Progress in Materials Science 155 (2026) 101533

Contents lists available at ScienceDirect

Progress in Materials Science

journal homepage: www.elsevier.com/locate/pmatsci

Smart micro/nanorobots for drug delivery in the brain

Di Shi [a], Xiang Wang [b], Yulin Deng [b,*], Huaijuan Zhou [a,*], Yilong Wang [c], Paul K. Chu [d,*], Jinhua Li [b,*]

[a] School of Interdisciplinary Science, Beijing Institute of Technology, Beijing 100081, China
[b] School of Medical Technology, Beijing Institute of Technology, Beijing 100081, China
[c] Department of Neurology, Beijing Tiantan Hospital, Capital Medical University, Beijing 100070, China
[d] Department of Physics, Department of Materials Science and Engineering, and Department of Biomedical Engineering, City University of Hong Kong, Tat Chee Avenue, Kowloon, Hong Kong, China

ARTICLE INFO

Keywords:
Nanocarriers
Micro/Nanorobots
Brain Diseases
Targeted Delivery

ABSTRACT

Pharmacotherapy is the core approach for treating various brain diseases. However, the intricate anatomical structure and the blood–brain barrier (BBB) of the brain present challenges for intracerebral drug delivery and therapeutic efficacy. Although systemic administration and surgical interventions can alleviate symptoms, they are limited by low therapeutic effects and potential adverse side effects. Moreover, due to their complex pathogenesis, insidious development, and deep-seated lesions, brain diseases are difficult to diagnose accurately. To address these challenges, there is an urgent need to develop intelligent nanocarriers that can efficiently load drugs and penetrate the BBB for precise therapy of brain diseases. In this connection, micro/nanorobots (MNRs) are multifunctional drug carriers at the micro-nano scale, which possess exceptional penetration and targeting capabilities. Employing externally powered propulsion or chemical self-propulsion, MNRs can navigate in the brain and cross the BBB. This review comprehensively summarizes the recent advances and future outlook of smart MNR drug delivery systems for brain disease treatment. It covers broad topics from nanocarriers to active smart MNRs. Furthermore, it elucidates the therapeutic mechanisms of these smart MNR drug delivery systems in brain diseases based on pathogenesis and pathology. Our aim is to provide a reference for designing and developing novel smart MNRs for drug delivery in the brain, paving the way for their clinical applications in treating brain diseases.

1. Introduction

Pharmacotherapy serves as a cornerstone of disease intervention in modern medical practice, requiring comprehensive consideration of pathological mechanisms, pharmacodynamic properties, and safety evaluations [1,2]. The brain, the most critical structure in the central nervous system (CNS), exhibits high metabolic demands and vulnerability [3,4]. The cerebral intricate anatomical structure and blood–brain barrier (BBB) pose severe challenges to the delivery and therapeutic efficacy of drugs [5–8]. Furthermore, cerebral pathologies (such as brain tumors [9,10], neurodegenerative disorders [11,12], and ischemic stroke [13,14]) present complex pathogenic mechanisms that severely threaten human health, presenting persistent difficulties in clinical treatment. These brain

* Corresponding authors.
E-mail addresses: deng@bit.edu.cn (Y. Deng), huaijuan.zhou@bit.edu.cn (H. Zhou), paul.chu@cityu.edu.hk (P.K. Chu), lijinhua@bit.edu.cn (J. Li).

https://doi.org/10.1016/j.pmatsci.2025.101533
Received 27 August 2023; Received in revised form 30 June 2025; Accepted 2 July 2025
Available online 6 July 2025

Abbreviations

Abbreviation	Full name
AD	Alzheimer's disease
AFM	atomic force microscopy
AIF	anti-inflammation
Ang	angiopep-2
APP	amyloid precursor protein
Arg	arginine
Aβ	β-amyloid
BACE1	β-site amyloid precursor protein cleaving enzyme-1
BBB	blood–brain barrier
bEnd.3	brain-derived Endothelial cells.3
B-LNPs	bridging-lipid nanoparticles
BPNSs	black phosphorus nanosheets
BTO	barium titanate
CAR	chimeric antigen receptor
CellBots	cell-based microrobots
CD	cluster of differentiation
CLSM	confocal laser scanning microscopy
CN	carbonaceous nanosphere
CNS	central nervous system
CRT	calreticulin
CSF	cerebrospinal fluid
Cur	curcumin
DMs	diatom microrobots
DOX	doxorubicin
DT	dihydrotanshinone I
EDX	energy dispersive X-ray
GBM	glioblastoma multiforme
GLUT1	glucose transporter 1
HNTSC	human nasal turbinate stem cell
hPSCs	human pluripotent stem cells
HSPG	heparan sulfate proteoglycan
ICG	indocyanine green
IF	inflammatory factor
iNOS	inducible nitric oxide synthase
LDL	low-density lipoprotein
LF	Lactoferrin
LFR	LF receptor
LMMRs	liquid metal microrobots
MB	methylene blue
MCA	middle cerebral artery
MCAO	middle cerebral artery occlusion
MCRs	magnetic continuum robots
MEA	multi-electrode array
MHC	major histocompatibility complex
MM	macrophage membrane
MNRs	micro/nanorobots
MOHRs	manipulated optoelectronic hybrid microrobots
MRI	magnetic resonance imaging
$mSiO_2$	mesoporous silica
NIR	near-infrared radiation
NMDARs	N-methyl-D-aspartate receptors
NPs	nanoparticles
OAT	optoacoustic tomography
OMV	outer membrane vesicle
PBS	phosphate-buffered saline
PD	Parkinson's disease
PD-L	programmed cell death-ligand

PDMS	polydimethylsiloxane
PEG	polyethylene glycol
PIF	pro-inflammation
PLGA	poly(lactic-co-glycolic acid)
PTX	paclitaxel
RMF	rotating magnetic field
ROS	reactive oxygen species
RT	radiation therapy
SAK	staphylokinase
SDF-1	stromal cell-derived factor 1
SFH	staphylokinase-hirudin fusion protein
siBACE1	β-site amyloid precursor protein cleaving enzyme-1 small interfering RNA
siRNA	small interfering RNA
siSNCA	α-synuclein small interfering RNA
STING	stimulator of interferon genes
TAMCs	tumor-associated myeloid cells
TBI	traumatic brain injury
TCR	T cell receptor
TfR	transferrin receptor
TLND	triphenylphosphonium lonidamine
tPA	tissue plasminogen activator
TPZ	tirapazamine
WT	wild-type
α-syn	α-synuclein

diseases often develop insidiously, with deep-seated lesions that are hard to diagnose accurately. Although traditional cerebral treatments (such as surgical resection or radiotherapy) can alleviate symptoms of brain diseases, they may cause irreversible neural damage [15,16]. Therefore, due to its non-invasiveness and broad applicability, pharmacotherapy has become an important therapy strategy. Current challenges in brain drug therapy include: (i) The BBB strictly limits drug permeation from the systemic circulation into the brain parenchyma, rendering over 98 % of small-molecule agents and nearly all macromolecular therapeutics (such as antibodies and gene-based medications) therapeutically ineffective [17–20]. (ii) Systemic administration may lead to off-target effects, inducing severe systemic toxicities [21–24].

In this context, intelligent drug delivery systems have progressively become key solutions to address therapeutic challenges in brain diseases. An ideal brain-targeted drug carrier should possess the following requirements: targeting specificity (precise lesion recognition), barrier penetrability (BBB penetration), drug-loading stability (prevention of off-target drug leakage), superior controllability, and biocompatibility. Although conventional carriers have partially improved drug delivery efficiency through passive targeting or surface modification, they still exhibit significant limitations. For example, liposomes exhibit rapid immune clearance and lack autonomous navigation to specific brain regions [25], while polymeric carriers rely on passive diffusion or material degradation for drug release, which fails to enable precise control [26,27]. It is well known that conventional drug carriers show limited BBB penetration efficiency, and typically require external physical fields, such as ultrasound [28–30] and near-infrared radiation (NIR) [31,32], to transiently disrupt the BBB for high-dose administration, which may induce cerebral tissue damage or systemic toxicity [33–35]. To overcome the challenges of brain drug therapy, there is an urgent requirement to develop multifunctional active drug delivery systems that can cross (or circumvent) physiological barriers and enable precise and controlled drug delivery, thereby breaking through current therapeutic bottlenecks in brain diseases.

Medical micro/nanorobots (MNRs) are microscopic mobile machines at the micrometer and nanometer scales designed to move to hard-to-reach locations (such as cerebral vessels and biliary ducts) and perform specific tasks (such as drug delivery and microsurgery) autonomously and/or driven by external power (such as magnetic field, ultrasound, light, heat, and electric field) [36–44]. As emerging drug carriers, MNRs offer a promising therapeutic strategy for brain diseases through their excellent locomotion and navigation [45–47], BBB penetration [48–50], and intelligent response capabilities [51–54]. Owing to their minuscule sizes and programmable designs, MNRs can simulate biological transport to cross BBB via versatile surface modification. For instance, MNRs can exploit biomimetic coatings to imitate lipoprotein particles for BBB crossing via receptor-mediated transcytosis [48,49]. Alternatively, they can travel along vascular pathways to reach deep-seated cerebral lesions (such as brain tumors and neuroinflammatory regions) under external powering or chemical propulsion and achieve precise drug delivery [55–59]. These strategies can not only significantly enhance localized drug concentrations but also minimize systemic drug dispersion, thereby substantially reducing adverse effects associated with toxic therapies such as chemotherapy.

In recent years, the research on drug delivery systems for the therapy of brain diseases has intensified significantly. Among the very few published reviews on the relevant topic of MNR-based drug delivery in the brain [60,61] (including a keynote review for cancer therapy and a comment), we identified a gap in comprehensive analyses in this field, especially from the perspective of nanocarriers to active MNR-based delivery systems, which is of great significance to deepen our understanding of and develop smart brain-targeted MNRs for active drug delivery, thereby unleashing their huge potential for treating a variety of brain diseases. In this review, we first

Table 1
Classification of passive nanocarriers.

Passive nanocarriers				Case analysis							
Classification		**Advantages**	**Disadvantages**	**Examples**	**Drugs**	**Brain diseases**	**Size**	**Loading degrees**	**Encapsulation efficiency**	**Zeta potential**	**Polydispersity**
Organic nanocarriers	Lipsomes [71,101,106,107]	Low toxicity Controlled drug release Superior biocompatibility and biodegradability	Low drug-loading stability Enzymatic degradation Low permeability	Oil/solid lipid/ phospholipid liposomes [108]	Quercetin	Neuron damage	74.61 ± 4.23 nm	17.98 ± 1.19 %	89.91 ± 6.41 %	–8.9 ± 0.5 mV	< 0.3
	Micelles [90,102,109,110]	Low toxicity Highly drug-loading efficiency Good biocompatibility and biodegradability	Low targeting and permeability Limited drug-loading stability Challenges in loading hydrophilic drugs	Electro-responsive micelles [111]	Phenytoin	Epilepsy	24.4 ± 1.3 nm	Around 3.2 %	N/A	Around –13.54 mV	0.31 ± 0.03
	Dendrimers [91,100,112–114]	High molecular uniformity and monodispersity Shielding drugs from biodegradation Theranostic integration	Hemolytic toxicity Long-term safety issues Unforeseeable drug release kinetics	Transferrin-bearing polypropylenimine dendrimer [115]	Luciferase gene	Glioma	N/A	N/A	N/A	Around 1.03 mV	N/A
	Nanogels [100,105,116–118]	Good bioadhesion and biocompatibility Fluid-like transport properties and excellent deformability Controlled drug release	Premature or burst release of the drug Long-term safety concerns Low targeting efficiency	Nanocomposite hydrogel [118]	Dexamethasone	Traumatic brain injury (TBI)	167.6 ± 2.47 nm	29.49 % ± 0.28 %	N/A	–36.69 ± 0.98 mV	Around 0.004
Inorganic nanocarriers	Metal-based nanocarriers [15,92,119–121]	Superior biocompatibility Imaging capability Small size effect	Interference with cellular signaling pathway Intracranial accumulation	Ultrasmall Au NPs [122]	Doxorubicin (DOX)	Glioblastoma multiforme (GBM)	1.1 ± 0.1 nm	13 DOX molecules/ 1 Au NP	N/A	–30 ± 2 mV	0.30 ± 0.40
	Metallic compound nanocarriers [92,103,104,123,124]	Low toxicity Good biodegradability Photothermal properties Nanozyme catalytic activity	Intensify oxidative stress Challenges in functionalizing targeting ligands Suboptimal drug-loading stability	Superparamagnetic iron oxide NPs [125]	Curcumin (Cur)	Alzheimer's disease (AD)	94.0 ± 2.1 nm	8 % (w/w)	99.00 ± 0.69 %	–0.01 ± 0.01 mV	0.14 ± 0.02

(*continued on next page*)

Table 1 (*continued*)

Passive nanocarriers				Case analysis							
Classification		**Advantages**	**Disadvantages**	**Examples**	**Drugs**	**Brain diseases**	**Size**	**Loading degrees**	**Encapsulation efficiency**	**Zeta potential**	**Polydispersity**
	Nonmetallic nanocarriers [15,93,126–128]	Highly colloidal stable Superior biocompatibility High penetration efficiency	Slow degradation kinetics Heavy metal leakage risks (quantum dot)	Cluster-like mesoporous silica [129]	Arctigenin	Spinal cord injury	Around 60–120 nm	1.56 ± 0.25 %	31.21 ± 3.60 %	N/A	N/A
Biomimetic nanocarriers	Cell-based nanocarriers [62,71,94,130–132]	Natural BBB penetration and targeting ability Immune modulation Lesion-specific accumulation	Limited drug-loading capacity Neurotoxicity and off-target effects Short cell lifespan	Mesenchymal stem cells [133]	Paclitaxel (PTX)	Glioma	Cells: micrometer scaleNPs: 135.3 ± 3.7 nm	4.34 ± 0.18 %	86.87 ± 3.63 %	–28.6 ± 3.6 mV	0.18 ± 0.02
	Cytomembrane-based nanocarriers [95,134–137]	Natural BBB penetration and targeting ability Immune escape Superior biocompatibility	Low drug-loading stability Complex preparation Unclear targeting mechanisms	Glioma C6 cancer cell membrane [138]	PTX nanosuspensions	Glioma	Around 169.2 nm	N/A	N/A	Around –29.80 mV	Highly monodisperse
	Extracellular vesicle-based nanocarriers [96,139–141]	Low immunogenicity Intrinsic targeting capabilities Modulation of tumor microenvironment	Challenges in isolation and purification Low drug-loading efficiency Short half-life	Peptide-modified extracellular vesicles [140]	Methotrexate	GBM	318.3 ± 15.5 nm	5.1 ± 0.5 %	1.4 ± 0.2 %	Around –10 mV	N/A
Stimuli-responsive nanocarriers	Internal stimuli-responsive nanocarriers [98,105,142,143]	No external equipment Controlled drug release High specific biological signals Ease of material modification	Uneven therapeutic responses Off-target drug release tissues Low penetrability	pH-Responsive diblock polymer [144]	DOX	GBM	55 ± 12 nm	Around 10 wt%	Almost 100 %	0 ± 1.5 mV	N/A
	External stimuli-responsive nanocarriers [97–99,145,146]	High precision of controlled drug release Controllable stimulus intensity Theranostic integration	Relies on external equipment Damage to healthy tissue Limited depth of stimulation response	Light-responsive black phosphorus [147]	Paeoniflorin	Parkinson's disease (PD)	Around 203.1 nm	N/A	N/A	Around −28.8 mV	0.152

Table 2
Comparison of MNRs for drug delivery in the brain.

Active propulsion		Advantages	Disadvantages	References
Chemical	Exogenous fuel	Propelled by local chemical reactions without external equipment Carried catalytic enzymes can effectively eliminate excessive reactive oxygen species (ROS) at brain lesion sites Fast diffusion	Reliance on external fuel, which can be toxic at high concentrations Random movement direction, making precise navigation challenging	[49,87,159]
	Endogenous fuel	Active propulsion Uses natural substances within the body as fuel, ensuring high biocompatibility and biodegradability Capacity of combine hydrogen therapy during propulsion to actively scavenge ROS and alleviate inflammation	Movement driven by chemical gradients, resulting in low control accuracy Poor penetration of brain tissues	[85,160,161]
External-field	Magnetic	No fuel required Highly controllable, capable of achieving sub-millimeter path planning Capacity of non-invasively penetrate the skull to manipulate deep brain regions	High requirements for magnetic control equipment, along with limited workspace Strong magnetic fields may cause brain tissue heating Magnetic particles are prone to aggregation, complicating swarm control	[41,48,156]
	Ultrasound	No fuel required Fast movement speed and able to tolerate high flow rates Microbubble carriers (lipid/polymer) naturally dissolve after completing tasks Miniaturized equipment suitable for bedside operation	High demands on chamber geometry, with uneven penetration depth Moving against blood flow requires higher sound pressure, potentially damaging the vascular endothelium Difficulty in controlling multiple swarms, with significant long-distance navigation loss	[155,157,162]
	Light	No fuel required NIR light can precisely trigger local photothermal/photochemical reactions NIR almost has no side effects on human organs and tissues	Limited speed and reliance on exogenous photosensitizers Poor penetration, making it hard to reach deep brain regions Overheating may damage normal neurons	[54,55,158]

introduce nanocarrier-based targeted brain drug delivery systems, encompassing organic nanocarriers, inorganic nanocarriers, biomimetic nanocarriers, stimuli-responsive nanocarriers. Then, we elaborate on the active targeted brain drug delivery systems based on MNRs, focus on the motion abilities of MNRs in the brain, and summarize strategies for MNRs to cross or circumvent the BBB to facilitate effective drug delivery. Next, the material design of intracranial MNRs was taken into consideration. Subsequently, we explore the applications of smart MNR delivery systems in brain diseases, including brain tumors, neuron recovery and regeneration, ischemic strokes, traumatic brain injuries, and neurodegenerative diseases. We illustrate their therapeutic mechanisms from the perspectives of pathogenesis and pathology. Finally, we propose an outlook on future directions and challenges in the emerging field of smart MNR drug delivery systems in the brain.

2. From nanocarriers to micro/nanorobots

In the treatment of brain disorders, due to the highly selective nature of the blood–brain barrier [48,62,63], the complexity of brain tissue microarchitecture [64–66], and limitations associated with passive diffusion mechanisms in nanocarriers [67–69], conventional nanocarriers exhibit limited delivery efficiency [7,70,71]. MNRs, a new type of intelligent drug delivery system with sizes ranging from several nanometers to several micrometers [39,59,72–78], demonstrate superior penetrability and targeting specificity [79,80]. Using externally powered propulsion [81–84] or chemical self-propulsion [85–87], MNRs can achieve controlled directional motion in biological environments, significantly enhancing transport efficiency and delivery precision for drug delivery.

2.1. Passive nanocarriers

Nanocarriers for drug delivery in the brain should possess the following fundamental functions: overcoming the BBB, loading and releasing drugs, targeted movement, and biocompatibility [88,89]. Current nanocarriers for drug delivery in the brain primarily include: (i) organic nanocarriers [71,90,91], (ii) inorganic nanocarriers [15,92,93], (iii) biomimetic nanocarriers [94–96], and (iv) stimuli-responsive nanocarriers [97–99] (Table 1). However, these passive nanocarriers exhibit limited efficacy in enhancing drug penetration and retention in the brain [71,100]. For instance, organic nanocarriers commonly exhibit low drug-loading stability and permeability [101,102]. Furthermore, the movement of passive nanocarriers in the brain relies on the natural flow of bodily fluids and passive diffusion driven by concentration gradients, which makes them unable to deliver drugs against countercurrent flow or concentration gradients. Although magnetic nanoparticle (NP)-based nanocarriers can be driven by external fields, they are easily recognized and phagocytosed by the immune system, leading to their accumulation in the brain and causing damage to healthy tissue

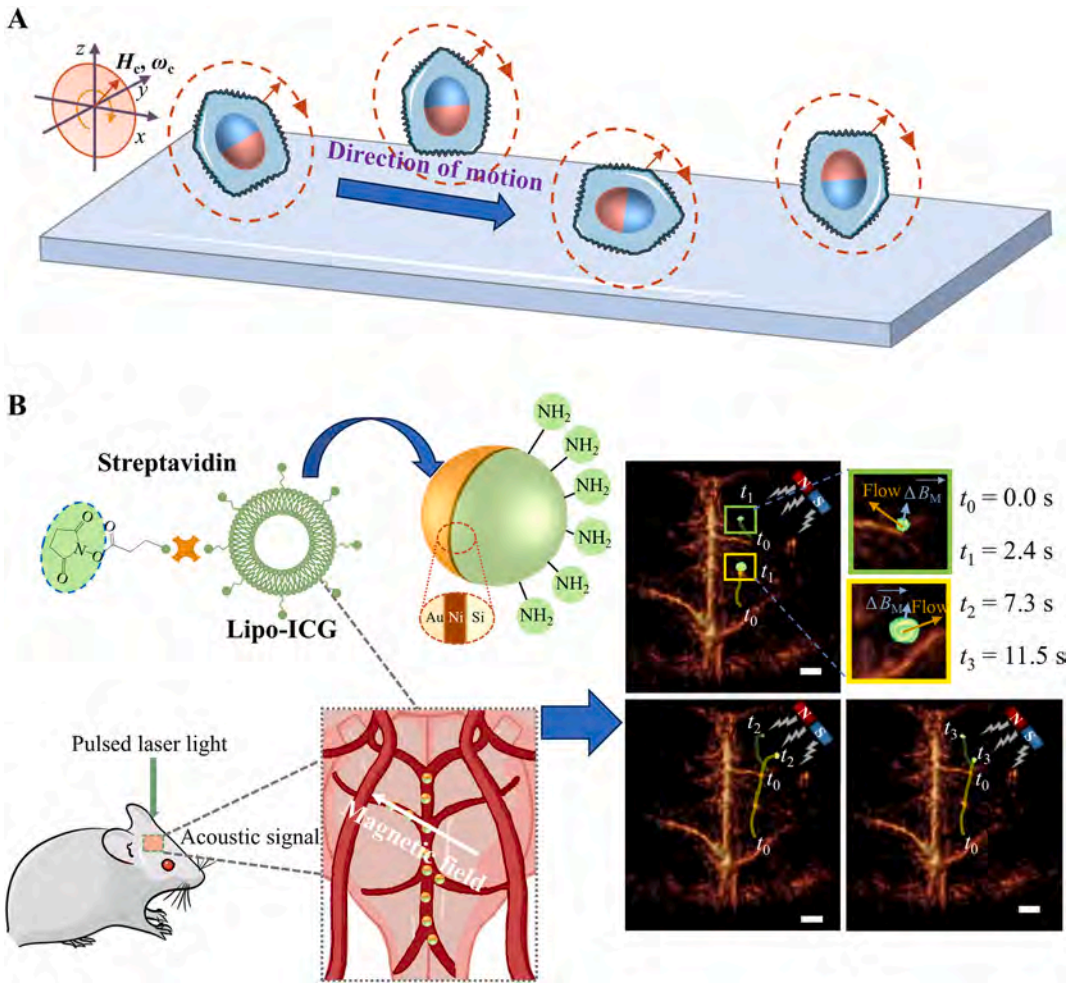

Fig. 1. (A) Schematic representation demonstrated magnetic MNRs rolling on a PDMS substrate under a rotating magnetic field. $\boldsymbol{H}_c$ and $\boldsymbol{\omega}_c$ represent the critical magnetic field intensity and the critical frequency of the RMF, respectively. Reproduced with permission from ref [48]. Copyright 2021, The Authors, some rights reserved; exclusive licensee American Association for the Advancement of Science. (B) Schematic illustration of the microrobot's composition and its motion monitoring in the brain. The core of the microrobot was composed of nanoliposomes, with its surface partially coated with a Ni layer, a Au layer, and ICG to form a Janus structure. The yellow arrow in OAT imaging represents the direction of blood flow, while the blue arrow indicates the direction of the magnetic field. The scale bar is 1 mm. Reproduced with permission from ref [166]. Copyright 2022, The American Association for the Advancement of Science. Abbreviation: ICG, indocyanine green.

[103,104]. Moreover, while biomimetic nanocarriers employ cells or cellular components to modulate immunity [94,95], their interference-prone targeted movement and high cost limit their clinical application in the brain. Stimuli-responsive nanocarriers face challenges in achieving precise control, posing risks of unintended stimulation to healthy tissues [98,105]. Consequently, to obtain superior targeted distribution and overcome physiological flow barriers, smart MNRs for drug delivery in the brain are urgently required to develop actively controllable motion, rapid drug delivery capabilities, and high permeability.

2.2. *Moving in the brain*

Drug delivery to the brain mainly depends on vascular transport and transcranial administration [148–152]. While craniotomy may cause infection and traumatic injury to healthy tissues [70,153,154], the minimally invasive nature of cerebrovascular transport significantly reduces these risks. Nevertheless, the intricate architecture of the cerebrovascular network and the dynamic fluid environment pose significant challenges for MNR precise navigation and propulsion in the brain [73,155,156]. Current MNRs for drug delivery in the brain primarily include: (i) magnetic propelled MNRs [41], (ii) self-propelled MNRs [49], (iii) utrasound-propelled MNRs [157], and (iv) light-propelled MNRs [158] (Table 2).

As a non-invasive manipulation strategy, magnetic actuation provides superior controllability and deep tissue penetration [72,163–165]. Notably, researchers have demonstrated that magnetic MNRs can be remotely controlled in the brain [63,166,167]. The translational mechanisms of magnetic MNR are fundamentally determined by the magnetic field category. Rotating magnetic field

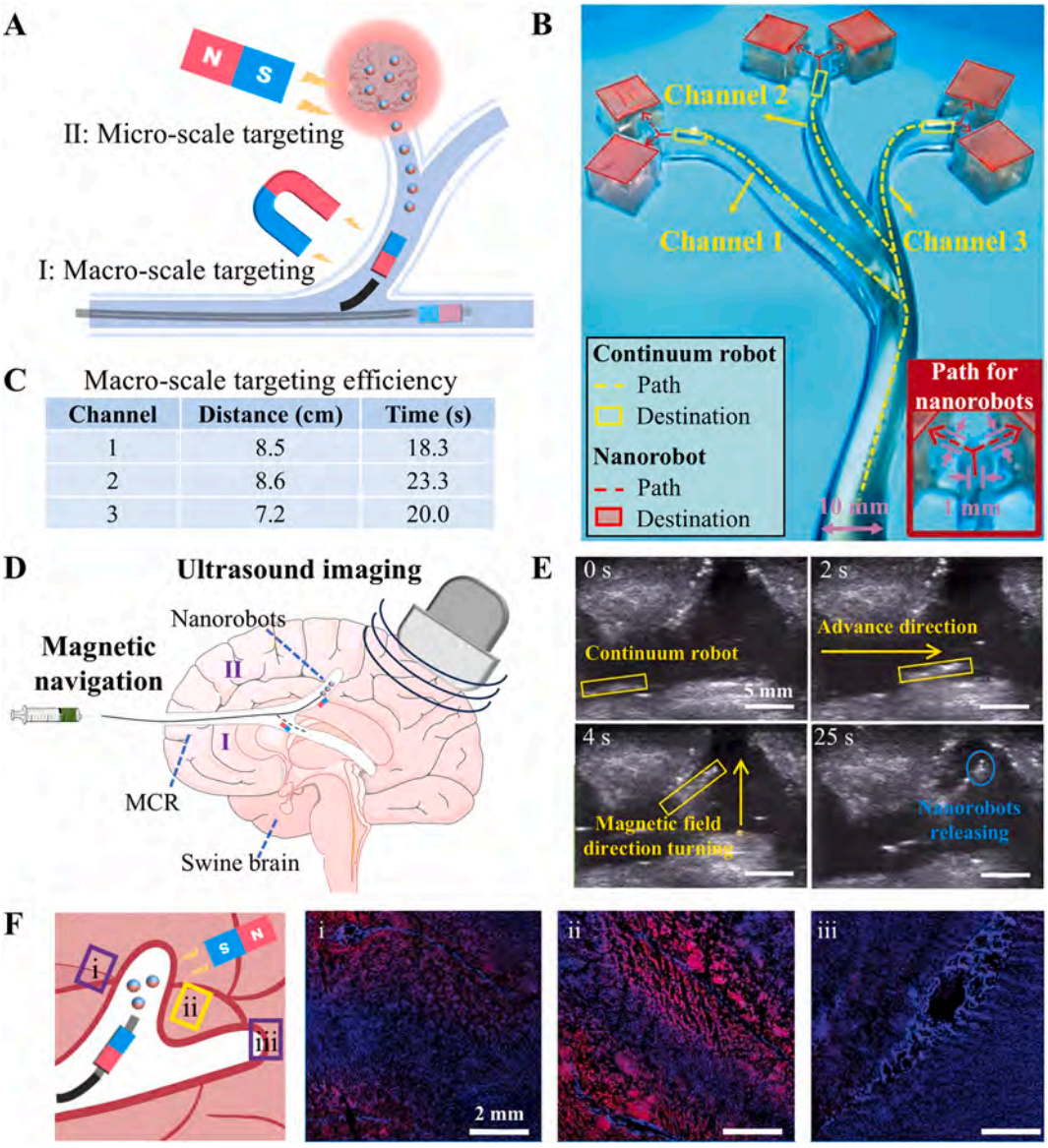

Fig. 2. Magnetically driven and navigated marsupial robotic system for rapid cross-scale targeting of drug delivery in the brain. (A) Schematic illustration of the use of a marsupial robotic system. (B) The marsupial robots based on MCR moved in the 3D-printed channel. (C) The macro-scale delivery efficiency of the continuum robots in 3D-printed channels with different distances. (D) Schematic demonstration and (E) experimental images of ultrasound imaging monitoring the targeted delivery of nanorobots assisted by MCR in a swine brain. The scale bar is 5 mm. (F) Schematic illustration of the micro-scale targeting of nanorobots in the brain and fluorescence images of brain tissue slices from different regions. Region (i) represented the area where nanorobots were transported solely by the MCRs, region (ii) represented the area where the marsupial robotic system was used to deliver nanorobots, and region (iii) served as the control group without nanorobots. Rhodamine B stained the nanorobots red, while 4′,6-diamidino-2-phenylindole (DAPI) stained the cell nuclei blue. Reproduced with permission from ref [156]. Copyright 2023, Wiley-VCH GmbH. Abbreviation: MCR, magnetic continuum robot.

(RMF) enables structurally heterogeneous drug-loading MNRs to simultaneously execute rotational and translational motions [41,168–171], enhancing their controllability in complex fluidic environments. Furthermore, RMF requires a lower amplitude under comparable MNR velocities compared to gradient magnetic field [48,172,173], providing a superior capability for multi-MNR system manipulation in the cerebral vasculature. As illustrated in Fig. 1**A**, Qiang He's group [48] used RMFs to actuate heterogeneous magnetic MNRs on a polydimethylsiloxane (PDMS) substrate, where the viscous PDMS was employed to simulate the resistance of blood counterflow against the MNRs. The MNRs showed translational helical motion under the actuation of the RMF, with both their rotation and translation directions aligned with the magnetic field, demonstrating excellent mobility and controllability. To enhance the precision of MNRs navigation in cerebral blood vessels, real-time tracking of the MNR is essential. However, the micro-size of the MNRs and the obstruction caused by deep tissues [166,174,175] make the detection and tracking of the MNR challenging. For this

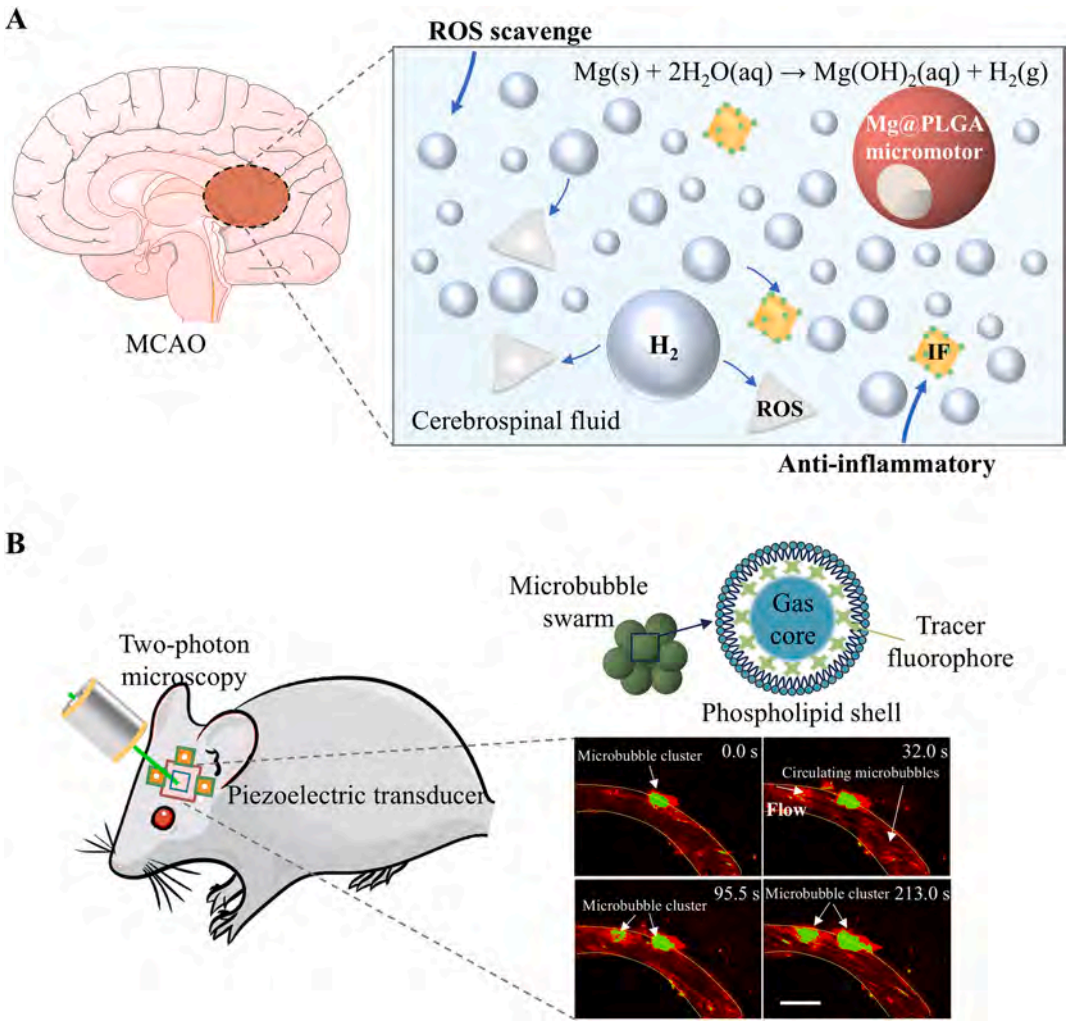

Fig. 3. Biocompatible endogenous fuels-driven microrobots for brain therapy. (A) Schematic representation demonstrated Mg atoms in the notch of the Mg@PLGA micromotor react with water to generate H_2 bubbles, which propel the micromotors in cerebrospinal fluid. Simultaneously, H_2 bubbles scavenged ROS and alleviated inflammatory factor expression. Reproduced with permission from ref [160]. Copyright 2021, Wiley-VCH GmbH. (B) Schematic illustration of the experimental setup and the microrobot. The evolution of microbubble (Mb) aggregation on vascular walls against ultrasound time. The microbubble clusters were labeled with green fluorescence, while the individual microbubbles were labeled with red fluorescence. The scale bar is 50 μm. Reproduced with permission from ref [155]. Copyright 2023, The Authors. Abbreviations: ROS, reactive oxygen species; IF, inflammatory factor; MCAO, middle cerebral artery occlusion.

purpose, Razansky's group [166] designed a nickel (Ni)-based Janus microrobot capable of safely navigating in the mouse brain and demonstrated its real-time three-dimensional tracking in cerebral blood vessels, as depicted in Fig. 1**B**. The introduction of the Ni coating enabled the microrobot to be manipulated by RMF, while the incorporation of the Au coating and indocyanine green (ICG) enhanced the optoacoustic tomography (OAT) contrast of the microrobot, allowing it to be imaged in deep tissues. Under the actuation of the RMF, the microrobot moved along the blood vessel in an approximately linear trajectory. In the OAT imaging, the pulsed laser responded to near-infrared light irradiation and emitted acoustic signals, enabling imaging and tracking of the microrobot's movement positions at different time points.

Although MNRs demonstrate remarkable mobility, their moving speed is limited, resulting in excessively long navigation distances in macro-scale blood vessels [176–179]. Additionally, the complex fluidic and physicochemical environment of the brain inevitably leads to the loss of carried drugs, limiting the therapeutic efficacy of nanorobots [156,180–182]. Consequently, there is an urgent need to develop strategies for localized MNRs to rapidly transport in the human body to address the challenge of long-distance transportation. Currently, numerous studies have employed endoscopes and catheters to transport MNRs into tubular tissues in the human body (such as bile ducts [183,184], nasolacrimal ducts [185], and blood vessels [186,187]). However, the large size of endoscopes and catheters makes it challenging to deliver MNRs to nearby disease sites in the brain. Magnetic continuum robots (MCRs) offer advantages such as small size [188,189], multi-degree-of-freedom motion [190,191], and biocompatibility [192], enabling precise movement deep in human tissues through external magnetic fields, making them excellent carriers for the high-precision navigation of

Table 3
Receptor-mediated transport for BBB crossing.

Receptors	Ligands	BBB crossing mechanism	References
TfR	Transferrin Anti-TfR receptor antibody (OX26, 8D3, and RI7-217) TfR-binding peptides (TfR-T12)	Transferrin and iron ions are endocytosed into cells under the TfR, and acidification occurs in endosomes to release transferrin and iron ions	[246–249]
Low-density lipoprotein (LDL) receptor	Apolipoproteins (apoprotein B100 and apolipoprotein E) Angiopep-2	LDL binds to LDL receptors through apolipoproteins, and the complex is internalized by the cell via receptor-mediated endocytosis	[249–251]
Insulin receptor	Insulin Insulin-like growth factors Anti-insulin receptor antibody (HIRMAb)	Insulin receptors on endothelial cells transport insulin from the peripheral blood in the brain	[252–254]
Scavenger receptor	Scavenger receptor are multiligand receptors with ability to bind a wide variety of endogenous and exogenous ligands, such as LDL derivatives, proteoglycans, and residues from apoptotic cells	Scavenger receptors play a role in LDL receptor-mediated endocytosis by binding to and internalizing modified LDL	[255–257]
Folate receptor	Folic acid Folate conjugates	Folate is released into the cerebrospinal fluid (CSF) via folate receptor exosome following receptor-mediated internalization	[258,259]
Nicotinic acetylcholine receptor	Acetylcholine D-peptide (^{D}CDX)	Receptor-mediated endocytosis is facilitated by the specific expression of nicotinic acetylcholine receptors at the endothelium	[260,261]
Leptin receptor	Leptin Leptin-derived peptides (LP16, LP31)	Leptin receptor-expressing pericytes facilitate increased permeability of leptin across the BBB	[262,263]
Diphtheria toxin receptor	Corynebacterium diphtheria toxin CRM197	CRM197 upregulates Caveolin-1 expression mediated by forkhead box protein O1 activity and enhances caveolae-mediated transcytosis	[264,265]
Heparan sulfate proteoglycan (HSPG)	Cationic cell-penetrating peptides	The negatively charged heparan sulfate chains of HSPG on the cell surface bind to cationic cell-penetrating peptides to induce endocytosis	[266,267]
Neonatal Fc receptor	Immunoglobulin G	Fc receptor mediates the flow of Immunoglobulin G from the brain into the blood through the reverse transcytosis process	[268]

nanorobots. Liu's group [156,181] proposed a marsupial robotic system for rapid cross-scale targeting of drug delivery in the brain. As shown in Fig. 2**A**, the system drove MCRs rapidly to localized transportation, followed by the release of nanorobots for micro-scale targeting delivery. They initially employed a 3D-printed tube made of transparent resin, designed with a gradually narrowing structure, to simulate the cross-scale (width: 10 mm to 1 mm) targeting drug delivery environment for MNRs. Fig. 2**B** depicts the 3D-printed tube featuring three branches of similar length to simulate the MCRs delivery (yellow path), with each branch terminating in two smaller branches to simulate the nanorobots delivery (red path). To quantify the delivery efficiency of the nanorobots, the average velocity of the marsupial robotic system was calculated. Fig. 2**C** demonstrated that the marsupial robotic system maintained a stable motion speed in each channel, with an average speed of 0.39 cm/s, showing the capability of nanorobots for macroscopic delivery. Subsequently, they combine ultrasound imaging to monitor the cross-scale delivery of the marsupial robotic system in a swine brain, as illustrated in Fig. 2**D**. The motion of the marsupial robotic system was visualized using ultrasound imaging (Fig. 2**E**). At the initial stage (0 ~ 4 s), the continuum robot reached the branching blood vessels and turned its motor direction under magnetic guidance. In the second phase (4 ~ 25 s), the nanorobots were released. Finally, fluorescence images of brain tissue slices (Fig. 2**F**) revealed that the majority of nanorobots were distributed in the region (ii), indicating that cross-scale delivery significantly enhanced the delivery efficiency of nanorobots in the brain. Although magnetic actuation enables non-invasive remote control of MNRs in the brain, scaling laws [165,193,194] pose challenges for driving microscale magnetic MNRs in clinical treatments. Additionally, residual magnetic materials from MNRs after drug delivery cannot be fully degraded [177,195,196]. Therefore, it is essential to develop and combine alternative propulsion mechanisms for MNRs in brain applications to reduce dependence on magnetic particles.

Considering the excessive ROS [197,198] and pro-inflammatory microenvironment [199,200] in brain diseases, self-propelled MNRs capable of changing local chemical environments have been employed in brain disease research [159,160]. Self-propelled MNRs can convert chemical energy into mechanical motion through chemical reactions. Based on the source of the "chemical fuels", these MNRs are classified as exogenous fuel-driven (such as H_2O_2 [87,201,202] and $NaBH_4$ [165,203,204]) and endogenous fuel-driven (such as glucose [205–207] and gastric acid [208–210], and water [85,211,212]) MNRs. However, most exogenous fuels exhibit high cytotoxicity and low concentration gradient, making it difficult to maintain stable propulsion and thus limiting their clinical application. Therefore, biocompatible endogenous fuels derived from physiological sources have gained significant attention for precise therapy of brain diseases. As shown in Fig. 3**A**, Tu's group [160] used water as the endogenous fuel, and Mg-based (Mg@PLGA) micromotors were injected into the middle cerebral artery occlusion (MCAO) mouse brain model to investigate the motion of micromotors in cerebral environments. The propulsion mechanism relies on H_2 generation through Mg-water reactions in the cerebrospinal fluid. These Mg@PLGA micromotors, composed of Mg microparticles and notched poly(lactic-co-glycolic acid) (PLGA) shells, actively release H_2 during their motion. The remarkable biological reducibility of H_2 [213,214] effectively scavenged excessive ROS and alleviated inflammatory factor (IF) expression, significantly reducing infarct volume in MCAO mice. Furthermore, the PLGA shell demonstrates excellent biocompatibility without causing cellular toxicity. Therefore, through chemical reactions, self-

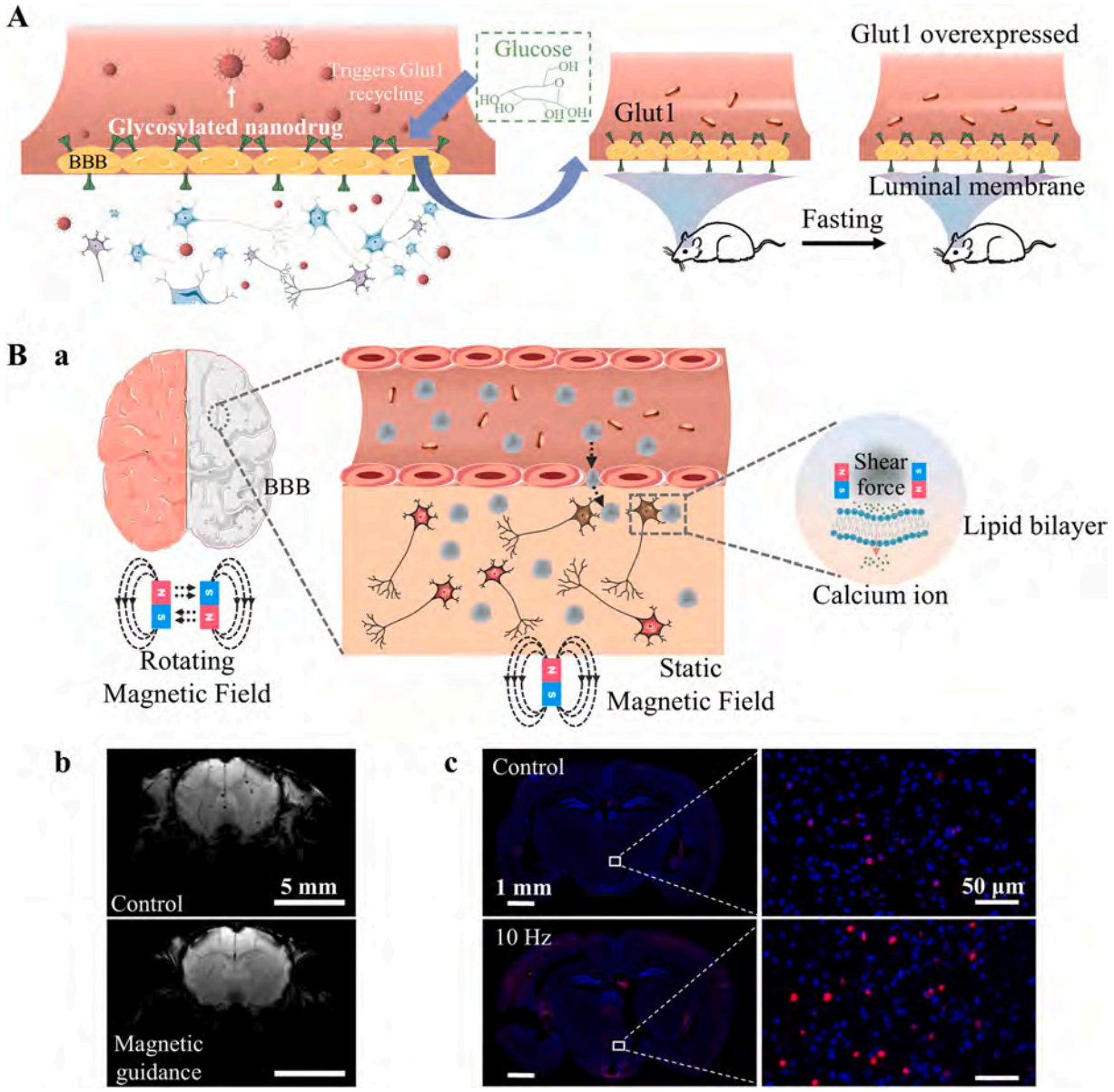

Fig. 4. Strategies for nanodrugs/microrobots to cross the BBB for brain targeting and therapy. (A) Schematic demonstration of the mechanism of glucose-regulated GLUT1-mediated transport of nanodrugs across the BBB. A 24-hour fasting in mice induced hypoglycemia, triggering GLUT1 overexpression on the luminal membrane of the BBB. Upon glucose supplementation, GLUT1 undergoes luminal membrane recycling, facilitating the transport of nanodrugs into brain tissue. Reproduced with permission from ref [50]. Copyright 2020, The American Association for the Advancement of Science. (B) (a) Schematic illustration of the BBB crossing process of magnetic LMMRs. (b) MRI images of the control group and LMMR-treated with magnetic guidance for 1 h. (c) Immunostaining images of the control group and LMMR-treated. Neuronal activation was assessed through c-Fos protein expression (red fluorescence). Experiments were conducted under a 10 Hz magnetic field, with a scale bar is 50 μm. Reproduced with permission from ref [63]. Copyright 2024, American Chemical Society. Abbreviation: BBB, blood–brain barrier.

propelled MNRs showed significant potential for precise therapy in the brain.

Ultrasound propulsion can drive MNRs in deep tissues, characterized by aggregation effect with fast response [83,215,216], and is easy to combine with imaging in practical applications. Furthermore, this propulsion exhibits minimal adverse effects on the human body at appropriate acoustic frequencies. Although ultrasound-propelled MNRs have been successfully demonstrated in human tissues and organs (such as ear vasculature [217], stomach [218], intestines [219], and cremaster muscle [220]), their application for microscale cerebrovascular navigation remains challenging. Motivated by this challenge, Ahmed's group [155] combined ultrasound propulsion and two-photon microscopy for real-time monitoring of microrobot motion. As shown in Fig. 3**B**, the experimental setup features a two-photon microscope positioned above a cranial window for microrobot visualization, along with piezoelectric

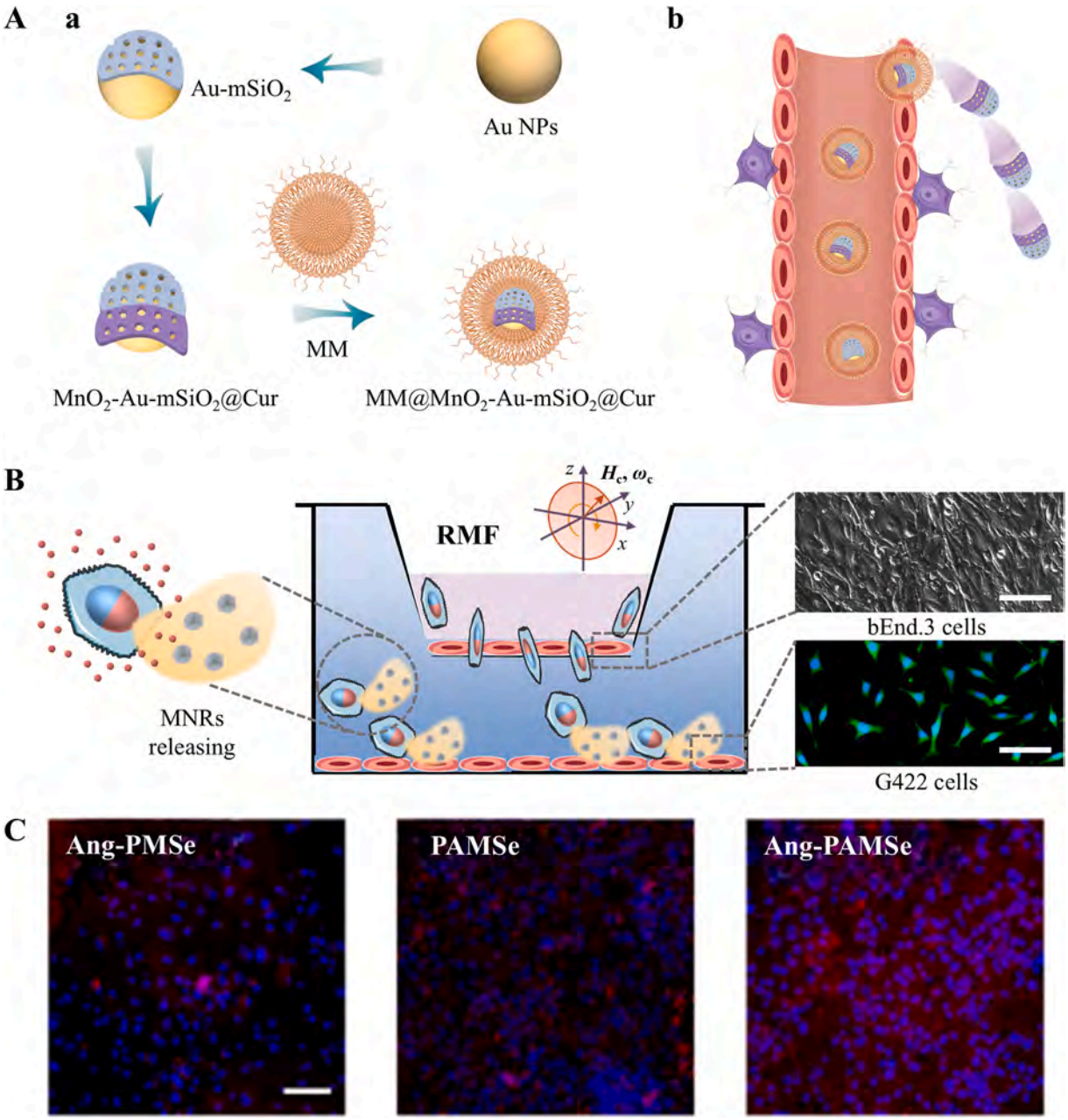

Fig. 5. The biomimetic camouflage tactics can enhance the immune escape and BBB-crossing capabilities of MNRs. (A) (a) Schematic illustration of the fabrication process of the MM@MnO_2-Au-mSiO_2@Cur. The fabrication process involved three steps: (i) Selective deposition of SiO_2 on Au nanoparticles to create Janus-structured Au-mSiO_2, (ii) formation of MnO_2-Au-mSiO_2@Cur nanorobots through Au-mediated potassium permanganate reduction and Cur loading, and (iii) coating with biomimetic MM to produce MM@MnO_2-Au-mSiO_2@Cur nanorobots. MM: macrophage membrane. (b) Schematic representation demonstrated MM@MnO_2-Au-mSiO_2@Cur crossing the BBB. Reproduced with permission from ref [49]. Copyright 2024, The Authors. Advanced Science published by Wiley-VCH GmbH. (B) Schematic illustration of the in vitro BBB model. The BBB was simulated using a bEnd.3 cell monolayer cultured on polycarbonate membranes, labeled with calcein-AM. A G422 cell layer was grown on the bottom of the Transwell system and labeled with Hoechst 33342. The scale bar is 75 μm. Reproduced with permission from ref [48]. Copyright 2021, The Authors, some rights reserved; exclusive licensee American Association for the Advancement of Science. (C) CLSM images of the cancer cell layer. MNRs crossed the BBB and were subsequently released into the cancer cell layer, with red fluorescence indicating MNRs and blue fluorescence indicating cell nucleus. The scale bar is 100 μm. Reproduced with permission from ref [56]. Copyright 2023, The Authors. Abbreviations: MM, macrophage membrane; Cur, curcumin; MM@MnO2-Au-mSiO2@Cur, biomimetic Cur-loaded self-propelled nanomotors; RMF, rotating magnetic field; bEnd.3, brain-derived Endothelial cells.3; G422, a model glioma cell; Ang-PAMSe, Ang-modified nanomotors; PAMSe, unmodified nanomotors, Ang-PMSe, Ang-modified NPs.

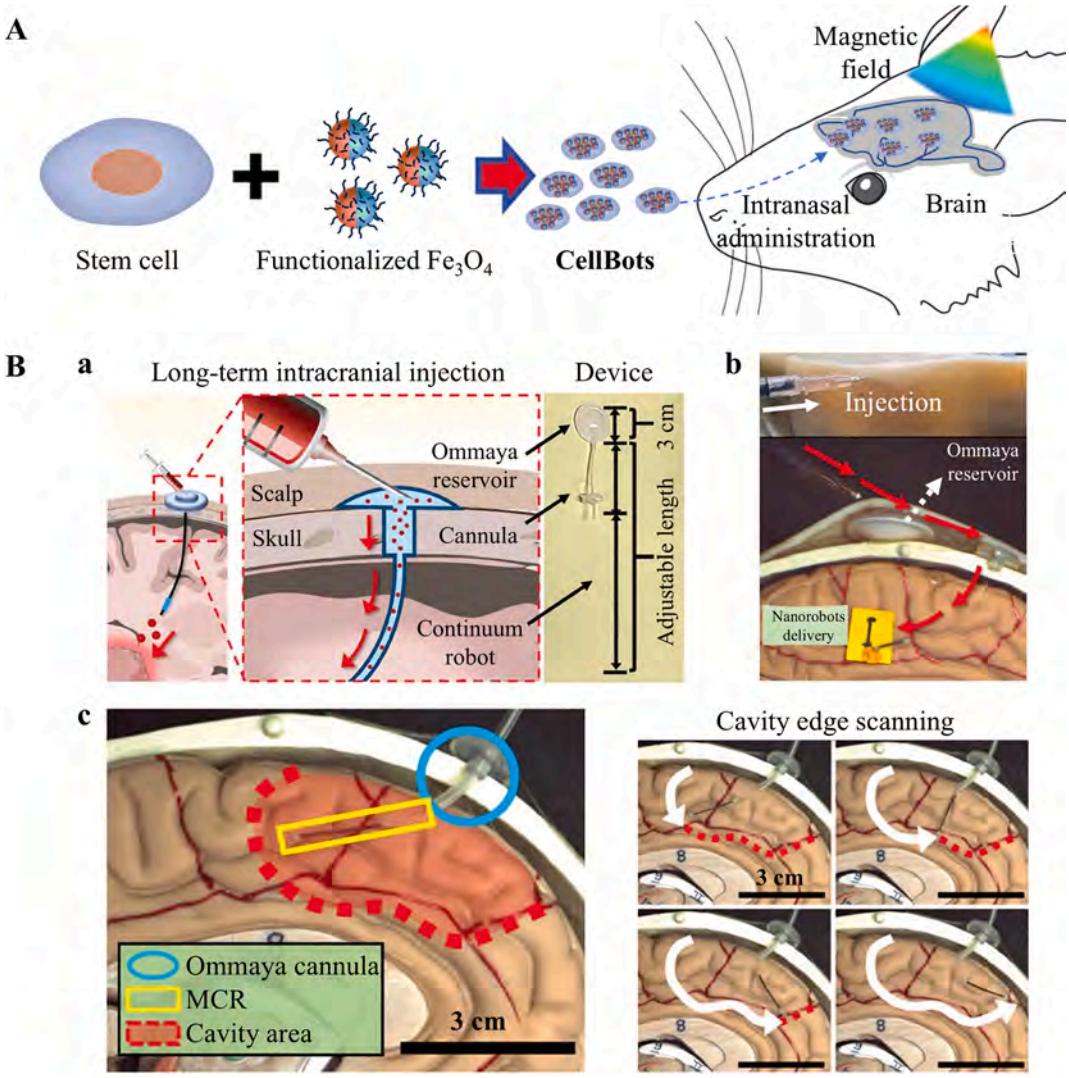

Fig. 6. Tactics for MNRs to circumvent the BBB for brain-targeted therapy. (A) Schematic illustration of the intranasal administration and delivery HNTSC in the brain of cell-based microrobots. Reproduced with permission from ref [297]. Copyright 2021, Wiley-VCH GmbH. (B) (a) Schematic illustration and (b) experiment images demonstrated intracranial drug delivery via an Ommaya reservoir. (c) Magnetic fields propelled MCRs for localized drug delivery in GBM. The scale bar is 3 cm. Reproduced with permission from ref [156]. Copyright 2023, Wiley-VCH GmbH. Abbreviations: CellBots, cell-based microrobots; MCR, Magnetic continuum robot.

transducers attached to the skull for ultrasound wave transmission. The microrobots were formed through microbubble aggregation, wrapping a phospholipid shell with inner-surface adsorbed tracer fluorophores, and encapsulating perfluoro butane gas. It can be found in Fig. 3B, microbubbles self-assembled to form microrobots (green fluorescence) on vascular walls under ultrasound stimulation. As ultrasound time proceeded (32 ~ 213 s), the microrobots captured individual microbubbles, moving against blood flow, while non-responsive microbubbles (red fluorescence) followed the bloodstream. Importantly, this approach demonstrated reproducible in vivo, exhibiting remarkable moving capabilities in the cerebral complex vascular networks. However, the limitations of ultrasound propulsion need to be resolved in the future: (i) Although microbubble cluster formation occurs rapidly, the probability of microrobot assembly remains low, which decreases drug delivery efficiency. (ii) Localized temperature increases in deep tissues during prolonged ultrasound transmission, presenting a potential security issue. In addition to the previous discussed MNRs for brain treatment, light-propelled MNRs have been preliminarily explored for brain applications [55]. Tu's group [55] employed polymeric nanomotors loaded with DOX and incorporating ICG as a photothermal agent. Under NIR irradiation, ICG generates heat to propel the nanomotors and provide photothermal ablation ability for tumor treatment, enhancing the synergistic treatment of GBM with DOX. However, due to the limited tissue penetration of NIR light, the study has so far been confined to mouse brain models and have not yet been extended to larger brain models.

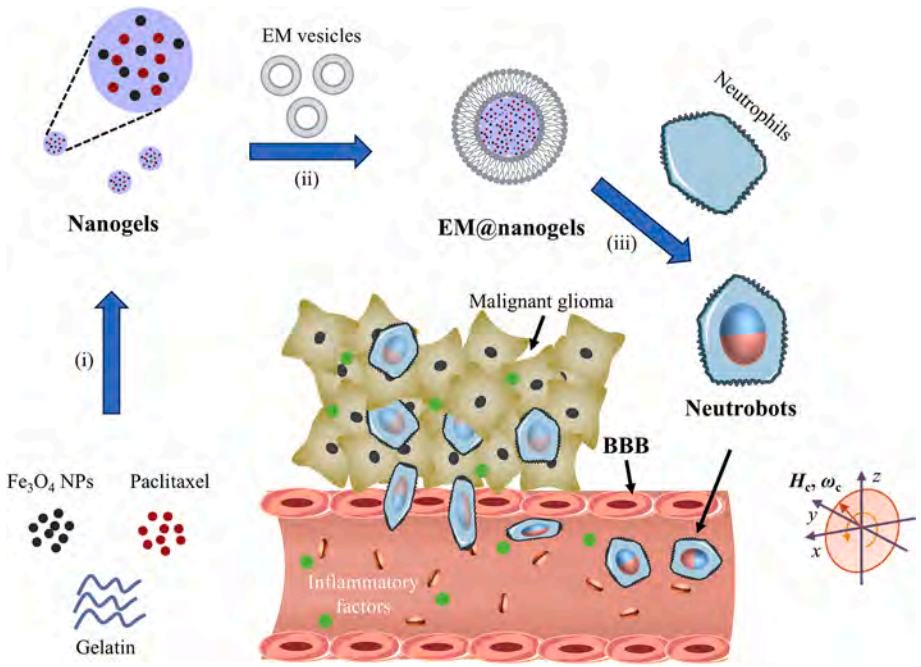

Fig. 7. Schematic representation demonstrated the fabrication process of neutrobots and they actively deliver PTX to malignant glioma. Fabrication process: (i) PTX loading into Fe_3O_4 NPs/gelatin complexes to form nanogels. (ii) Encapsulating the nanogels with E. coli membrane vesicles to form EM@nanogels. (iii) Phagocytosis of EM@nanogels by neutrophils to obtain neutrobots. Delivery process: (i) Magnetic actuation and chemotaxis along inflammatory factor gradients guide neutrobots toward the BBB. (ii) Neutrobots rely on the natural properties of neutrophils to cross the BBB. (iii) Targeted accumulation in malignant glioma. H_c and ω_c represent the critical magnetic field intensity and the critical frequency of the RMF, respectively. The loading per milligram of nanogel was 57, 76, 86, 90, 118, and 183 μg for PTX additions of 1, 2, 4, 6, 8, and 10 mg, respectively. The EM@nanogels exhibited an average diameter of approximately 105 nm, with a Zeta potential measuring − 13.4 ± 0.7 mV. The maximum velocity of individual neutrobots reached 16.4 μm/s. Reproduced with permission from ref [48]. Copyright 2021, The Authors, some rights reserved; exclusive licensee American Association for the Advancement of Science. Abbreviations: EM, Escherichia coli membrane; BBB, blood–brain barrier; neutrobots, neutrophil-encapsulated microrobots.

2.3. Crossing/circumventing the blood–brain barrier

The blood–brain barrier is a selective barrier composed of endothelial cells of the cerebral capillary wall, basement membrane, astrocyte end-feet, and pericytes [221–223]. To maintain cerebral homeostasis, only a few small lipophilic molecules can cross this barrier [7,17,18], significantly limiting drug delivery. Therefore, it is challenging to develop strategies for drug delivery that cross [224–227] or circumvent [8,228–230] the BBB.

2.3.1. Crossing the blood–brain barrier

Current strategies to cross the BBB mainly include: (i) carrier-mediated transport, such as glucose transporter 1 (GLUT1) [231,232] and L-type amino acid transporter 1 (Lat1) [233,234]; (ii) receptor-mediated transport, such as transferrin receptor (TfR) [235,236] and insulin receptor [237,238] (Table 3); (iii) chemical modifications, such as liposomes [239,240] and prodrug formulations [241,242]; (iv) nanocarrier systems [243,244]; (v) external-field disruption, such as focused ultrasound [33,245] and near-infrared radiation [31,93], which can effectively enhance drug diffusion into brain tissue.

As the center of the nervous system, the brain consumes nearly 20 % oxygen and glucose [50,269,270]. BBB regulates its channels to allow substantial glucose transport from blood to brain tissue. As depicted in Fig. 4**A**, Shi's group [50] controlled GLUT1-mediated glucose recycling to facilitate glycosylated nanodrug cross the BBB. Upon glucose supplementation in mice, GLUT1 recycling was triggered. The nanomedicine was injected into mice along with glucose, leading to GLUT1 overexpression on the luminal membrane as glucose enters brain tissue. The glycosylated components of nanodrugs bind to GLUT1, allowing their transcytosis across the BBB and transport into brain tissue. However, conventional methods struggle to maintain stable drug concentrations at disease sites, while high-dose systemic administration potentially induces off-target effects.

As previously discussed in Section 2.2, MNRs have demonstrated extraordinary capabilities in precise navigation, tissue penetration, and drug-loading stability in cerebral vasculature and cerebrospinal fluid, representing a promising strategy for BBB crossing. Consequently, investigating BBB crossing remains a critical challenge in developing MNR-based therapeutic strategies for brain diseases. As shown in Fig. 4**B**, Guan's group [63] fabricated magnetic liquid metal microrobots (LMMRs) by embedding Fe nanoparticles into liquid metal (gallium/indium (Ga/In) alloys) matrices. This innovative design combined the shape-adaptive properties of liquid metal with the magnetic responsivity of Fe nanoparticles, enabling effective crossing of the BBB. Initially, RMFs propelled the LMMRs

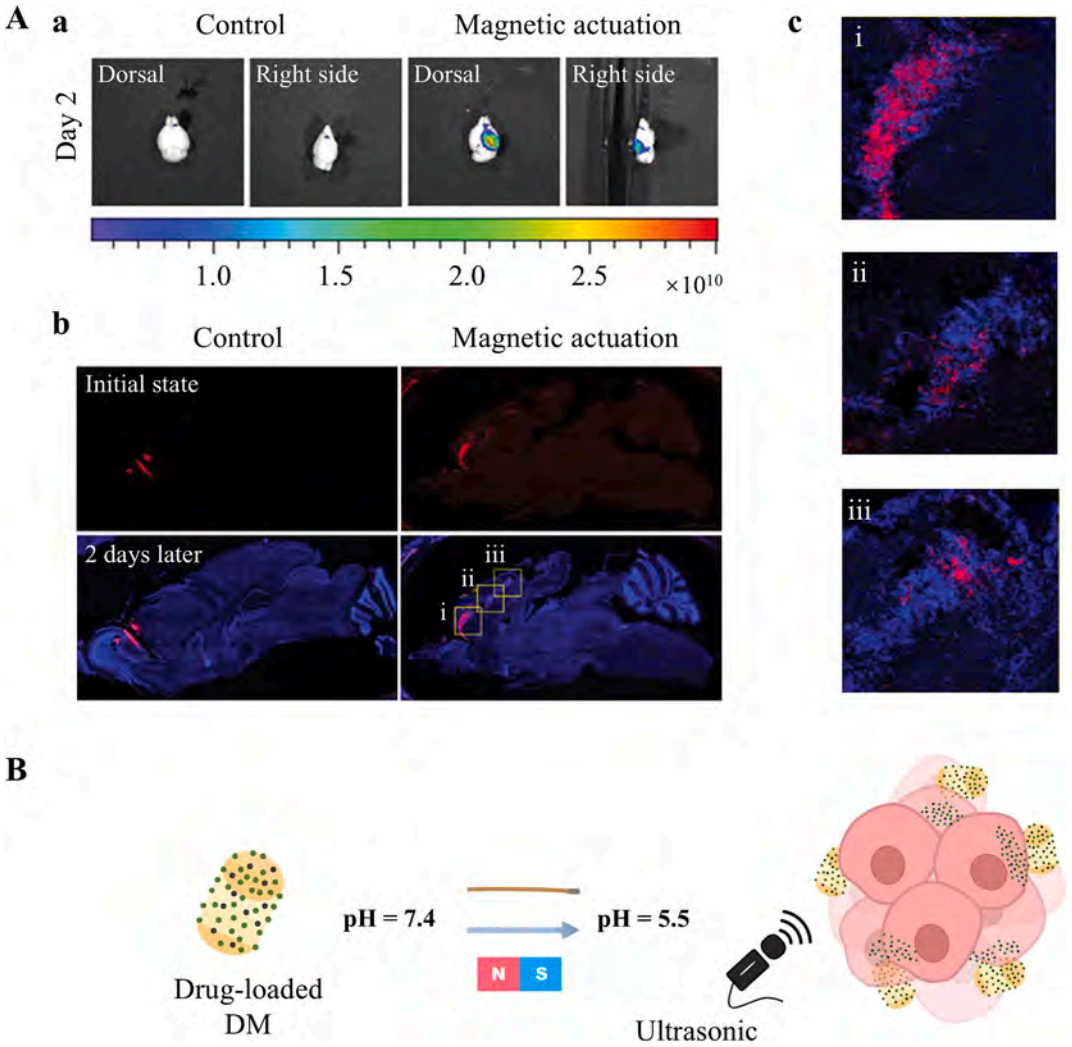

Fig. 8. Field-controlled locomotion and stimuli-responsive drug release of MNRs for brain targeting and therapy. (A) (a) Fluorescence images of the control group and experimental group in dorsal and right side after two days. (b) Immunofluorescence staining of the brain sections with (c) corresponding magnified local regions (i, ii, and iii). The HNTSCs were labeled with red fluorescence. Reproduced with permission from ref [297]. Copyright 2021, Wiley-VCH GmbH. (B) Schematic demonstration of the controlled drug release of MNRs in the brain. Under vacuum conditions, the maximum drug loading efficiency of temozolomide reached 51.22%. Under magnetic field actuation, DMs were transported to nearby brain regions via the MCR system, where ultrasonic vibration triggered drug release. The localized pH reduction further enhanced drug liberation. Reproduced with permission from ref [181]. Copyright 2024, Wiley-VCH GmbH. Abbreviation: DM, diatom microrobot.

toward BBB channels. Subsequently, under static magnetic field actuation, the LMMRs crossed the BBB through controlled shape transformation. In the brain tissue, the LMMR moves along cell membrane surfaces, inducing lipid bilayer stretching that triggers calcium ion influx and subsequent neuronal activation. The presence of LMMRs in brain tissue was confirmed through magnetic resonance imaging (MRI) characterization. Furthermore, immunostaining images of activated (c-Fos positive) cell expression demonstrated that LMMRs effectively stimulated neuronal cells, indicating maintained mobility and functionality after crossing the BBB.

As the brain inflammatory responses, the immune system actively clears foreign entities [271], and the exogenous MNRs make them susceptible to recognition and elimination [49,272]. Therefore, biomimetic camouflage of MNRs is necessary for crossing the BBB during brain inflammation. A few immune cells (such as macrophages [49,273] and neutrophils [48,274]) can cross the BBB during brain inflammation. Consequently, the components of immune cells have become superior materials for MNR biomimetic camouflage. Receptor proteins of the macrophage membrane (MM) capable of crossing the BBB and accumulating in inflammatory regions have been investigated [274–276]. As illustrated in Fig. 5**A**, Ji's group [49] designed MM-coated MNRs (MM@MnO_2-Au-mSiO_2@Cur) that successfully enter brain inflammatory regions while avoiding the disturbances of the immune system and BBB. These biomimetic MNRs were fabricated by encapsulating MnO_2-Au-mSiO_2@Cur with macrophage membranes. The Janus mesoporous silica (mSiO_2) structure serves as a Cur carrier, while the internal MnO_2 catalyzes endogenous H_2O_2 decomposition, propelling MNRs across

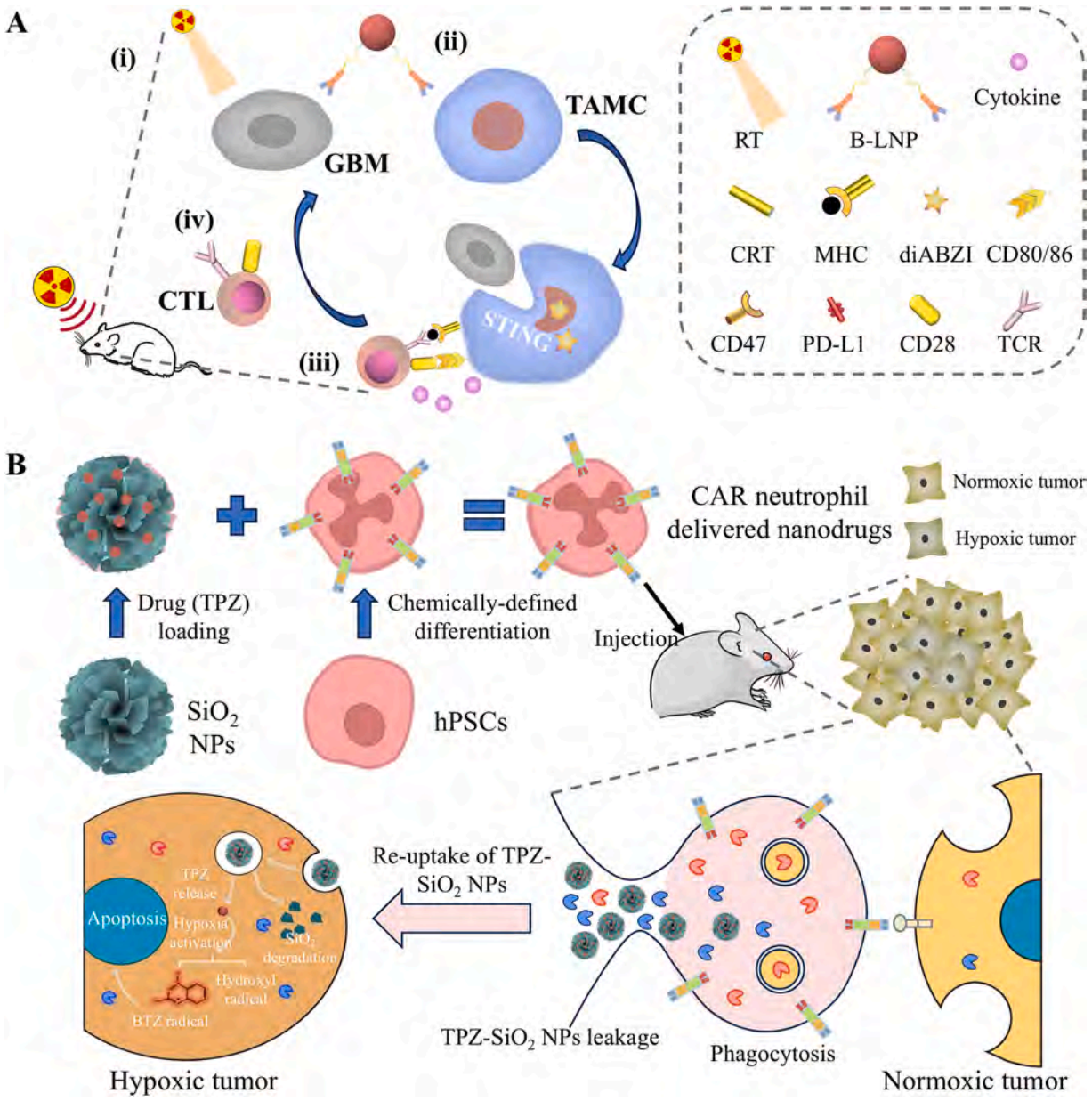

Fig. 9. Applications of drug-loaded nanosystems for targeted brain tumor therapy. (A) Illustration of the antitumor mechanism of B-LNPs. B-LNPs exhibited a uniform particle size distribution with an average diameter of approximately 90 nm and a Zeta potential of –4.41 mV. Reproduced with permission from ref [10]. Copyright 2023, The Authors. (B) Schematic demonstration of the fabrication process and the antitumor mechanism of CAR neutrophils. Fabrication process: (i) TPZ loading into mesoporous SiO_2. (ii) Chemically-defined differentiation of hPSCs. (iii) Embedding TPZ-SiO_2 NPs into hPSCs to obtian CAR neutrophils@TPZ-SiO_2 NPs. Hydrodynamic sizes of @TPZ-SiO_2 NPs was around 260.8 nm, and the maximum drug loading efficiency of TPZ reached 11.2 %. Antitumor mechanism: (i) Phagocytosis of normoxic tumor cells by CAR neutrophils@TPZ-SiO_2 NPs. (ii) Release of TPZ-SiO_2 NPs. (iii) Re-uptake of TPZ-SiO_2 NPs by tumor cells. (iv) Intracellular TPZ release from TPZ-SiO_2 NPs, inducing hypoxic tumor cell death, followed by degradation of residual SiO_2 NPs. BTZ represented benzotriazinyl. Reproduced with permission from ref [9]. Copyright 2023, The Authors. Abbreviations: GBM, glioblastoma multiforme; STING, stimulator of interferon genes; TAMC, tumor-associated myeloid cell; RT, radiation therapy; B-LNP, bridging-lipid nanoparticle; CRT, calreticulin; diABZI, STING agonist; TCR, T cell receptor; CD28, T cell activators; CD80/86, co-stimulatory factors of TAMCs; MHC, major histocompatibility complex; CTL, CD8 with T cell; TPZ, tirapazamine; hPSCs, human pluripotent stem cells.

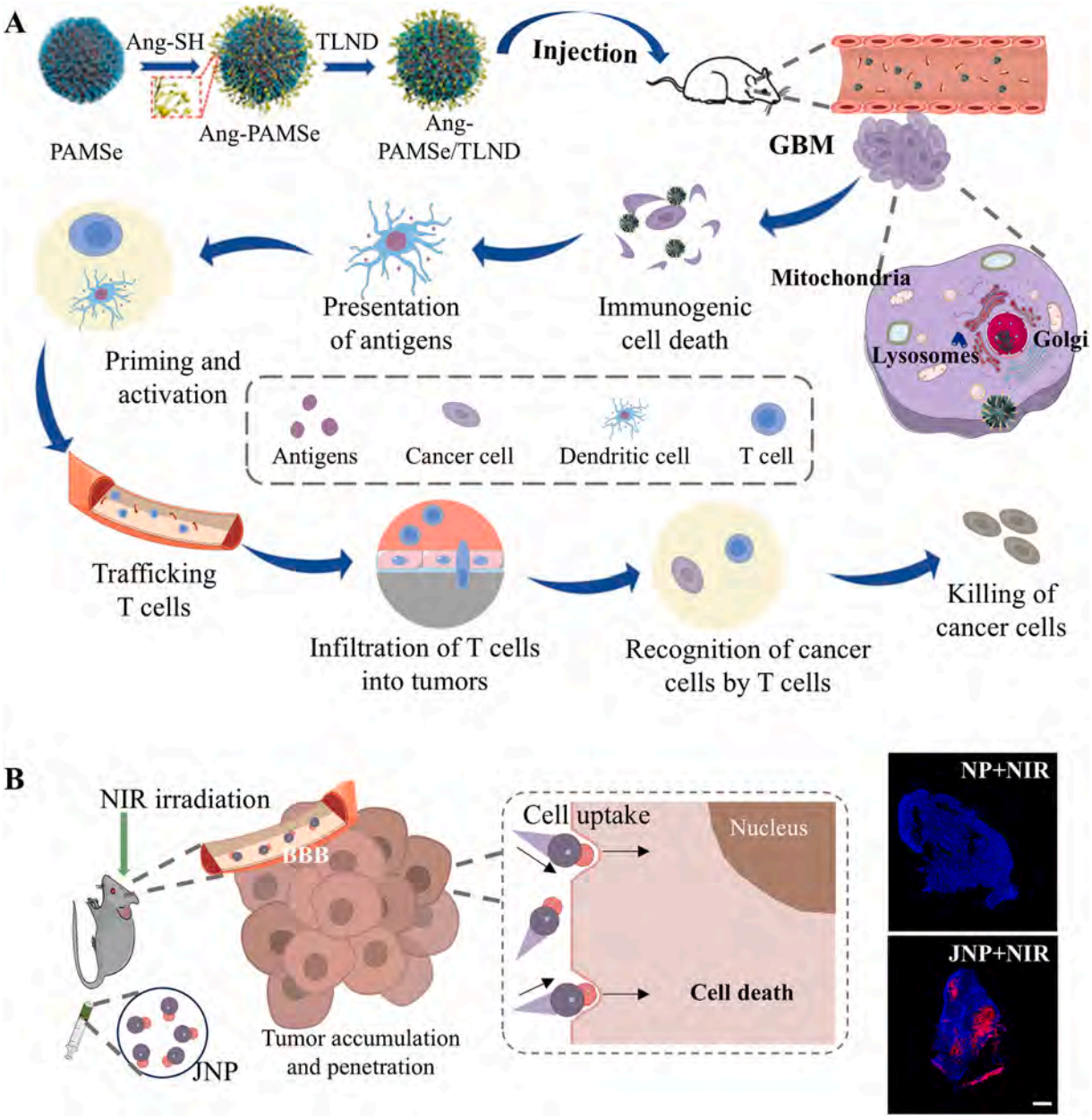

Fig. 10. Applications of intelligent MNRs for active brain tumor therapy. (A) Schematic demonstration of the fabrication process and the antitumor mechanism of Ang-PAMse/TLND. Fabrication process: (i) Polymerization of L-Arg derivatives to form PAMse, (ii) Ang functionalization of PAMse polymers, and (iii) TLND loading to obtain Ang-PAMse/TLND. Ang-PAMse demonstrated a diameter of approximately 200 nm with a Zeta potential of –34 ± 0.7 mV. The TLND achieved a loading degrees of 20.4 % and an encapsulation efficiency of 87.1 %. Antitumor mechanism: (i) Triggering immunogenic cell death, (ii) NO-mediated enhancement of antigen presentation, (iii) and T cell activation. (iv) NO-facilitated T cell trafficking. (v) NO-ROS reaction improving T cell infiltration. (vi) T cells recognized and the tumor cells. (vii) TLND targeted tumor cell mitochondria, inducing tumor cell apoptosis. Reproduced with permission from ref [56]. Copyright 2023, The Authors. (B) Schematic demonstration of the antitumor process of the JNP, and fluorescence images of sliced tumors treated with conventional drug-loaded NPs and drug-loaded JNPs under NIR irradiation. The red signals represented DOX and the blue represented DAPI. The scale bar is 100 μm. JNPs exhibited a diameter of 122.7 ± 4.4 nm, a polydispersity of 0.122 ± 0.023, and a Zeta potential of –26.8 ± 2.5 mV. The DOX loading degree of JNPs was 79.8 ± 2.6 μg/mg. Reproduced with permission from ref [55]. Copyright 2023, Elsevier B.V. All rights reserved. Abbreviations: PAMse, a NO-driven nanomotor; TLND, triphenylphosphonium lonidamine; Ang-SH, modified Angiopep-2; GBM, glioblastoma multiforme; BBB, blood–brain barrier; NIR, near-infrared radiation; JNP, a light-driven nanomotor.

the BBB. To evaluate the BBB-crossing capability of MNRs, an in vitro BBB model was established using a porous Transwell system [48,56,277]. From Fig. 5**B**, MNRs crossed the BBB membrane which is composed of brain-derived Endothelial cells.3 (bEnd.3) cells, and diffused into the lower chamber containing G422 cells (a model glioma cell) layer [48]. The number of MNRs crossing the BBB was indirectly quantified using fluorescence viability indicators through confocal laser scanning microscopy (CLSM), which reflects the activation level of lower chamber cells. As shown in Fig. 5**C**, Wan's group [56] employed in vitro BBB model to assess the crossing efficiency of angiopep-2 (Ang)-modified nanomotors (Ang-PAMSe). The CLSM imaging revealed that Ang-PAMSe exhibited higher BBB-crossing capability than both unmodified nanomotors (PAMSe) and Ang-modified NPs (Ang-PMSe). The results demonstrated that the combination of MNR motility and Ang-mediated targeting synergistically enhances BBB penetration.

2.3.2. Circumventing the blood–brain barrier

Because the BBB cannot distinguish between drugs and toxins, when drugs pass through the opened BBB, other detrimental compounds may also cross the BBB and enter brain tissue [278–280]. Moreover, certain physical and chemical stimuli can cause damage to healthy brain cells [35,281,282]. These limitations can be solved through direct drug delivery methods that circumvent the BBB [283]. Current BBB-circumventing methods primarily transport drugs through brain parenchyma [284,285], CSF [286,287], and cervical lymph nodes [288,289]. As a direct intracerebral delivery method, intraparenchymal administration effectively reduces drug loss, thereby enhancing therapeutic efficacy [290,291]. Hanes's group [292] developed brain-penetrating nanoparticles capable of rapid diffusion through brain parenchyma, which is composed of NPs coated with low molecular weight polyethylene glycol (PEG). The hydrophilicity and electrical neutrality of PEG significantly increase the number of freely diffusing NPs in brain parenchyma, reducing drug loss due to NP adsorption. Furthermore, intrathecal drug delivery strategies through the CSF can achieve high-concentration drug delivery and reduce off-target effects [293,294]. Perello's group [295] demonstrated that ghrelin can be taken up by the blood-CSF barrier cells. After injecting ghrelin, high concentrations of ghrelin were detected in the CSF, indicating that ghrelin was delivered to the brain via the CSF.

Although these BBB-circumventing strategies have demonstrated superior drug transport capabilities, their drug diffusion remains slow and uneven. The application of MNRs can effectively address these issues. Notably, the minimally invasive intranasal administration route circumvents the BBB indirectly, enabling direct drug delivery to brain tissue [296,297]. As shown in Fig. 6**A**, Choi's group [297] developed a magnetically propelled microrobot system for human nasal turbinate stem cell (HNTSC) delivery in the brain. Functionalized Fe_3O_4 NPs were integrated into HNTSCs to obtain cell-based microrobots (CellBots), which transported HNTSCs to the brain via intranasal administration under magnetic guidance. The skull marrow connects to the CSF through the dura mater, allowing intracranial injections to circumvent the BBB [298–300]. As shown in Fig. 6**B**, Liu's group [156] used an Ommaya reservoir to deliver a drug-loaded marsupial robotic system intracranially. The catheter of the Ommaya reservoir connects the intracranial cavity to the external environment through a minimally invasive approach, with its upper reservoir implanted subcutaneously for long-term intracranial injection. After injection into the reservoir, MCRs cross through the catheter to release drug-loaded nanorobots intracranially (Fig. 2), effectively circumventing the BBB. From Fig. 6**B**, computed tomography imaging simulated the cavity following GBM removal. In this cavity area, magnetically driven MCRs followed expected trajectories along the cavity edges, enabling localized drug delivery in the complex GBM microenvironment. While MNRs enhance the targeting precision of intraosseous skull administration, the safety of this strategy for cranial bone injuries remains unassessed.

2.4. Drug delivery to the brain

Compared to conventional nanocarrier-based drug delivery, MNRs with enough medication enable a shift from passive drug resistance to active treatment in brain diseases. Moreover, MNRs targeting specific tissue sites exhibit superior drug-loading stability, allowing local treatment with low drug concentrations, thereby reducing systemic toxicity and enhancing drug delivery efficiency. Besides delivering traditional drugs (such as antibiotics [301–303], anticancer drugs [304,305], anti-inflammatory drugs [49,306,307], and alkaloids [308]) to disease sites, MNRs can deliver specialized "drugs" including ions (such as Fe^{3+} [309], Ga^{3+} [209], and Ca^{2+} [310]), gases (such as NO [86,311], H_2 [160,312], and O_2 [313,314]), stem cells [315,316], embryonic cells [317], cytokines [86], and mitochondria [318]. For cerebral drug delivery, MNRs primarily move through the bloodstream to cross the BBB and reach brain tissue. As depicted in Fig. 7, Qiang He's group [48] developed neutrophil-encapsulated microrobots (neutrobots) for targeted malignant glioma therapy. These dual-functional neutrobots exhibited both magnetically driven propulsion and inflammatory factor gradient chemotaxis. Initially, under combined RMF actuation and inflammatory factor gradient chemotaxis, the neutrobots navigate through the bloodstream toward the BBB. Subsequently, they leverage inherent neutrophil properties to traverse the BBB. Finally, the nanorobots deliver PTX directly to malignant glioma.

As previously discussed in Section 2.3, HNTSCs can circumvent the BBB through MNR-mediated delivery to brain tissue. As shown in Fig. 8**A**, Choi's group [297] used fluorescence imaging to show that non-magnetically actuated CellBots (control group) primarily accumulated in nasal cavities, while magnetically actuated CellBots exhibited significant dispersion in brain tissue. Moreover, immunofluorescence staining was performed on brain tissue sections at different times. The control group exhibited red fluorescence signals localized in the nasal cavity, indicating failed HNTSC delivery. In contrast, the experimental group demonstrated red fluorescence signals in brain regions, with signal intensity decreasing gradually from proximal to distal brain regions (i > ii > iii), demonstrating successful HNTSC delivery to the brain. Consequently, this BBB-circumventing drug delivery strategy demonstrates exceptional potential for clinical translation in precise therapy of brain diseases.

To reduce drug loss during delivery, strict requirements have been established for controlled drug release systems. Previous research works have demonstrated that MNRs can achieve controlled drug release through various triggered mechanisms, including

external triggers (such as magnetic fields [177,319,320], ultrasound [321,322], temperature [323–325], and light [326–328]), internal environmental triggers (such as pH [329–331] and enzymes [332–334]), and combined stimulus triggers [181,335]. As illustrated in Fig. 8**B**, Jiao's group [181] developed diatom microrobots (DMs) for controlled drug release in brain therapy. They implemented a dual-trigger strategy combining ultrasound and pH responsiveness: ultrasonic cavitation disrupted the DM outer structure to initiate drug release, while the acidic microenvironment (pH = 5.5) further enhanced drug liberation. Given the vulnerability of brain tissue, controlled drug release from MNRs requires attention to reduce adverse effects and develop trigger mechanisms specifically adapted to the cerebral microenvironment.

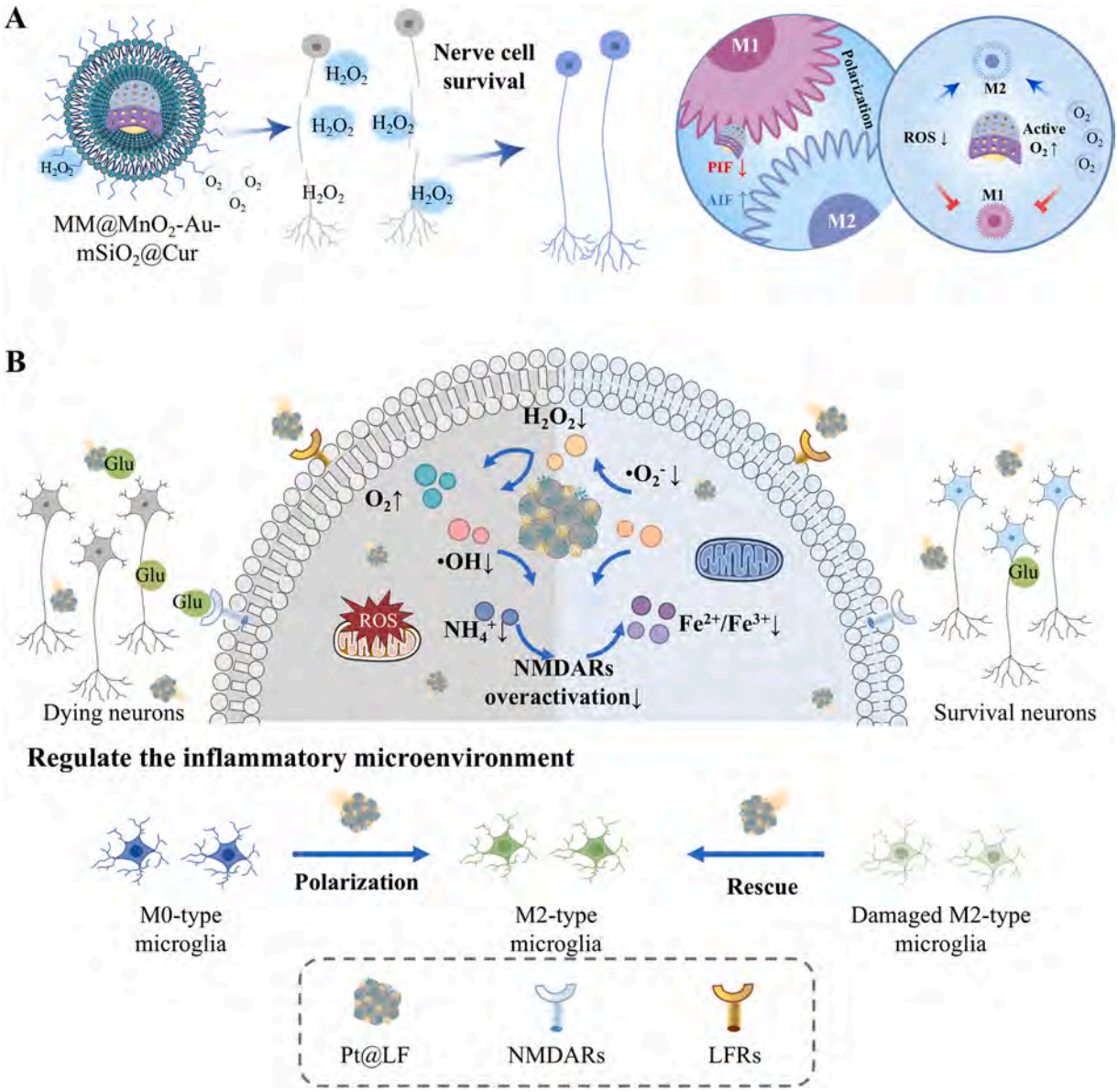

Fig. 11. Applications of intelligent MNRs for active neuroinflammation therapy. (A) Schematic illustration of the neuron recovery process of the MM@MnO_2-Au-mSiO_2@Cur. MM@MnO_2-Au-mSiO_2@Cur modulates macrophage phenotype switching through O_2 generation and Cur release. MM@MnO_2-Au-mSiO_2@Cur exhibiedt a diameter of approximately 100 nm with a Zeta potential of –10.3 mV.Reproduced with permission from ref [49]. Copyright 2024, The Authors. Advanced Science published by Wiley-VCH GmbH. (B) Schematic representation demonstrated that Pt@LF regulated the inflammatory microenvironment and recovery neuron. Hydrodynamic sizes of Pt@LF was 62.85 ± 1.12 nm, and its Zeta potential was 16.5 ± 1.12 mV. Upon entering cerebral inflammatory microenvironments, Pt@LF protects M2 macrophages and promotes M0/M2 polarization, restoring neurons through Fe ion/NH_4^+/ROS depletion, reducing glutamate release, and inhibiting NMDAR activation. Reproduced with permission from ref [57]. Copyright 2024, Wiley-VCH GmbH. Abbreviations: MM, macrophage membrane; Cur, curcumin; ROS, reactive oxygen species; PIF, Pro-inflammation; AIF, Anti-inflammation; MM@MnO2-Au-mSiO2@Cur, biomimetic Cur-loaded self-propelled nanomotors; LFRs, LF receptors; NMDARs, N-methyl-D-aspartate receptors; Glu, glutamate.

Overall, current MNRs for drug delivery in the brain face three main challenges: (i) Efficient and precise navigation: The macroscopic scale of the brain contrasts with the microscale movement of MNRs, which leads to long-term transportation for MNRs. For deep brain tissue, such as brain tumors, MNR penetration depth directly determines drug delivery precision. Moreover, real-time monitoring can effectively guide the movement trajectory of the MNR, directly affecting the navigation accuracy of the MNR. Due to the tiny size of MNR, the existing imaging technologies lack enough temporal resolution for tracking MNRs [88]. (ii) Overcoming the resistance of BBB: Current strategies primarily focus on enhancing BBB permeability or biomimetic traversal, with insufficient exploration of BBB circumventing. Intranasal or transcranial delivery could circumvent the BBB entirely, preventing the entrance of harmful substances.

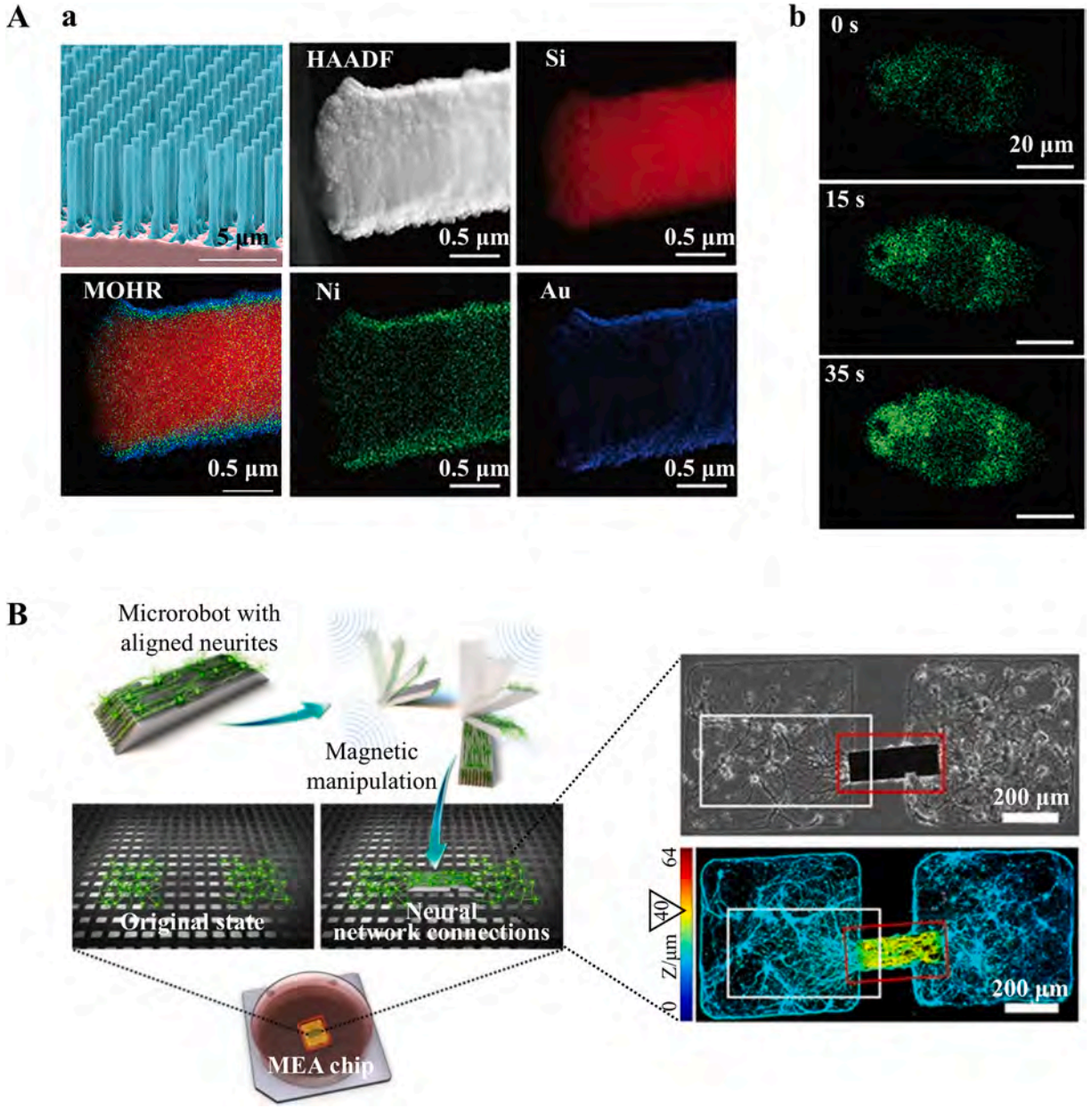

Fig. 12. Applications of intelligent MNRs for active brain stimulation and neuronal connection. (A) (a) Scanning electron microscopy images of MOHRs (with a scale bar of 5 μm) and EDX mapping (with a scale bar of 0.5 μm). The MOHRs exhibited a rod-like morphology with an average length of approximately 7 μm and a mean diameter of 0.8 μm. (b) Fluorescence images showing MOHR-induced Ca^{2+} activation over increasing laser irradiation time. Ca^{2+} was labeled with green fluorescence. The scale bar is 20 μm. Reproduced with permission from ref [398]. Copyright 2023, Wiley-VCH GmbH. (B) Schematic of microrobot-mediated neuronal cluster repair on MEA chips (left). Bright-field and height-coded confocal fluorescence microscopy images of hippocampal neurons (right). Neurites: green, neuron nucleus: blue. The Scale bar is 200 μm. Reproduced with permission from ref [404]. Copyright 2020, The American Association for the Advancement of Science. Abbreviations: HAADF, highangle annular dark field; MOHR, manipulated optoelectronic hybrid microrobots; MEA, multi-electrode array.

However, intranasal administration faces diffusion barriers from mucosal layers, while transcranial approaches require further safety validation. (iii) Drug delivery and controlled release: Drug-loading stability of MNRs directly affects the drug delivery efficiency, yet the cerebral complex microenvironment can easily lead to drug leakage or inactivation. Additionally, limited drug loading capacity due to the micro size of MNR necessitates advanced loading strategies. Crucially, achieving spatiotemporally controlled drug-releasing remains necessary for lengthening the therapeutic effect and retention time of drugs in cerebral tissues.

2.5. *Material design considerations for intracranial micro/nanorobots*

According to the previous discussion, MNRs for brain drug delivery have characteristics such as controllable rapid movement, BBB overcoming, and local drug delivery. Beyond these basic functions, clinical applications impose critical material design requirements

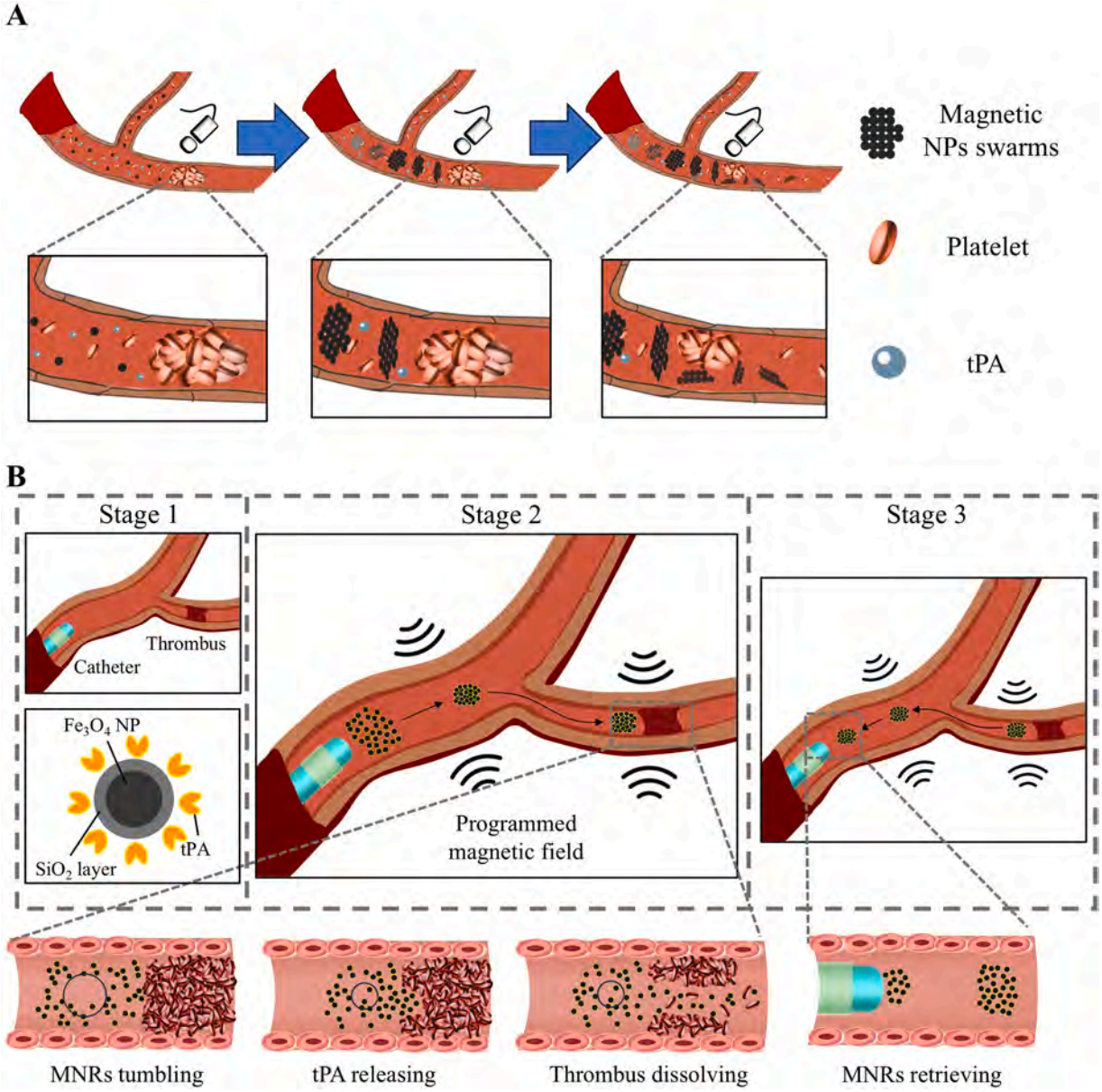

Fig. 13. Applications of intelligent MNRs for active thrombolysis and ischemic stroke therapy. (A) Schematic representation demonstrated that magnetic NPs swarms deliver tPA for enhanced thrombolysis. Reproduced with permission from ref [411]. Copyright 2021, Wiley-VCH GmbH. (B) Schematic diagram revealed that tPA-anchored nanorobots can generate retrievable magnetic colloidal microswarms and dissolve submillimeter vascular thrombus. Reproduced with permission from ref [340]. Copyright 2024, The American Association for the Advancement of Science. Abbreviations: tPA, tissue plasminogen activator; MNRs, micro/nanorobots.

for intracranial MNRs. The human immune system can recognize and eliminate antigenic foreign substances, which determines that MNR needs to have good biocompatibility. Some liposomes can cross through BBB. They can control drug release after modification, becoming excellent substrate material for MNR [108]. Moreover, the strategy of biological camouflage using cells or cellular components enables the surface of MNR to have some of the functions of cells, allowing it to naturally cross BBB without external triggers while avoiding immune clearance. Currently, the main disguises of camouflage MNRs in the brain are neutrophils [48] and macrophages [321], with future development potential for red blood cells [336], stem cells [337], and tumor cells [338]. However, biocompatibility alone remains insufficient for intracranial MNRs. The accumulation of the nondegradable substrate materials of MNR can cause toxicity and inflammation in the brain. For this reason, the main material of MNRs usually needs to be degradable. For instance, Zn [329] or Mg-based [160] bubble-propelled MNRs, gradually decompose without being harmless in a liquid environment. Furthermore, Stimuli-responsive hydrogel MNRs also show promise for controlled release. Xu's group [339] developed a magnetic-responsive hydrogel robot for the treatment of brain tumors. The hydrogel was decomposed through magnetic stimulation after MNRs targeted brain tumors achieving precise local drug delivery. In addition to degradation, recycling is also a strategy to deal with the accumulation of foreign particles. After using MNR to eliminate thrombosis, Zhang's group [340] successfully recovered magnetic MNR with a catheter under a magnetic field after thrombus dissolution, preventing the accumulation of magnetic NPs.

The size of MNRs must be small enough to move in the biological environment and to come into contact with molecules and cells [320]. Nanoparticles larger than 200 nm generally fail to cross the BBB [100], limiting the size of larger MNRs. However, MNRs that are too small (<10 nm) restrict their drug loading capacity [323] and are difficult to manipulate by the magnetic field and to visualize

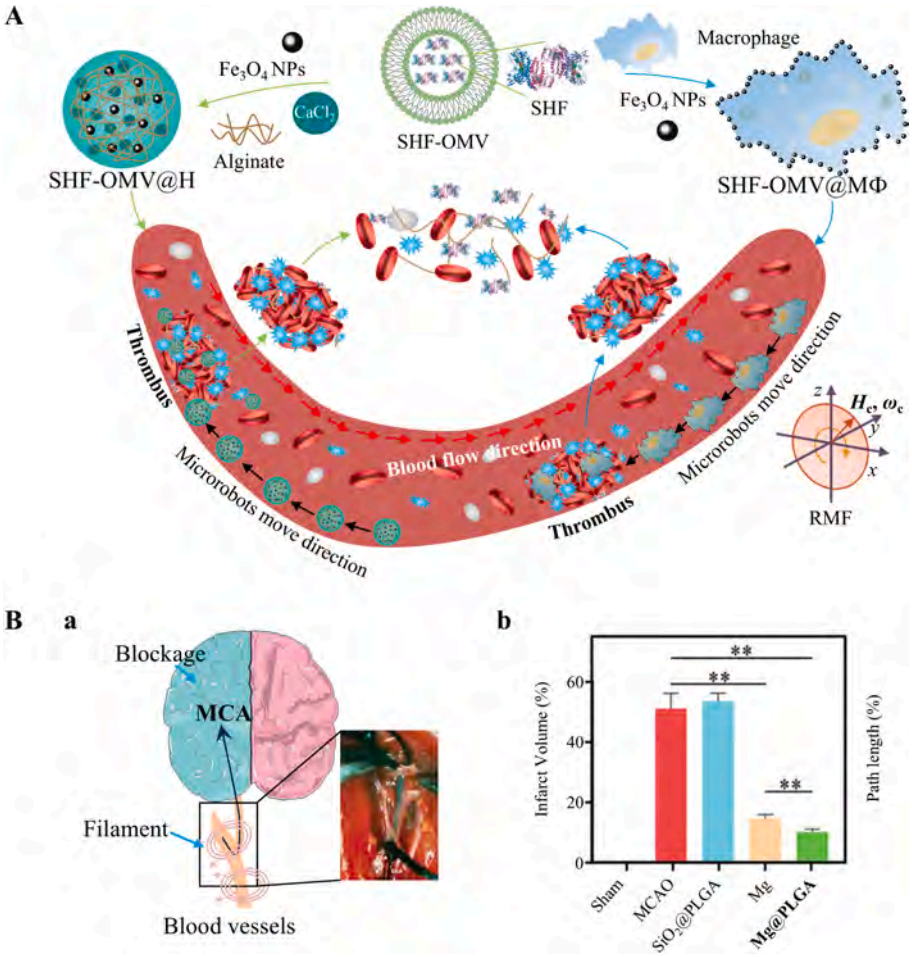

Fig. 14. Applications of intelligent MNRs for active synergistic ischemic stroke treatment. (A) Schematic illustration of SFH-OMV-based microrobots for thrombus treatment. SFH-OMV@H comprised SFH-OMV and hydrogel, while SHF-OMV@MΦ consisted of SFH-OMV and macrophages. These two types of SFH-OMV exhibited comparable size (approximately 86–89 nm) and Zeta potential (around –7mV). Reproduced with permission from ref [321]. Copyright 2024, Wiley-VCH GmbH. (B) (a) MCAO rat model established by filament ligation of MCA ends. (b) Quantification of infarct volume/ischemic brain hemisphere after seven days (n = 5) treatment. **p < 0.01. Sham: control group without arterial occlusion; Si@PLGA: control group with incompletely PLGA-coated SiO_2. Reproduced with permission from ref [160]. Copyright 2021, Wiley-VCH GmbH. Abbreviation: SFH, staphylokinase-hirudin fusion protein; SFH-OMV, SFH-antithrombotic outer membrane vesicle; RMF, rotating magnetic field; MCA, middle cerebral artery.

[41]. Operating at micro/nanoscales, MNRs exhibit motion patterns fundamentally distinct from macroscopic movement, making them difficult to move in low Reynolds numbers liquid environments [182,341]. The Reynolds number reflects the ratio of fluid inertia to viscous force. Viscous friction dominates the movement of objects with negligible inertia at low Reynolds numbers. Once the MNRs stop driving without energy input, they will stop moving [342]. Consequently, the material design of MNRs needs to enable them to overcome the viscous resistance inherent to low Reynolds numbers. In brain applications, MNRs can adapt to specific environments depending on their shapes. Most common nanoparticles are spherical, leading to a spherical MNR based on such nanoparticles [166,343]. This shape gives MNRs the advantage of being easy to modify and combine with cell membrane components. Rod-shaped NPs exhibit stronger brain endothelial adhesion and enhanced cerebral accumulation [344]. Moreover, the interaction between rod-shaped MNR and the brain endothelium directly affects the absorption of particles by cells. Their high-curvature tips concentrate positive charges [345], while positively charged particles are more easily absorbed by cells than negatively charged or neutral NP-based MNRs [346]. However, positively charged particles can lead to potential ROS generation and cellular damage, necessitating rigorous safety validation for rod-shaped MNR charge loading. Further, ciliary-type MNRs employ a hair-like extension pattern to overcome the viscous resistance of the fluid environment in the brain [347]. For specific applications, such as stroke-induced vascular occlusion, helical MNRs imitate the rotational movement of screws to penetrate thrombi efficiently, mechanically disrupting them [348,349]. To reply to the hindrance of BBB, some MNRs with deformation capabilities have also attracted attention. As shown in Fig. 4B, deformable MNRs (LMMRs) utilize the highly flexible deformation [350] and near-zero Young's modulus [351] of liquid metal to adaptively cross the BBB. Thus, the size and shape of MNRs can be specifically designed according to their intended applications.

3. Micro/nanorobotic therapy of brain diseases

3.1. Brain tumor

Current tumor therapies primarily include radiation therapy (RT) [352–354], chemotherapy [355–357], and immunotherapy [358–360]. Among these, immunotherapy preserves normal cells while reducing systemic side effects [361]. In the GBM microenvironment, a majority of myeloid compartments exhibit immunosuppressive and tumor-supportive properties, significantly compromising antitumor immune responses [10,362]. Furthermore, the BBB presents a selective barrier to drug delivery for GBM therapy, posing major challenges for cerebral immunotherapy applications. As previously discussed, nanocarriers have demonstrated remarkable capabilities in drug loading, reduced systemic toxicity, and BBB penetration, significantly enhancing targeted drug delivery to the brain. There are a large number of tumor-associated myeloid cells (TAMCs) with immunosuppressive effect in GBM, but insufficient infiltrating effector T cells [363]. Therefore, therapeutic strategies for the treatment of brain tumors primarily are GBM-related TAMCs. Activation of the stimulator of interferon genes (STING) pathway reprograms TAMCs, enhancing their antitumor immune functions [364,365], which has shown promising trends in targeted tumor therapy. Lesniak's group [10] developed dual-targeting cluster of differentiation (CD)47/programmed cell death-ligand (PD-L)1 (checkpoint molecules) bridging-lipid nanoparticles (B-LNPs) that selectively activate STING while reducing T cell suppression. As shown in Fig. 9**A**, the antitumor mechanism of B-LNPs can be described in four sequential steps: (i) Initially, RT induced upregulation of pro-phagocytic signals calreticulin (CRT) and CD47 in GBM. (ii) Next, B-LNPs connected GBM and TAMCs through CD47/PD-L1 binding, effectively blocking checkpoint molecules. (iii) Subsequently, the diABZI (STING agonist) carried by B-LNPs acted on TAMCs, synergistically triggering T cell activation and infiltration. (iv) Finally, T cell-mediated antitumor responses were accelerated by reprogrammed TAMCs, leading to the reduction of GBM cells. As previously discussed in Section 2.3, neutrophils can cross the BBB due to their native properties. Fig. 7 demonstrates that neutrophil-mediated drug delivery significantly enhances targeting specificity, offering substantial potential for GBM immunotherapy. Bao's group [9] engineered chimeric antigen receptor (CAR)-modified neutrophils to deliver nanodrugs for targeted GBM therapy. As illustrated in Fig. 9**B**, they developed CAR neutrophils@TPZ-SiO_2 NPs by embedding tirapazamine (TPZ)-loaded mesoporous SiO_2 NPs into chemically-defined differentiated human pluripotent stem cells (hPSCs). Upon injection into mice, CAR neutrophils@TPZ-SiO_2 NPs initially attacked and phagocytosed normoxic tumor cells. Subsequently, TPZ-SiO_2 NPs were released and rea-uptaken by tumor cells. Finally, TPZ was released in the hypoxic tumor microenvironment, inducing normoxic tumor cells to transform into hypoxic states and apoptosis.

GBM formation in the brain creates a microenvironment characterized by high concentration ROS and inducible nitric oxide synthase (iNOS) [56,366,367], presenting significant challenges for conventional nanocarrier-based drug delivery. As discussed in Section 2.4, self-propelled MNRs capable of transporting gases (such as NO [311], H_2 [160], and O_2 [313]) offer an effective solution to excessive ROS and iNOS. Under iNOS catalysis, arginine (Arg) can react with ROS to generate NO [83,368,369]. The concentration gradients of ROS and iNOS allow MNRs to chemically respond to the GBM microenvironment for targeted drug delivery. As illustrated in Fig. 10**A**, Wan's group [56] developed a NO-driven nanomotor (PAMse) fueled by L-Arg derivatives. PAMse was synthesized through L-Arg derivatives monomer polymerization and functionalized with Ang peptides, followed by loading with triphenylphosphonium lonidamine (TLND) to fabricate Ang-PAMse/TLND. Upon injection into mouse brains, Ang-PAMse/TLND crossed the BBB via Ang recognition. Subsequently, as Ang-PAMse/TLND infiltrated tumor tissue, TLND targeted tumor cell mitochondria, inducing tumor cell apoptosis. A high concentration of H_2O_2 is another important feature of the GBM microenvironment [370]. Self-propelled MNRs that use H_2O_2 as fuel can simultaneously eliminate high concentration of H_2O_2 and excess ROS. Qiang He's group [161] developed a drug delivery system (Trojanbot) based on catalase-driven nanobots (CatNbot) and neutrobots for targeted GBM therapy. CatNbot was fabricated by encapsulating DOX-loaded collagen nanoparticles in bacterial membrane vesicles. Under this biomimetic camouflage, neutrophils internalize CatNbot to obtain the Trojanbot. Take advantage of neutrophil chemotaxis [48], Trojanbot crosses the BBB and reaches the GBM. Subsequently, inflammatory stimuli trigger Trojanbot to release CatNbots. CatNbots catalyze the decomposition of

H_2O_2, allowing them to penetrate the tumor and deliver DOX to the core of GBM.

As previously discussed in Section 2.2, magnetic propelled MNRs exhibit superior controllability and deep tissue penetration [63,166,167]. However, inorganic magnetic propelled MNRs are easily recognized and phagocytized by immune cells [371], making it necessary to modify their surface to avoid the immune response. Xu's group [339] fabricated magnetic hydrogel microrobots by encapsulating magnetic NPs in drug-loaded biohybrid blood hydrogel fibres. During in vivo experiments in porcine models, the microrobots were navigated to intracranial tumor. Then, intensification of the applied magnetic field triggered biohybrid blood hydrogel fibre structural disintegration, enabling localized DOX release for targeted tumor therapy. Furthermore, non-invasive photothermal therapy can synergistically enhance tumor treatment efficacy. NIR light can not only propel MNRs but also induce tumor cell apoptosis [55,372,373]. Tu's group [55] developed a light-driven nanomotor (JNP) co-loaded with photothermal agent ICG and chemotherapeutic DOX for combined GBM therapy. As shown in Fig. 10**B**, JNPs crossed the BBB and accumulated in tumor tissue under NIR irradiation. Additionally, the motility of JNP demonstrated a positive correlation with NIR irradiation power, showing excellent controllability. As JNPs were uptaken by tumor cells, the combined photothermal effect and DOX's pharmacological action induced tumor cell death. Compared to the non-light-driven control group (NP + NIR), NIR-driven JNPs (JNP + NIR) exhibited deeper DOX fluorescence signal (red) penetration in tumors, indicating better tissue infiltration.

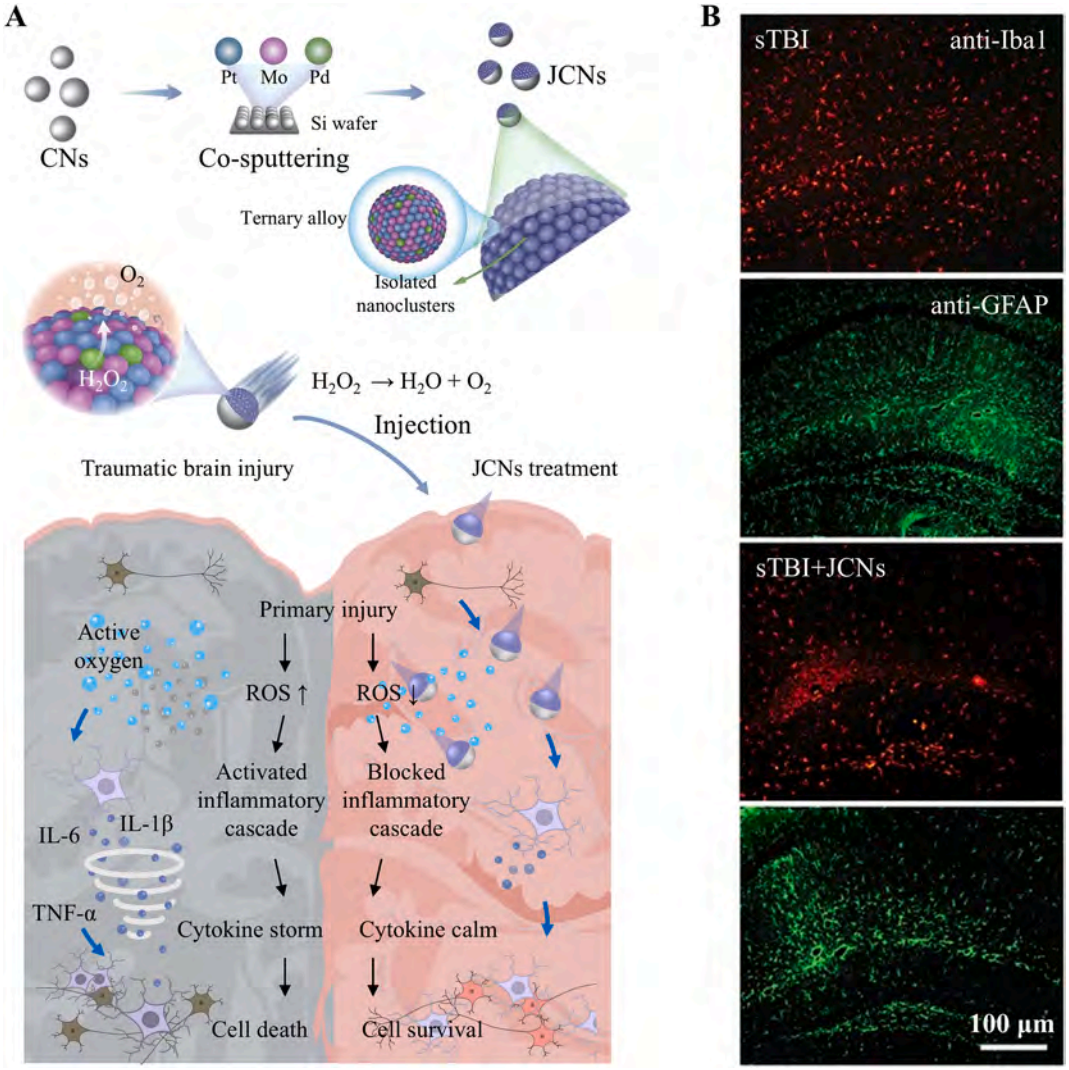

Fig. 15. Applications of intelligent MNRs for active traumatic brain injury therapy. (A) Schematic illustration of the fabrication process and the therapy mechanism of JCNs. (B) Immunofluorescence co-staining of TBI-model mice using CLSM after 1 day post injury with JCNs and control group. Green: astrocytes were labeled by glial fibrillary acidic protein. Red: microglia were labeled by ionized calcium binding adaptor molecule 1 (Iba-1). The scale bar is 100 μm. Reproduced with permission from ref [159]. Copyright 2022, Wiley-VCH GmbH. Abbreviations: CNs, carbonaceous nanospheres; JCNs, self-propelled nanomotors; GFAP, glial fibrillary acidic protein; Iba-1, ionized calcium binding adaptor molecule 1; sTBI, severe traumatic brain injury.

3.2. Neuron recovery and regeneration

Neuronal damage and loss can lead to a series of severe physiological and pathological consequences, affecting the structure and function of the nervous system [374,375]. Current neuronal therapeutic methods include pharmacological interventions [376–378], stem cell transplantation [297,379], and brain stimulation [380–382]. Zhang's group [383] developed a switchable gene-chemical co-delivery system based on drug-loaded NPs for neurodegenerative disease treatment. The NPs crossed the BBB and escaped from lysosomes/endosomes via protonation of the poly-(carboxybetaine), releasing α-synuclein (α-syn) siRNA (siSNCA), followed by Cur release in the high-ROS microenvironment. The released Cur and siSNCA synergize to recover neuronal function. Axonal regeneration in neurons occurs very slowly [384]. In the neuronal deficiency regions, distal axons have limited regenerative capacity exhibit limited capacity, and this deficit may result in neuroma formation [385–387]. Kumbar's group [388] developed a porous chitosan sponge conduit scaffold to bridge injured neurons and facilitate drug delivery. The scaffold, composed of a composite structure of chitosan and halloysite nanotubes, showed exceptional drug-loading capacity. The scaffold delivered 4-aminopyridine to accelerate neuronal regeneration, while its aligned microtubular structure guided directional axon regeneration.

Conventional drug delivery faces limitations such as systemic administration and low BBB penetration, as previously discussed. Therefore, intelligent nanocarrier systems are essential for targeted drug delivery. Neuroinflammation is typically accompanied by excessive ROS production, while neurons are particularly vulnerable to hypoxic conditions exacerbated by ROS accumulation

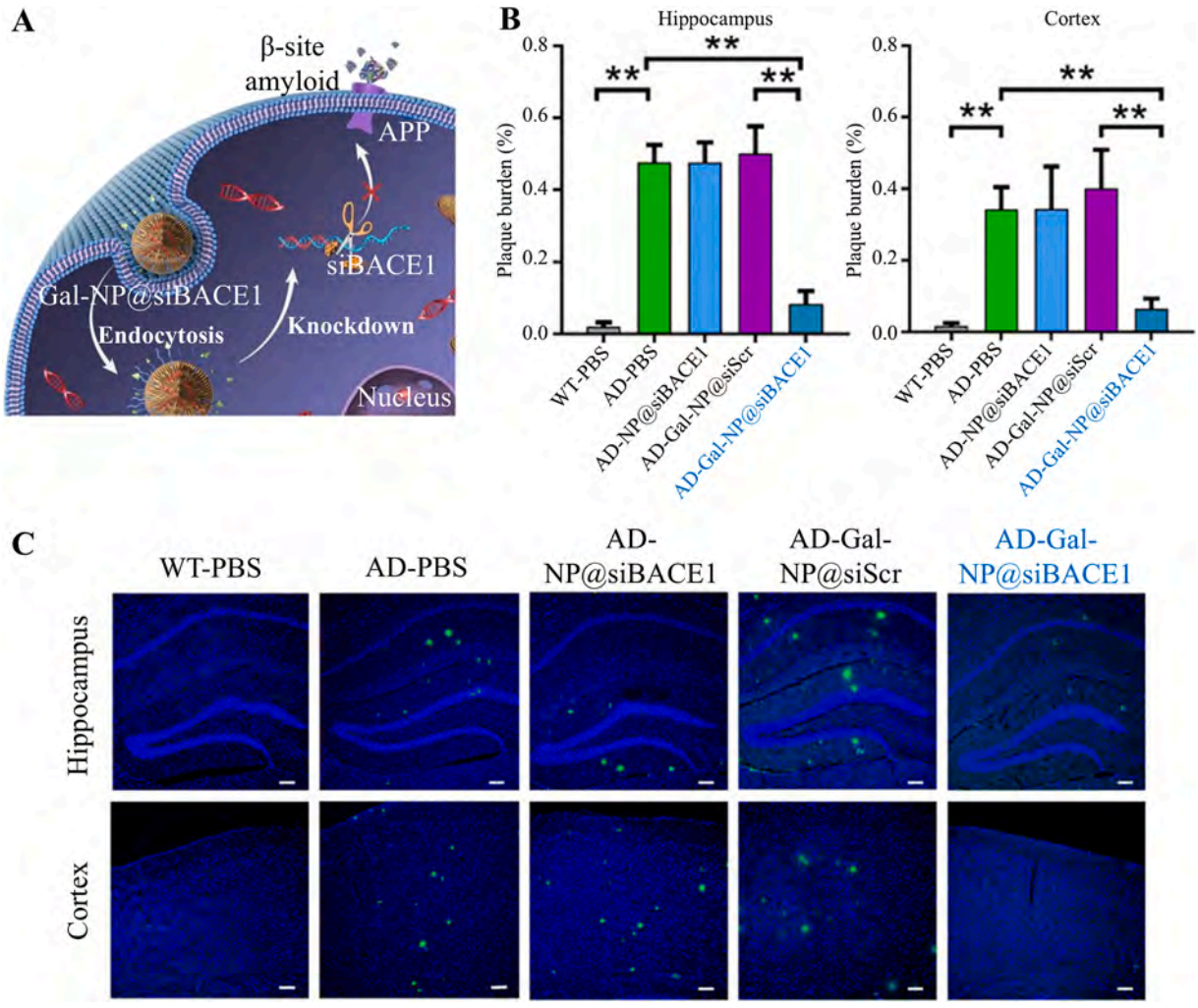

Fig. 16. Applications of drug-loaded nanosystems for targeted neurodegenerative disease therapy. (A) Schematic representation demonstrated Gal-NP@siRNA knockdown BACE1 mRNA. (B) Amyloid plaque burden in hippocampal (left) and cortical (right) regions. WT-PBS: healthy controls; AD-PBS: untreated AD controls; AD-NP@siBACE1: unmodified NP controls; AD-Gal-NP@siScr: non-targeting siRNA controls. (C) CLSM images of hippocampal (up) and cortical (down) sections. Nucleus was labeled with green fluorescence, while Aβ was labeled with green fluorescence. The scale bar is 100 μm. Reproduced with permission from ref [50]. Copyright 2020, The American Association for the Advancement of Science. Abbreviations: APP, amyloid precursor protein; siBACE1, β-site amyloid precursor protein cleaving enzyme-1 small interfering RNA; WT, wild-type; PBS, phosphate-buffered saline.

[389,390]. To resolve this, Ji's group [49] designed MM@MnO_2-Au-mSiO_2@Cur (fabrication process illustrated in Fig. 5**A**) for targeted neuroinflammation therapy. As shown in Fig. 11**A**, MM@MnO_2-Au-mSiO_2@Cur catalyzed endogenous H_2O_2 decomposition, generating O_2 bubbles that propelled it toward damaged neurons and alleviated local hypoxia. Subsequently, the O_2 bubbles and released Cur synergistically promoted macrophage polarization from pro-inflammatory (M1) to anti-inflammatory (M2) phenotypes, facilitating neuronal repair. Additionally, ferroptosis induced by ischemic stroke is another critical factor in neuronal damage [391–393]. Reduced expression of ferroportin 1 leads to iron accumulation, indirectly causing overactivation of N-methyl-D-aspartate receptors (NMDARs) and subsequent excitotoxic neuronal death [57,394]. Lactoferrin (LF) effectively chelates iron, significantly inhibiting ferroptosis. Sha's group [57] developed biomimetic MNRs (Pt@LF) by combining LF with platinum (Pt) nanoclusters. The Pt nanozyme metabolized excess ROS into O_2, serving as the propulsion source for Pt@LF. From Fig. 11**B**, Pt@LF entered inflammatory microenvironments, where LF consumed Fe ions and NH_4^+, reducing glutamate release and inhibiting NMDAR activation. Additionally,

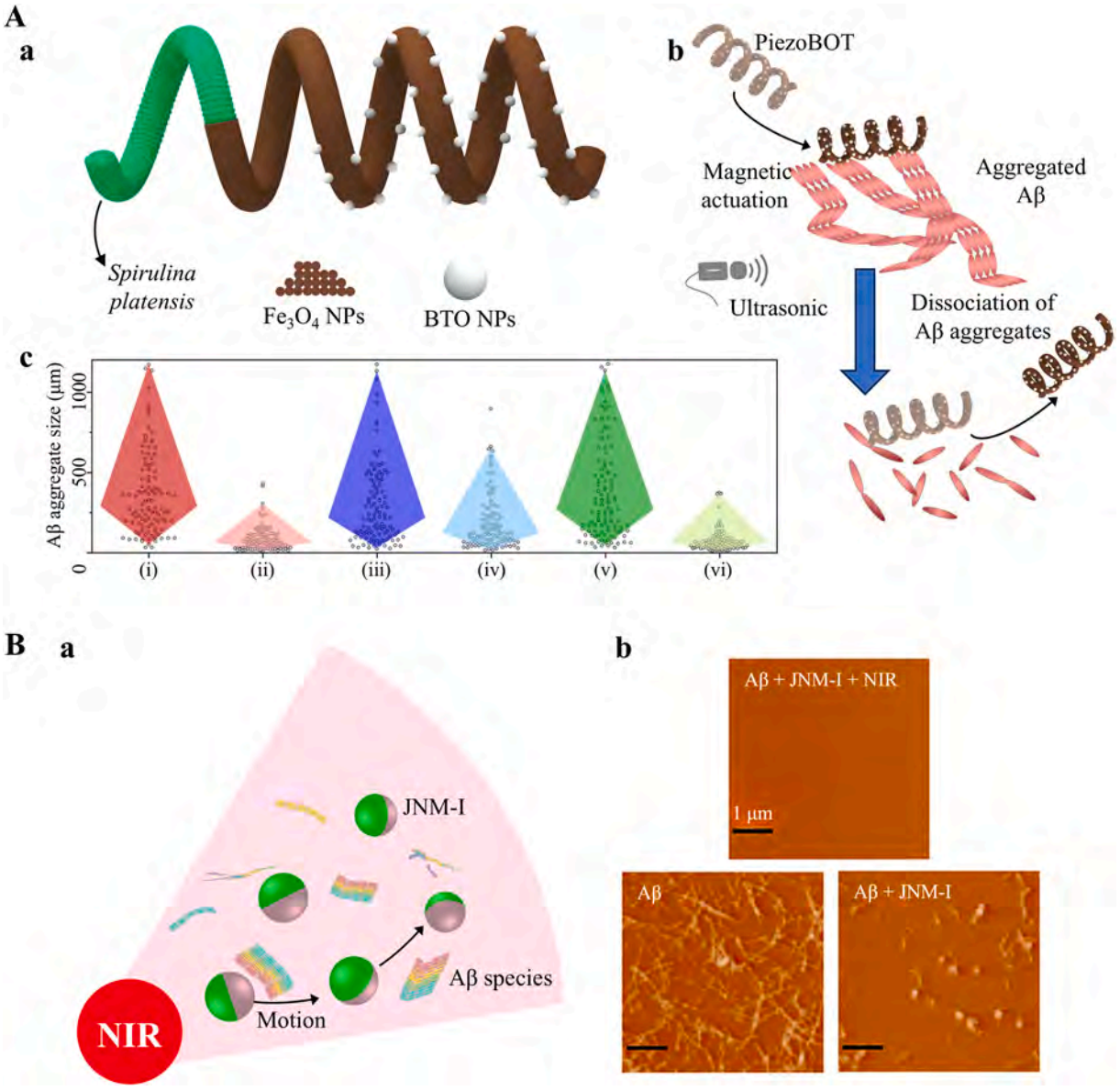

Fig. 17. Applications of intelligent MNRs for active neurodegenerative disease therapy. (A) (a) Schematic illustration of the structure of PiezoBOT. (b) Schematic representation demonstrated PiezoBOT dissociate Aβ. (c) The histogram demonstrated Aβ aggregation size across different environments. i: Aβ + BTO; ii: Aβ + BTO + ultrasound stimulation; iii: Aβ-only; iv: Aβ + ultrasound stimulation; v: Aβ + PiezoBOT; vi: Aβ + PiezoBOT + ultrasound stimulation. Reproduced with permission from ref [468]. Copyright 2023, The Authors. (B) (a) Schematic representation demonstrated JNM-I dissociate Aβ under the excitation of NIR. (b) AFM images of Aβ (25 μM) incubated with JNM-I under NIR irradiation. Reproduced with permission from ref [476]. Copyright 2020, American Chemical Society. Abbreviations: BTO, barium titanate; PiezoBOTs, NP-based microrobots; NIR, near-infrared radiation; Aβ, β-amyloid; JMN-I, a light-propelled nanomotor.

Pt@LF scavenged excess ROS to generate oxygen, promoting M0/M2 macrophage polarization and alleviating local hypoxia. Overall, this LF delivery strategy effectively restored neuronal function.

Brain stimulation lacks specificity and requires craniotomy, posing potential side effects. Photosensitive nanomaterials exhibit multifunctionality and high biocompatibility, enabling targeted delivery through surface modifications [395–397]. Photosensitive-based MNRs enable minimally invasive brain stimulation, circumventing the need for traditional craniotomy procedures. As shown in Fig. 12**A**, Li's group [398] synthesized magnetically driven manipulated optoelectronic hybrid microrobots (MOHRs) for precise neuronal targeting. Energy dispersive X-ray (EDX) mapping revealed a Si base layer, followed by Ni and Au layers in MOHRs. The MOHRs transformed optical signals into electrical signals under photostimulation, effectively stimulating neurons, with calcium flux indicating neuronal excitation levels. As the laser irradiation proceeded, more Ca^{2+} (green) were progressively activated, demonstrating sustained neuronal stimulation by MOHRs. Consequently, MNR-mediated delivery holds significant promise for advancing brain stimulation therapies.

Neuronal connectivity forms the foundation of nervous system function, crucial for information transmission, learning, memory, and behavioral regulation [399,400]. A number of researchers have employed physical and chemical methods to guide neurite outgrowth for neuronal connections in vitro neural network restoration [401–403]. However, these methods face limitations in spatial resolution and precision at microscopic scales. As previously discussed in Section 2.4, magnetically driven MNRs have demonstrated exceptional stem cell transport capabilities and precise brain targeting, showing potential for neural circuit repair. For this purpose, Choi's group [404] developed 3D magnetically driven microrobots as "bridges" for neural network repair. As illustrated in Fig. 12**B**, microrobots carrying aligned neurites were magnetically guided between neuronal clusters, with neurite growth tracked via a multi-electrode array (MEA) system. Confocal fluorescence microscopy bright-field images demonstrate that the microrobot formed a bridge between the two neuronal clusters. Furthermore, immunofluorescence imaging revealed interconnected neurites (green) with directional growth toward adjacent clusters. While this strategy successfully establishes neural network connections in vitro, further in vivo studies are necessary for brain disease applications.

3.3. Ischemic stroke

Ischemic stroke results from cerebral blood flow interruption, leading to localized brain tissue ischemia and necrosis, representing a prevalent cerebrovascular disorder [13,14,405]. Blood clotting-induced thrombus is the primary pathological event of ischemic stroke [406–408]. Current therapeutic methods include mechanical thrombectomy [348,409,410], intravenous thrombolysis [411–413], antiplatelet therapy [414,415], and anticoagulation therapy [416,417]. Tissue plasminogen activator (tPA), capable of effectively dissolving thrombus, is limited by the low delivery efficiency of systemic administration and a short therapeutic time window of thrombolysis [411,418]. Consequently, there is an urgent need to develop nanocarriers with high drug-loading stability and delivery efficiency for local drug delivery. As shown in Fig. 13**A**, Zheng's group [411] delivered tPA to thrombosed carotid arteries in a rabbit model using magnetic NP swarms. Under RMF actuation, tPA-loaded Fe_3O_4 NPs assembled into magnetic NP swarms that penetrated the thrombus, significantly enhancing tPA permeation and subsequent thrombolysis. Experimental results showed that these NP swarms enhanced tPA diffusion, significantly improving thrombolytic efficacy without increasing the clinical tPA dosage. Furthermore, in addition to thrombolysis, preventing thrombus formation represents an effective strategy for thrombus therapy [419]. Argatroban, as an anticoagulant, directly restrains the formation of thrombus [420,421]. Gong's group [422] employed platelet membrane-coated NPs to deliver argatroban through the vasculature. The NPs have taken advantage of the thrombus-homing properties of platelet membranes to target thrombus regions, releasing argatroban to inhibit the formation of thrombus.

Owing to their small size and high-precision navigation, MNRs have been widely used as drug carriers for intravenous thrombolysis in previous research works [423–425]. Notably, MNRs can convert external energy into mechanical motion, thereby breaking thrombus mechanically [426,427]. Thus, the drug delivery strategy that uses the mechanical motion of MNRs to assist thrombolysis can effectively enhance the therapeutic efficacy of thrombolytic agents. As depicted in Fig. 13**B**, Zhang's group [340] developed tPA-anchored nanorobots that form retrievable magnetic colloidal microswarms to dissolve submillimeter vascular thrombus. The nanorobot is composed of a Fe_3O_4 NP core and a SiO_2 shell, with tPA chemically adsorbed on the SiO_2 shell. The nanorobots were delivered via a catheter and subsequently released near the thrombus under magnetic actuation, inducing localized thrombus fragmentation through their tumbling motion. Upon contacting the thrombus, the nanorobots release tPA to enhance chemical thrombolysis. The synergistic combination of physical disruption from nanorobot motion and tPA-mediated thrombolysis removed blood vessel blockages. Crucially, the nanorobots can be retrieving via catheter under magnetic actuation, addressing potential biocompatibility concerns associated with incompletely degradable magnetic materials. In vitro experiment, compared to systemic tPA administration, tPA-anchored nanorobots achieved a 20 times increase in thrombolytic efficiency.

However, some pharmacological treatments have narrow therapeutic windows and cause reocclusion post-reperfusion. Therefore, adjunct anticoagulation therapy can significantly enhance therapeutic outcomes after thrombolysis. To address this, Wu's group [321] developed an antithrombotic outer membrane vesicle (OMV) composed of thrombolytic drug staphylokinase (SAK)-hirudin fusion protein (SFH). SFH combines hirudin's anticoagulant properties with SAK's thrombolytic activity for synergistic ischemic stroke treatment. As shown in Fig. 14**A**, SFH-OMV can combine with different substances to achieve various therapeutic effects. Both SFH-OMV formulations incorporated Fe_3O_4 NPs for magnetic propulsion: (i) SFH-OMV and hydrogel were used to synthesize hydrogel microrobots in emulsion (oil/$CaCl_2$ solution). SFH-OMV@H can navigate against blood flow to directly target and dissolve the thrombus. (ii) Macrophages phagocytosed SFH-OMV to form SHF-OMV@MΦ. Due to the adhesive properties of macrophages, SHF-OMV@MΦ can counteract blood flow to eliminate thrombi and adhere to the vascular wall to protect the surrounding brain tissue. Excessive ROS production is another primary mechanism underlying ischemic stroke formation [391,428]. As previously discussed in

Section 2.4, self-propelled MNRs generate therapeutic hydrogen gas (H_2) during propulsion, effectively regulating ROS. As shown in Fig. 14**B**, Tu's group [160] employed Mg-based micromotors to treat MCAO. The MCAO rat model was created by proximally ligating the left common carotid artery and external carotid artery. Mg-based micromotors react with water to generate H_2, which serves as both a propulsion force and a ROS scavenger, while modulating inflammatory factor expression (Fig. 3**A**). The treatment efficacy was indirectly assessed by calculating the infarct volume/ischemic hemisphere ratio. Experimental results demonstrated that Mg@PLGA exhibited the second-lowest occlusion volume after the sham group, indicating that H_2 transported by Mg@PLGA effectively mitigated thrombotic occlusion. This research work provides the first conceptual validation of MNRs' mechanism for active ROS scavenging and inflammation mitigation in vivo, paving the way for their therapeutic application in ischemic stroke.

3.4. Traumatic brain injury

TBI, caused by external mechanical forces acting on brain tissue, is associated with high mortality rates [429–431]. The pathophysiological progression of TBI involves primary injury (immediate damage from direct/indirect force impact) [432,433] and secondary injury. The secondary injury includes a series of complex pathophysiological alterations (such as inflammatory responses, oxidative stress, and neuronal apoptosis) [159,434] that develop over time following the primary injury. Thus, rapidly enhancing neuroprotection and halting secondary injury progression are critical for emergency rescue of TBI. Several neuroprotective agents with anti-inflammatory and neuroprotective properties (such as methylene blue (MB) [435–437], edaravone [438–440], and minocycline [441–443]) have been investigated for TBI treatment. Kim's group [444] developed a biocompatible Pluronic surfactant-based solubilization system for MB delivery, which significantly improved its targeting efficiency. In this system, anionic sodium oleate forms electrostatic complexes with cationic MB, which subsequently self-assemble with Pluronic surfactants via hydrophobic interactions to form mixed micelles (Pluronic-surfaced nanocomplexes). The nanocomplexes reduced inflammatory cytokine expression in mice, effectively mitigating TBI-induced neuroinflammation. However, the limited regenerative capacity of brain tissue presents tough challenges for neural repair after TBI. To address this challenge, Negah's group [445] first synthesized a nanoscaffold with a Young's modulus of 3.21 kPa to deliver stromal cell-derived factor 1 (SDF-1) in the brain, alleviating TBI-induced neural damage. The scaffold was fabricated by combining self-assembling peptide RADA16 with SDF-1. Experimental results demonstrated that the functional motif derived from SDF-1 enhanced stem cell regeneration and synaptogenesis at the injury site.

In addition to neuroprotection, rapid mitigation of neuroinflammation is crucial. As previously discussed in Section 2.4, self-propelled MNRs generate therapeutic hydrogen gas during propulsion, demonstrating excellent anti-inflammatory and ROS-scavenging abilities. As shown in Fig. 15**A**, Xue's group [159] developed self-propelled nanomotors (JCNs) by asymmetrically coating carbonaceous nanospheres (CNs) with ultrathin metal layers (Pt, Pd and Mo). The JCNs catalytically decompose H_2O_2 to: (i) Generate oxygen, alleviating hypoxia. (ii) Scavenge ROS, reducing oxidative stress. (iii) Restrain pro-inflammatory cytokines, blocking inflammatory cascades. Immunofluorescence co-staining (Fig. 15**B**) demonstrated significantly weaker fluorescence signals for both microglia (red) and astrocytes (green) in the JCN-treated group compared to TBI controls, indicating that JCN therapy substantially reduced glial activation in the hippocampal region. Therefore, JCNs effectively alleviate oxidative stress and neuroinflammation, offering a feasible strategy for emergency TBI intervention.

3.5. Neurodegenerative diseases

Neurodegenerative diseases are characterized by progressive degeneration and death of neurons, typically accompanied by pathological protein aggregation [446–448], oxidative stress [449–451], and neuroinflammation [452–454]. Common neurodegenerative diseases include PD and AD. The abnormal accumulation of α-syn serves as the primary pathological event of PD [11,455,456]. Zhang's group [457] developed black phosphorus nanosheets (BPNSs) to scavenge α-syn aggregates. As multifunctional nanomaterials, BPNSs serve as both drug carriers and therapeutic agents, owing to their high reducibility, antioxidant properties, and layered structure [458,459]. Experimental results demonstrated that BPNSs directly combined α-syn fibrils and activated autophagy to restrain α-syn aggregation [457]. However, aggregated α-syn promotes ROS generation and activates microglia to secrete pro-inflammatory factors, leading to the death of dopamine neurons. To address this, Wang's group [460] designed extracellular vesicle-based nanoformulations composed of extracellular vesicles and dihydrotanshinone I (DT)-loaded $mSiO_2$, which modulated inflammation and restrained immune overactivation. The released DT activated nuclear factor erythroid 2-related factor 2 expression, scavenging ROS and alleviating inflammation, thereby modulating the PD microenvironment and enhancing therapeutic outcomes. Moreover, the reduction of endogenous H_2S is believed to have a crucial impact on the progression of PD, so the supplementation of exogenous H_2S is regarded as one of the key strategies for treating PD. Inspired by this, researchers have developed nanomotors with the capabilities of releasing H_2S and targeting mitochondria and demonstrated their favorable therapeutic effect on PD [461,462].

The deposition of β-amyloid (Aβ) serves as the primary pathological event of AD [12,463,464]. Small interfering RNA (siRNA), which directly blocks aberrant protein gene expression, represents a promising gene therapy [50,465,466]. Wang's group [467] designed biomimetic nanovesicles carrying β-site amyloid precursor protein cleaving enzyme-1 (BACE1) siRNA (siBACE1) to synergistically regulate microglial function and interfere with Aβ metabolism. These nanovesicles enhanced Aβ phagocytosis by triggering receptor expressed on myeloid cell 2 expression, thereby inhibiting BACE1 from producing Aβ. As previously discussed in Section 2.3, the BBB imposes restrictions on macromolecular drug delivery to the brain. As shown in Fig. 16**A**, Shi's group [50] employed a carrier-mediated strategy to deliver glycosylated siRNA nanodrugs (Gal-NP@siBACE1) into the brain to restrain Aβ production. Gal-NP@siBACE1 knocked down BACE1 mRNA expression after being internalized by brain cells, thereby preventing cleavage of amyloid precursor protein (APP) and reducing Aβ production. Fig. 16**B** quantifies therapeutic efficacy in AD through the measurement of

amyloid plaque burden. Compared to all AD control groups, the Gal-NP@siBACE1 group showed a significant reduction in amyloid plaque deposition, approaching levels observed in the healthy control group of wild-type (WT) mice treated with phosphate-buffered saline (PBS) (WT-PBS). Furthermore, the CLSM imaging of mice (Fig. 16**C**) showed a reduction in amyloid plaque areas in the Gal-NP@siBACE1 group, demonstrating the therapeutic efficacy of siRNA delivery for AD treatment.

While the pathological mechanisms of neurodegenerative diseases have not been completely revealed, current therapies mainly target pathological events. Notably, MNRs built from functional materials and biomaterials can be designed to dissociate or phagocytose Aβ aggregates [468–470], offering a promising non-invasive therapeutic strategy for neurodegenerative disorders. Piezoelectric nanomaterials, characterized by high biocompatibility and piezocatalytic properties, are especially suitable for in vivo applications [471–473]. Pané's group [468] developed barium titanate (BTO) NP-based microrobots (PiezoBOTs) that use BTO's strong piezocatalytic effect to disaggregate Aβ, as shown in Fig. 17**A**. The PiezoBOTs feature a helical *Spirulina platensis* template coated with an Fe_3O_4 NP layer for magnetic actuation, followed by the loading of BTO NPs. The piezocatalytic activity of BTO NPs effectively catalyzes Aβ dissociation under combined magnetic and ultrasonic fields. To analyze the therapeutic effect of PiezoBOTs, the Aβ aggregate size were calculated in Fig. 17A. The control groups (Aβ without ultrasound stimulation and Aβ-only) exhibited similar Aβ aggregate sizes, showing that ultrasound stimulation can cause the disaggregation of Aβ aggregates. Although ultrasound-mediated mechanical effects (iv group) reduced the Aβ aggregate size, the catalytic effect of PiezoBOT (ii group) can further decrease Aβ aggregate size. Moreover, Aβ can be eliminated by cellular autophagy. However, since Aβ predominantly accumulates extracellularly, intracellular autophagy mechanisms exhibit limited efficacy in its clearance [474,475]. For this purpose, Wang's group [469] developed functional peptide-polymer-based nanosweepers, which capture and clear Aβ peptides. The functional peptides on the nanosweepers can recognize Aβ and deliver it to cells through self-assembly, where it is eliminated via cellular autophagy.

Previous research works have demonstrated that light-propelled MNRs under NIR irradiation, improve targeted delivery and local photothermal therapy for Aβ inhibition [476–478]. As high-energy external fields, NIR irradiation induces rapid movement of MNRs, which greatly improves interactions with surrounding materials. For example, Sun's group [476] developed Aβ inhibitor-modified light-propelled nanomotors (JMN-I) to restrain Aβ fibrillogenesis. As shown in Fig. 17**B**, JNM-I, collides with Aβ in the microenvironment under the excitation of NIR, increasing the contact frequency among the inhibitor and Aβ, thereby effectively inhibiting Aβ aggregation. To visualize the morphology of Aβ aggregates, the atomic force microscopy (AFM) imaging were depicted in Fig. 17B. AFM images showed distinct fibrillar morphologies of Aβ. After introducing JNM-I (without NIR), the inhibitor reduced Aβ fibrillogenesis, with partial aggregated plaques observed. Under NIR activation, Aβ aggregate morphology was nearly undetectable, aligning with theoretical predictions. To further enhance therapeutic effects, Sun's group [477] incorporated double carbon dots composite materials into MNRs, employing their photooxygenation and photothermal properties to synergistically inhibit Aβ fibrillogenesis. The double carbon dots composite is composed of previously reported NIR-carbon dots [479] and carbonized polymer dots [480]. Their MNRs can degrade mature Aβ fibrils and inhibit Aβ aggregation at an extremely low concentration (0.5 μg mL^{-1}).

Because neurodegenerative diseases cause irreversible damage to neurons [481,482], neuronal repair has emerged as an auxiliary therapeutic for neurodegenerative diseases. Additional research on MNRs in neurodegenerative diseases has focused on neuron recovery [398] and stem cell delivery [483]. Experimental results from Li's group [398] demonstrated that neurons damaged by Aβ could effectively restore activity under stimulation by MOHRs microrobots (Fig. 12**A**). Furthermore, Pané's group [483] synthesized biodegradable magnetically propelled microrobots capable of delivering neuronal cells under static magnetic field actuation, and promoting cell differentiation under alternating magnetic field. As previously discussed in Section 2, MNRs exhibit extraordinary mobility, BBB penetration, and drug-loading capability. Therefore, MNRs have significant potential to develop other therapies (such as gene therapy) in neurodegenerative disease treatment.

Taken together, micro/nanorobots enable periodical and quantitative controlled drug release via environmental responsiveness or external stimuli [177,321,329,334]. For example, ultrasound-induced cavitation can disrupt the shell of micro/nanorobots to trigger drug release [181], while pH-responsive carriers selectively disassemble in acidic pathological microenvironments [329], preventing premature drug leakage in healthy tissues. These "on-demand drug release" intelligent properties of micro/nanorobots extend the effective action time of drugs and reduce the frequency and dosage of drug administration, significantly improving the utilization efficiency of brain drugs. Notably, micro/nanorobots' multifunctional integration capability expands their applications. Micro/nanorobots can carry therapeutic drugs and radiographic contrast agents, enabling in vivo monitoring through X-ray imaging [484]. Additionally, incorporating materials such as a gold layer into micro/nanorobots enhances imaging and monitoring capabilities [166,195,485], improves the precision of drug delivery, and promotes the integration of theranostics.

4. Conclusion and future outlook

This review summarizes recent advances in smart micro/nanorobots for drug delivery in the brain. Nanocarrier-based brain drug delivery systems were reviewed and discussed in terms of their advantages, disadvantages, and physicochemical properties. The precision, stability, and efficiency of drug delivery systems are the key to treating brain diseases. Due to the limitation of the BBB, conventional nanocarriers primarily rely on passive targeting through the enhanced permeability and retention effect or surface modifications for BBB penetration, resulting in imperfect drug-loading stability and delivery efficiency, which are insufficient for clinical requirements. Furthermore, as a passive drug delivery strategy, conventional nanocarriers have limited control over the targeting precision of lesions. Micro/nanorobots with capabilities for precise navigation, deep tissue penetration, and high drug loading stability demonstrate significant potential to address these limitations. Therefore, the recent advancements in smart active micro/nanorobots are summarized in detail, focusing on their motor abilities in cerebral environments, BBB-overcoming strategies, drug delivery performance, and material design. The therapeutic applications of these intelligent drug delivery systems across

representative brain diseases are systematically analyzed and discussed, elucidating their therapeutic efficacy and mechanism corresponding to distinct pathogenesis and pathology.

It should be noted that the design and development principles of traditional nanocarriers can lay a solid foundation for devising functional micro/nanorobots and understanding their therapeutic effects. This review is set to comprehensively overview the rational design and development of smart micro/nanorobot drug delivery systems, and bridge the gap between traditional nanosystems and active micro/nanorobots for brain-targeted drug delivery, ultimately unleashing the potential of micro/nanorobots for precision therapeutic applications in a variety of brain diseases. In recent years, researchers have made great efforts in this emerging research field of micro/nanorobots-based intelligent drug delivery systems and have made significant progress. However, further investigation and improvement are essential for their practical applications in brain disease therapy in a precise manner. To this end, the following points can be taken into consideration in the design and development of novel micro/nanorobots for brain health in the future.

4.1. Driving and navigating micro/nanorobots in the brain

At present, micro/nanorobots face many challenges in driving and navigating in the complex environment of the brain. In the future, it is expected that more efficient and precise drive mechanisms will be developed. For example, a driving method based on a new energy conversion principle, such as using chemical energy in the body (such as energy generated by glucose oxidation) to directly power micro/nanorobots, allowing them to move continuously and stably in the brain. In terms of navigation, multimodal fusion navigation technology will become a research hotspot. Combining high-resolution anatomical information from MRI, real-time dynamic monitoring from ultrasound, and chemical navigation based on biomarkers, micro/nanorobots can reach the target lesion site with submicron accuracy in the intricate cerebrovascular network and brain tissue gaps, and achieve precise drug delivery to subtle lesion areas in the brain.

(1) Magnetically propelled micro/nanorobots will be widely used in the brain due to their non-invasiveness and high penetration [41]. The small size of micro/nanorobots limits their transport speed and extends the targeting time to the lesion area, which is not conducive to the treatment of stroke and traumatic brain injury. Therefore, it is necessary to use aids like catheters or magnetic continuum robots for cross-scale transport. This also provides a way to recycle magnetic substances that cannot be completely degraded in the human body.
(2) Self-propelled micro/nanorobots have shown excellent therapeutic effects in the brain and have minimal impact on the physiological environment. However, their movement is difficult to control. A biomimetic strategy can enhance the targeting and motion control of self-propelled micro/nanorobots in the brain [178]. Moreover, self-propelled micro/nanorobots have limitations in “fuel” quantity, thereby requiring improved in vivo residence time and adaptability to the surrounding environment conditions (such as local pH changes, enzyme catalysis, and ROS).
(3) Ultrasound-propelled micro/nanorobots face challenges such as locomotion attenuation in complex media and potential biological damage from cavitation. The complicated microvasculature and anatomy of the brain also pose challenges for route planning of externally propelled micro/nanorobots (under ultrasound and magnetic fields). Therefore, there is an urgent need to enhance the imaging and real-time signal feedback of micro/nanorobots to monitor their position and adjust their trajectory based on the pathological environment. In addition, micro/nanorobots with multimodal propulsion and/or multiple functions can be developed for treating brain diseases. For example, light-propelled micro/nanorobots, though limited by low penetration depth, exhibit excellent photothermal and photodynamic effects, showing potential for cerebral therapy.

With the continuous development of artificial intelligence and machine learning algorithms, micro/nanorobots will have higher intelligent response and autonomous control capabilities. They can sense changes in the brain microenvironment in real-time, such as the pH value, temperature, and concentration of specific biomolecules at the lesion site, and autonomously adjust the movement trajectory and drug release strategy based on this information. For example, when a high concentration of a specific protein is detected in the tumor microenvironment, the micro/nanorobots can autonomously start the drug release program and dynamically adjust the drug release rate according to the metabolic activity of the tumor cells to achieve the best therapeutic effect while reducing drug exposure to normal brain tissue.

4.2. Overcoming the BBB for brain drug delivery

(1) In the research field of micro/nanorobots for brain drug delivery, current strategies mainly focus on crossing the BBB rather than circumventing it. Circumventing the BBB may find its wide applications for micro/nanorobots in intelligent drug delivery to the brain due to the unique advatages. For example, by circumventing the BBB through intranasal and intracranial approaches, micro/nanorobots can prevent harmful substances from entering the brain. In terms of the BBB-circumventing tactics, greater efforts should be made in the future to fully address the current challenges faced by micro/nanorobots for brain drug delivery. For instance, although micro/nanorobots-based intranasal drug delivery can directly target the brain tissue, the nasal mucus layer may hamper drug diffusion and reduce absorption efficiency. Therefore, it is necessary to further enhance the mucus-penetrating ability and drug-loading stability of micro/nanorobots by virtue of elaborate design of material composition, geometrical structure, and functional properties. Furthermore, current transcranial micro/nanorobots can enhance the drug targeting and loading stability, but the safety of this invasive strategy regarding skull injury needs further evaluation.

(2) There are several unique microchannels between the skull bone marrow and the brain surface [228,300,486]. We envision that taking full advantage of these mysterious microchannels holds great promise for smart micro/nanorobots to actively circumvent the BBB and deliver drugs to the brain, particularly to the brain parenchyma. For example, researchers have demonstrated the existence of numerous skull bone marrow-dura microchannels to connect each other [298,487–489]. Therefore, the skull bone marrow microenvironment near the brain can supply monocytes and neutrophils that pass through these skull bone marrow-dura microchannels to the meninges and CNS parenchyma in homeostasis and upon injury. Inspired by this, biohybrid microrobots based on living monocytes, macrophages, and neutrophils, especially skull bone marrow-derived immune cells, can be developed to go through the skull bone marrow-dura microchannels and deliver various therapeutic agents to the brain parenchyma. Alternatively, multifarious biohybrid micro/nanorobots camouflaged with cell membranes derived from diverse immunocytes can be developed to pass through these skull bone marrow-dura microchannels for brain-targeted drug delivery. There are also direct vascular channels that connect the skull bone marrow and the brain surface to enable myeloid cell migration [490]. It has been found that leukaemia cells can path through these vessel channels to metastasize to the CNS [491]. Similarly, multifarious biohybrid micro/nanorobots can be created for brain-targeted drug delivery on the basis of living cancer cells or cancer cell membranes. Theoretically, a variety of micro/nanorobots with the dimensions adaptable to the mysterious microchannels can be designed and developed to pass through these natural microchannels, which is able to unleash the huge potential of these mysterious microchannels for micro/nanorobots-based active brain drug delivery and disease treatment. Taken together, the combination of smart micro/nanorobots and these mysterious microchannels will open up a new era of developing active micro/nanorobots for precision brain targeting, drug delivery, and disease therapy.

(3) The drug delivery efficiency of micro/nanorobots in the brain is closely related to their biocompatibility and controlled release. Once micro/nanorobots overcome the BBB and enter inflammatory brain areas, they have the risk of phagocytosis by immune cells, highlighting the importance of immune evasion for the development of micro/nanorobots in brain disease therapy. Innate immune cells (such as macrophages, neutrophils, and dendritic cells) can phagocytose various foreign bodies, including micro/nanorobots [371]. When performing medical tasks for which innate immune cells are not the target cells, microrobots should be able to evade phagocytic uptake through rational design, or at least complete the medical task before phagocytosis. For this purpose, a promising tactic is to design and create biohybrid micro/nanorobots from host cells (such as immune cells) or cell components (such as cell membranes). Moreover, it is necessary to carry out in-depth research to understand the interaction between medical micro/nanorobots and brain immune cells, which can finally optimize the rational designs of micro/nanorobots and induce the desired immune responses for brain disease therapy.

4.3. The challenges of micro/nanorobot design for brain drug delivery

(1) It is of great importance to endow micro/nanorobots with active targeting ability upon design. Nanocarriers need to have a high degree of targeting to accurately deliver drugs to the lesion site. However, the brain tissue structure is complex, and the physiological characteristics and pathological states of different brain regions vary greatly. Existing targeting ligands often have difficulty in achieving specific recognition of specific brain regions or cells. For example, nanocarriers for neurodegenerative diseases need to accurately reach the diseased neurons or glial cells, but the commonly used targeting molecules, such as antibodies and peptides, are limited in their targeting efficiency and stability in the complex brain microenvironment and are prone to nonspecific binding, which affects the therapeutic effect and may cause side effects. To overcome this, more efforts should be made in the future to design and create smart micro/nanorobots for brain drug delivery. For example, it will be a promising strategy to modify or functionalize micro/nanorobots with various targeting molecules that are commonly adopted for developing traditional nanocarriers.

(2) The safety and biocompatibility of micro/nanorobots in vivo are crucial. Some nanomaterials themselves may be potentially toxic. For example, metal nanoparticles may release metal ions, causing oxidative stress and cell damage; some polymers or functional molecules modified on the surface of nanocarriers may also trigger immune responses. In addition, the metabolic pathways and long-term accumulation effects of nanocarriers in the body are still unclear. They may accumulate in organs such as the liver and spleen, causing damage to other tissues and organs, which makes the clinical application of nanocarriers have greater risks. In particular, for micro/nanorobots as an emerging nanocarrier type, more attention should be paid to these concerns, which will be discussed further later.

(3) The microscale size of micro/nanorobots necessitates specialized material design strategies to overcome viscous resistance in low Reynolds number environments. Furthermore, MNR geometry critically influences cerebral functionality. Spherical MNRs offer advantages for facile surface modification and biomimetic design, while ciliary-type micro/nanorobots counteract fluidic resistance in brain tissues. For specialized applications, MNRs of special shapes are required. For example, the spiral-shaped MNRS can effectively destroy cerebral vascular blockage caused by stroke during the driving process. However, surface charge loading requires cautious optimization for rod or needle-shaped MNRs, while positive charge concentration enhances brain endothelial adhesion, it carries potential adverse effects. Consequently, MNR development for neurological applications demands disease-specific and microenvironment-adapted material engineering.

(4) Micro/nanorobots need to have sufficient drug-loading capacity to ensure that the drug reaches an effective therapeutic concentration in the brain. However, many nanocarriers have low drug-loading efficiency, especially for drugs with poor water solubility or large molecular weight, it is difficult to achieve efficient loading. At the same time, achieving controlled release of drugs is also a major challenge. After crossing the BBB, nanocarriers need to accurately control the release rate and time of the drugs according to the needs of the lesion site to maintain a stable drug concentration. However, current nanocarriers often find

it difficult to meet this requirement. Either the drugs are released too quickly, resulting in large fluctuations in drug concentration and increased risk of side effects; or the drugs are released too slowly and cannot play a therapeutic role in time.

4.4. Clinical application expansion

(1) Micro/nanorobots represent a new dawn in the treatment of neurological diseases. For brain neurodegenerative diseases, such as Alzheimer's disease and Parkinson's disease, micro/nanorobots are expected to carry neuroprotective drugs, neurotrophic factors, or gene therapy vectors to directly act on diseased neurons or glial cells. Through precise delivery, the function of damaged nerve cells can be repaired, neuroinflammatory response can be inhibited, and disease progression can be delayed. In terms of cerebrovascular diseases, such as acute stroke, micro/nanorobots can quickly reach the site of a thrombus, release thrombolytic drugs or perform physical thrombus removal, restore brain blood perfusion, reduce brain tissue damage caused by ischemia, and greatly improve the patient's chance of recovery.
(2) Micro/nanorobots can provide key support for personalized medicine. The physiological structure and disease characteristics of each person's brain are different. Micro/nanorobots can be customized according to the individual conditions of patients, such as through the analysis of patients' brain imaging data and genetic test results, to design the size, shape, surface functionalization modification, and drug loading scheme of the robot. This personalized drug delivery system can maximize the therapeutic effect, reduce adverse drug reactions, and open up a new path for precision medicine for brain diseases. Moreover, MNRs can be employed to deliver drugs to the brain in space in the future. Their propulsion and navigation become more complex due to the extreme environmental conditions of space, such as microgravity or zero-gravity [492], radiation [493], cosmic magnetic fields [494,495], and the truth that sound cannot travel through space. In this context, multi-field driving may find its way into precise brain drug delivery in space and provide astronauts with promising healthcare solutions.

4.5. Ethical and safety considerations

(1) The long-term biosafety of micro/nanorobots is required to assess. With the increasing application of micro/nanorobots in brain-targeted drug delivery, their long-term biosafety has become a key issue. It is necessary to conduct in-depth research on the degradation products, metabolic pathways, and potential long-term effects of micro/nanorobots on brain tissue and neural function in the brain environment. To this end, it is essential to establish a complete animal model and clinical trial system to track and observe the behavior of micro/nanorobots in the body for months or even years to ensure that they do not cause chronic inflammation, gene mutations, or other unforeseen health risks.
(2) Micro/nanorobots are concerned with ethical and privacy issues for brain-targeted drug delivery and disease therapy. The entry of micro/nanorobots into the brain, the most sensitive and complex organ in the human body, will raise a series of ethical and privacy issues. For example, how to ensure patients' right to know and make their own choices about micro/nanorobots treatment, and how to prevent micro/nanorobots technology from being abused to violate personal privacy or conduct inhumane brain interventions. Formulating strict ethical guidelines and regulatory policies, regulating the research and application of micro/nanorobots in the field of brain-targeted drug delivery, and protecting the rights and interests of patients and the bottom line of social ethics are indispensable links in future development.

CRediT authorship contribution statement

Di Shi: Writing – original draft, Formal analysis, Investigation, Data curation. **Xiang Wang:** Investigation. **Yulin Deng:** Conceptualization. **Huaijuan Zhou:** Conceptualization, Supervision, Funding acquisition, Writing – review & editing, Writing – original draft. **Yilong Wang:** Conceptualization. **Paul K. Chu:** Supervision, Funding acquisition. **Jinhua Li:** Conceptualization, Supervision, Funding acquisition, Writing – review & editing, Writing – original draft.

Declaration of competing interest

The authors declare that they have no known competing financial interests or personal relationships that could have appeared to influence the work reported in this paper.

Acknowledgments

This work is supported by the Beijing Nova Program of Science and Technology (20240484527), Beijing Natural Science Foundation (2242059), National Natural Science Foundation of China (52302343), City University of Hong Kong Donation Research Grants (DON-RMG 9229021 and 9220061), and Guangdong - Hong Kong Technology Cooperation Funding Scheme (TCFS GHP/212/22GD and CityU 9440399).

Data availability

Data will be made available on request.

References

[1] Berk M, Köhler-Forsberg O, Turner M, Penninx BWJH, Wrobel A, Firth J, et al. Comorbidity between major depressive disorder and physical diseases: a comprehensive review of epidemiology, mechanisms and management. World Psychiatry 2023;22:366–87.
[2] Nowotny B, Thomas D, Schwers S, Wiegmann S, Prange W, Yassen A, et al. First randomized evaluation of safety, pharmacodynamics, and pharmacokinetics of BAY 1831865, an antibody targeting coagulation factor XI and factor XIa, in healthy men. J Thromb Haemost 2022;20:1684–95.
[3] Daniele SG, Trummer G, Hossmann KA, Vrselja Z, Benk C, Gobeske KT, et al. Brain vulnerability and viability after ischaemia. Nat Rev Neurosci 2021;22:553–72.
[4] Huang W-C, Peng Z, Murdock MH, Liu L, Mathys H, Davila-Velderrain J, et al. Lateral mammillary body neurons in mouse brain are disproportionately vulnerable in Alzheimer's disease. Sci Transl Med 2023;15:eabq1019.
[5] Ruan S, Zhou Y, Jiang X, Gao H. Rethinking CRITID procedure of brain targeting drug delivery: circulation, blood brain barrier recognition, intracellular transport, diseased cell targeting, internalization, and drug release. Adv Sci 2021;8:2004025.
[6] Banks WA. From blood–brain barrier to blood–brain interface: new opportunities for CNS drug delivery. Nat Rev Drug Discov 2016;15:275–92.
[7] Tsou Y-H, Zhang X-Q, Zhu H, Syed S, Xu X. Drug delivery to the brain across the blood–brain barrier using nanomaterials. Small 2017;13:1701921.
[8] Correia AC, Monteiro AR, Silva R, Moreira JN, Sousa Lobo JM, Silva AC. Lipid nanoparticles strategies to modify pharmacokinetics of central nervous system targeting drugs: crossing or circumventing the blood–brain barrier (BBB) to manage neurological disorders. Adv Drug Deliv Rev 2022;189:114485.
[9] Chang Y, Cai X, Syahirah R, Yao Y, Xu Y, Jin G, et al. CAR-neutrophil mediated delivery of tumor-microenvironment responsive nanodrugs for glioblastoma chemo-immunotherapy. Nat Commun 2023;14:2266.
[10] Zhang P, Rashidi A, Zhao J, Silvers C, Wang H, Castro B, et al. STING agonist-loaded, CD47/PD-L1-targeting nanoparticles potentiate antitumor immunity and radiotherapy for glioblastoma. Nat Commun 2023;14:1610.
[11] Elabi O, Gaceb A, Carlsson R, Padel T, Soylu-Kucharz R, Cortijo I, et al. Human α-synuclein overexpression in a mouse model of Parkinson's disease leads to vascular pathology, blood brain barrier leakage and pericyte activation. Sci Rep 2021;11:1120.
[12] Huang D, Wang Q, Cao Y, Yang H, Li M, Wu F, et al. Multiscale NIR-II imaging-guided brain-targeted drug delivery using engineered cell membrane nanoformulation for Alzheimer's disease therapy. ACS Nano 2023;17:5033–46.
[13] Wang Q, Yang F, Duo K, Liu Y, Yu J, Wu Q, et al. The role of necroptosis in cerebral ischemic stroke. Mol Neurobiol 2024;61:3882–98.
[14] Liu W, Liu L, Li H, Xie Y, Bai J, Guan J, et al. Targeted pathophysiological treatment of ischemic stroke using nanoparticle-based drug delivery system. J Nanobiotechnol 2024;22:499.
[15] Tan Q, Zhao S, Xu T, Wang Q, Zhang M, Yan L, et al. Inorganic nano-drug delivery systems for crossing the blood–brain barrier: advances and challenges. Coord Chem Rev 2023;494:215344.
[16] Allen BD, Limoli CL. Breaking barriers: neurodegenerative repercussions of radiotherapy induced damage on the blood-brain and blood-tumor barrier. Free Radic Biol Med 2022;178:189–201.
[17] Xiong B, Wang Y, Chen Y, Xing S, Liao Q, Chen Y, et al. Strategies for structural modification of small molecules to improve blood–brain barrier penetration: a recent perspective. J Med Chem 2021;64:13152–73.
[18] Mhaske A, Shukla S, Ahirwar K, Singh KK, Shukla R. Receptor-assisted nanotherapeutics for overcoming the blood–brain barrier. Mol Neurobiol 2024;61:8702–38.
[19] Rawal SU, Patel BM, Patel MM. New drug delivery systems developed for brain targeting. Drugs 2022;82:749–92.
[20] Ling Q, Herstine JA, Bradbury A, Gray SJ. AAV-based in vivo gene therapy for neurological disorders. Nat Rev Drug Discov 2023;22:789–806.
[21] Shaha S, Rodrigues D, Mitragotri S. Locoregional drug delivery for cancer therapy: preclinical progress and clinical translation. J Control Release 2024;367:737–67.
[22] Mayer FP, Niello M, Cintulova D, Sideromenos S, Maier J, Li Y, et al. Serotonin-releasing agents with reduced off-target effects. Mol Psychiatry 2023;28:722–32.
[23] Manzari MT, Shamay Y, Kiguchi H, Rosen N, Scaltriti M, Heller DA. Targeted drug delivery strategies for precision medicines. Nat Rev Mater 2021;6:351–70.
[24] Kuang X, Chi D, Li J, Guo C, Yang Y, Zhou S, et al. Disulfide bond based cascade reduction-responsive Pt(IV) nanoassemblies for improved anti-tumor efficiency and biosafety. Colloids Surf B Biointerfaces 2021;203:111766.
[25] Xia J, Chen C, Dong M, Zhu Y, Wang A, Li S, et al. Ginsenoside Rg3 endows liposomes with prolonged blood circulation and reduced accelerated blood clearance. J Control Release 2023;364:23–36.
[26] De R, Mahata MK, Kim K-T. Structure-based varieties of polymeric nanocarriers and influences of their physicochemical properties on drug delivery profiles. Adv Sci 2022;9:2105373.
[27] Alshaikh RA, Waeber C, Ryan KB. Polymer based sustained drug delivery to the ocular posterior segment: barriers and future opportunities for the treatment of neovascular pathologies. Adv Drug Deliv Rev 2022;187:114342.
[28] Sonabend AM, Gould A, Amidei C, Ward R, Schmidt KA, Zhang DY, et al. Repeated blood–brain barrier opening with an implantable ultrasound device for delivery of albumin-bound paclitaxel in patients with recurrent glioblastoma: a phase 1 trial. Lancet Oncol 2023;24:509–22.
[29] Carpentier A, Canney M, Vignot A, Reina V, Beccaria K, Horodyckid C, et al. Clinical trial of blood-brain barrier disruption by pulsed ultrasound. Sci Transl Med 2016;8. 343re2.
[30] Rezai AR, Ranjan M, D'Haese P-F, Haut MW, Carpenter J, Najib U, et al. Noninvasive hippocampal blood−brain barrier opening in Alzheimer's disease with focused ultrasound. Proc Natl Acad Sci 2020;117:9180–2.
[31] Liu Y, Hong H, Xue J, Luo J, Liu Q, Chen X, et al. Near-infrared radiation-assisted drug delivery nanoplatform to realize blood–brain barrier crossing and protection for parkinsonian therapy. ACS Appl Mater Interfaces 2021;13:37746–60.
[32] Xue D, Wang Y, Zhang H. Advances of NIR light responsive materials for diagnosis and treatment of brain diseases. Adv Opt Mater 2023;11:2202888.
[33] De Maio A, Huang Y, Lin F-H, Stefanovic B, Stanisz GJ, O'Reilly MA. Evaluation of focused ultrasound modulation of the blood-brain barrier in gray and white matter. J Control Release 2025;381:113631.
[34] Pang L, Wang Y. Overview of blood-brain barrier dysfunction in methamphetamine abuse. Biomed Pharmacother 2023;161:114478.
[35] Obermeier B, Daneman R, Ransohoff RM. Development, maintenance and disruption of the blood-brain barrier. Nat Med 2013;19:1584–96.
[36] Chen C, Ding S, Wang J. Materials consideration for the design, fabrication and operation of microscale robots. Nat Rev Mater 2024;9:159–72.
[37] Wu Z, Chen Y, Mukasa D, Pak OS, Gao W. Medical micro/nanorobots in complex media. Chem Soc Rev 2020;49:8088–112.
[38] Ceylan H, Yasa IC, Kilic U, Hu W, Sitti M. Translational prospects of untethered medical microrobots. Prog Biomed Eng 2019;1:012002.
[39] Wang B, Kostarelos K, Nelson BJ, Zhang L. Trends in micro-/nanorobotics: materials development, actuation, localization, and system integration for biomedical applications. Adv Mater 2021;33:2002047.
[40] Li J, Dekanovsky L, Khezri B, Wu B, Zhou H, Sofer Z. Biohybrid micro- and nanorobots for intelligent drug delivery. Cyborg Bionic Syst 2022;2022:9824057.
[41] Zhou H, Mayorga-Martinez CC, Pané S, Zhang L, Pumera M. Magnetically driven micro and nanorobots. Chem Rev 2021;121:4999–5041.
[42] Schwarz L, Medina-Sánchez M, Schmidt OG. Hybrid BioMicromotors. Appl Phys Rev 2017;4:031301.
[43] Nelson BJ, Kaliakatsos IK, Abbott JJ. Microrobots for minimally invasive medicine. Annu Rev Biomed Eng 2010;12:55–85.
[44] Han K, Shields Iv CW, Velev OD. Engineering of self-propelling microbots and microdevices powered by magnetic and electric fields. Adv Funct Mater 2018;28:1705953.
[45] Ma X, Jannasch A, Albrecht U-R, Hahn K, Miguel-López A, Schäffer E, et al. Enzyme-powered hollow mesoporous janus nanomotors. Nano Lett 2015;15:7043–50.
[46] Ren L, Nama N, McNeill JM, Soto F, Yan Z, Liu W, et al. 3D steerable, acoustically powered microswimmers for single-particle manipulation. Sci Adv 2019;5:eaax3084.

[47] Yan X, Zhou Q, Yu J, Xu T, Deng Y, Tang T, et al. Magnetite nanostructured porous hollow helical microswimmers for targeted delivery. Adv Funct Mater 2015; 25:5333–42.
[48] Zhang H, Li Z, Gao C, Fan X, Pang Y, Li T, et al. Dual-responsive biohybrid neutrobots for active target delivery. Sci Rob 2021;6:eaaz9519.
[49] Ye J, Fan Y, She Y, Shi J, Yang Y, Yuan X, et al. Biomimetic self-propelled asymmetric nanomotors for cascade-targeted treatment of neurological inflammation. Adv Sci 2024;11:2310211.
[50] Zhou Y, Zhu F, Liu Y, Zheng M, Wang Y, Zhang D, et al. Blood-brain barrier–penetrating siRNA nanomedicine for Alzheimer's disease therapy. Sci Adv 2020;6: eabc7031.
[51] Palagi S, Singh DP, Fischer P. Light-controlled micromotors and soft microrobots. Adv Opt Mater 2019;7:1900370.
[52] Yu J, Jin D, Chan K-F, Wang Q, Yuan K, Zhang L. Active generation and magnetic actuation of microrobotic swarms in bio-fluids. Nat Commun 2019;10:5631.
[53] Xuan M, Wu Z, Shao J, Dai L, Si T, He Q. Near infrared light-powered janus mesoporous silica nanoparticle motors. J Am Chem Soc 2016;138:6492–7.
[54] Zhou H, Dong G, Gao G, Du R, Tang X, Ma Y, et al. Hydrogel-based stimuli-responsive micromotors for biomedicine. Cyborg Bionic Syst 2022;2022.
[55] Li H, Zhang X, Miao J, Shi Z, Li Z, Wen M, et al. Dual drug-loaded calabash-like nanomotor as an active therapeutic for enhanced chemo-photothermal therapy of orthotopic glioblastoma. Chem Eng J 2023;473:145413.
[56] Chen H, Li T, Liu Z, Tang S, Tong J, Tao Y, et al. A nitric-oxide driven chemotactic nanomotor for enhanced immunotherapy of glioblastoma. Nat Commun 2023;14:941.
[57] Wang R, Nie W, Yan X, Luo K, Zhang Q, Wang T, et al. Biomimetic nanomotors for deep ischemia penetration and ferroptosis inhibition in neuroprotective therapy of ischemic stroke. Adv Mater 2025;37:2409176.
[58] An M, Feng Y, Liu Y, Yang H. External power-driven micro/nanorobots: design, fabrication, and functionalization for tumor diagnosis and therapy. Prog Mater Sci 2023;140:101204.
[59] Nelson BJ, Pané S. Delivering drugs with microrobots. Science 2023;382:1120–2.
[60] Ghosh S, Bhaskar R, Mishra R, Arockia Babu M, Abomughaid MM, Jha NK, et al. Neurological insights into brain-targeted cancer therapy and bioinspired microrobots. Drug Discov Today 2024;29:104105.
[61] Yoo J, Tang S, Gao W. Micro- and nanorobots for biomedical applications in the brain. Nat Rev Bioeng 2023;1:308–10.
[62] Tylawsky DE, Kiguchi H, Vaynshteyn J, Gerwin J, Shah J, Islam T, et al. P-selectin-targeted nanocarriers induce active crossing of the blood–brain barrier via caveolin-1-dependent transcytosis. Nat Mater 2023;22:391–9.
[63] Wu X, Zhang L, Tong Y, Ren L, Guo H, Miao Y, et al. Self-adaptive magnetic liquid metal microrobots capable of crossing biological barriers and wireless neuromodulation. ACS Nano 2024;18:29558–71.
[64] Orive G, Anitua E, Pedraz JL, Emerich DF. Biomaterials for promoting brain protection, repair and regeneration. Nat Rev Neurosci 2009;10:682–92.
[65] Budday S, Sarem M, Starck L, Sommer G, Pfefferle J, Phunchago N, et al. Towards microstructure-informed material models for human brain tissue. Acta Biomater 2020;104:53–65.
[66] Karahan E, Tait L, Si R, Özkan A, Szul MJ, Graham KS, et al. The interindividual variability of multimodal brain connectivity maintains spatial heterogeneity and relates to tissue microstructure. Commun Biol 2022;5:1007.
[67] Zhang Q, Dehaini D, Zhang Y, Zhou J, Chen X, Zhang L, et al. Neutrophil membrane-coated nanoparticles inhibit synovial inflammation and alleviate joint damage in inflammatory arthritis. Nat Nanotechnol 2018;13:1182–90.
[68] Geng H, Pan Y-c, Zhang R, Gao D, Wang Z, Li B, et al. Binding to amyloid-β protein by photothermal blood-brain barrier-penetrating nanoparticles for inhibition and disaggregation of fibrillation. Adv Funct Mater 2021;31:2102953.
[69] Chen MS, Sun R, Wang R, Zuo Y, Zhou K, Kim J, et al. Fillable magnetic microrobots for drug delivery to cardiac tissues in vitro. Adv Healthc Mater 2024;13: 2400419.
[70] Wilhelm S, Tavares AJ, Dai Q, Ohta S, Audet J, Dvorak HF, et al. Analysis of nanoparticle delivery to tumours. Nat Rev Mater 2016;1:16014.
[71] Wang L, Shi Y, Jiang J, Li C, Zhang H, Zhang X, et al. Micro-nanocarriers based drug delivery technology for blood-brain barrier crossing and brain tumor targeting therapy. Small 2022;18:2203678.
[72] Zhang L, Wang S, Hou Y. Magnetic micro/nanorobots in cancer theranostics: from designed fabrication to diverse applications. ACS Nano 2025.
[73] Alapan Y, Bozuyuk U, Erkoc P, Karacakol AC, Sitti M. Multifunctional surface microrollers for targeted cargo delivery in physiological blood flow. Sci Rob 2020;5:eaba5726.
[74] Palagi S, Fischer P. Bioinspired microrobots. Nat Rev Mater 2018;3:113–24.
[75] Peng F, Tu Y, Wilson DA. Micro/nanomotors towards in vivo application: cell, tissue and biofluid. Chem Soc Rev 2017;46:5289–310.
[76] Rajabasadi F, Schwarz L, Medina-Sánchez M, Schmidt OG. 3D and 4D lithography of untethered microrobots. Prog Mater Sci 2021;120:100808.
[77] Li J, Pumera M. 3D printing of functional microrobots. Chem Soc Rev 2021;50:2794–838.
[78] Zhang F, Zhuang J, Li Z, Gong H, de Ávila B-E-F, Duan Y, et al. Nanoparticle-modified microrobots for in vivo antibiotic delivery to treat acute bacterial pneumonia. Nat Mater 2022;21:1324–32.
[79] Ren E, Hu J, Mei Z, Lin L, Zhang Q, He P, et al. Water-stable magnetic lipiodol micro-droplets as a miniaturized robotic tool for drug delivery. Adv Mater 2025; 37:2412187.
[80] Liu WS, Cheng CK, Chan KF, Zhang L. Chapter 14 - In vitro diagnostics via micro/nanorobotic platform. In: Zhang L, Chiu PWY, Chan KF, editors. Recent Progress in Medical Miniature Robots. Academic Press; 2025. p. 365–91.
[81] Chatzipirpiridis G, Ergeneman O, Pokki J, Ullrich F, Fusco S, Ortega JA, et al. Electroforming of implantable tubular magnetic microrobots for wireless ophthalmologic applications. Adv Healthc Mater 2015;4:209–14.
[82] Chen B, Ding M, Tan H, Wang S, Liu L, Wang F, et al. Visible-light-driven TiO_2@N-Au nanorobot penetrating the vitreous. Appl Mater Today 2022;27:101455.
[83] Wu Z, Zhou M, Tang X, Zeng J, Li Y, Sun Y, et al. Carrier-free trehalose-based nanomotors targeting macrophages in inflammatory plaque for treatment of atherosclerosis. ACS Nano 2022;16:3808–20.
[84] Liang X, Chen Z, Deng Y, Liu D, Liu X, Huang Q, et al. Field-controlled microrobots fabricated by photopolymerization. Cyborg Bionic Syst 2023;4:0009.
[85] Xu C, Wang S, Wang H, Liu K, Zhang S, Chen B, et al. Magnesium-based micromotors as hydrogen generators for precise rheumatoid arthritis therapy. Nano Lett 2021;21:1982–91.
[86] Li N, Huang C, Zhang J, Zhang J, Huang J, Li S, et al. Chemotactic NO/H_2S nanomotors realizing cardiac targeting of G-CSF against myocardial ischemia-reperfusion injury. ACS Nano 2023;17:12573–93.
[87] Sánchez S, Soler L, Katuri J. Chemically powered micro- and nanomotors. Angew Chem Int Ed 2015;54:1414–44.
[88] Liu D, Wang T, Lu Y. Untethered microrobots for active drug delivery: from rational design to clinical settings. Adv Healthc Mater 2022;11:2102253.
[89] Liu J, Wang T, Dong J, Lu Y. The blood–brain barriers: novel nanocarriers for central nervous system diseases. J Nanobiotechnol 2025;23:146.
[90] Kaur J, Gulati M, Kapoor B, Jha NK, Gupta PK, Gupta G, et al. Advances in designing of polymeric micelles for biomedical application in brain related diseases. Chem Biol Interact 2022;361:109960.
[91] Zhu Y, Liu C, Pang Z. Dendrimer-based drug delivery systems for brain targeting. Biomolecules 2019.
[92] Alaei M, Koushki K, Taebi K, Yousefi Taba M, Keshavarz Hedayati S, Keshavarz SS. Metal nanoparticles in neuroinflammation: impact on microglial dynamics and CNS function. RSC Adv 2025;15:5426–51.
[93] Yang S, Chen Z, Zhou P, Xia J, Deng T, Yu C. Carbon dots based on endogenous nutrients with visible and NIR fluorescence to penetrate blood-brain barrier. Carbon 2023;202:130–40.
[94] Timin AS, Litvak MM, Gorin DA, Atochina-Vasserman EN, Atochin DN, Sukhorukov GB. Cell-based drug delivery and use of nano-and microcarriers for cell functionalization. Adv Healthc Mater 2018;7:1700818.
[95] Wu H, Zhang T, Li N, Gao J. Cell membrane-based biomimetic vehicles for effective central nervous system target delivery: insights and challenges. J Control Release 2023;360:169–84.

[96] Meng W, Chuanshi H, Yaying H, Linlin W, Ling L, Zhu G. Prospects and challenges of extracellular vesicle-based drug delivery system: considering cell source. Drug Deliv 2020;27:585–98.
[97] Mura S, Nicolas J, Couvreur P. Stimuli-responsive nanocarriers for drug delivery. Nat Mater 2013;12:991–1003.
[98] Ismail M, Wang Y, Li Y, Liu J, Zheng M, Zou Y. Stimuli-responsive polymeric nanocarriers accelerate on-demand drug release to combat glioblastoma. Biomacromolecules 2024;25:6250–82.
[99] Das SS, Bharadwaj P, Bilal M, Barani M, Rahdar A, Taboada P, et al. Stimuli-responsive polymeric nanocarriers for drug delivery, imaging, and theragnosis. Polymers 2020.
[100] Hersh AM, Alomari S, Tyler BM. Crossing the blood-brain barrier: advances in nanoparticle technology for drug delivery in neuro-oncology. Int J Mol Sci 2022.
[101] Agrawal M, Saraf S, Saraf S, Dubey SK, Puri A, Patel RJ, et al. Recent strategies and advances in the fabrication of nano lipid carriers and their application towards brain targeting. J Control Release 2020;321:372–415.
[102] Abourehab MA, Ahmed OA, Balata GF, Almalki WH. Self-assembled biodegradable polymeric micelles to improve dapoxetine delivery across the blood–brain barrier. Int J Nanomed 2018;13:3679–87.
[103] Qiao R, Fu C, Forgham H, Javed I, Huang X, Zhu J, et al. Magnetic iron oxide nanoparticles for brain imaging and drug delivery. Adv Drug Deliv Rev 2023;197:114822.
[104] Kheirkhah P, Denyer S, Bhimani AD, Arnone GD, Esfahani DR, Aguilar T, et al. Magnetic drug targeting: a novel treatment for intramedullary spinal cord tumors. Sci Rep 2018;8:11417.
[105] Lin F-W, Chen P-Y, Wei K-C, Huang C-Y, Wang C-K, Yang H-W, et al. Rapid in situ MRI traceable gel-forming dual-drug delivery for synergistic therapy of brain tumor stimuli-responsive nanocarriers for drug delivery, tumor imaging, therapy and theranostics. Theranostics 2017;7:2524–36.
[106] Vieira DB, Gamarra LF. Getting into the brain: liposome-based strategies for effective drug delivery across the blood–brain barrier. Int J Nanomed 2016;11:5381–414.
[107] Shariare MH, Rahman M, Lubna SR, Roy RS, Abedin J, Marzan AL, et al. Liposomal drug delivery of Aphanamixis polystachya leaf extracts and its neurobehavioral activity in mice model. Sci Rep 2020;10:6938.
[108] Kumar P, Sharma G, Kumar R, Singh B, Malik R, Katare OP, et al. Promises of a biocompatible nanocarrier in improved brain delivery of quercetin: Biochemical, pharmacokinetic and biodistribution evidences. Int J Pharm 2016;515:307–14.
[109] Alotaibi BS, Manal B, Abdalla IN, Jaber KZ, Munazza I, Sobia N, et al. Potential of nanocarrier-based drug delivery systems for brain targeting: a current review of literature. Int J Nanomed 2021;16:7517–33.
[110] Yin Y, Wang J, Yang M, Du R, Pontrelli G, McGinty S, et al. Penetration of the blood–brain barrier and the anti-tumour effect of a novel PLGA-lysoGM1/DOX micelle drug delivery system. Nanoscale 2020;12:2946–60.
[111] Zhang Q, Yang L, Zheng Y, Wu X, Chen X, Fei F, et al. Electro-responsive micelle-based universal drug delivery system for on-demand therapy in epilepsy. J Control Release 2023;360:759–71.
[112] Mishra V, Kesharwani P. Dendrimer technologies for brain tumor. Drug Discov Today 2016;21:766–78.
[113] Li H, Zha S, Li H, Liu H, Wong K-L, All AH. Polymeric dendrimers as nanocarrier vectors for neurotheranostics. Small 2022;18:2203629.
[114] Sheikh MA, Malik YS, Xing Z, Guo Z, Tian H, Zhu X, et al. Polylysine-modified polyethylenimine (PEI-PLL) mediated VEGF gene delivery protects dopaminergic neurons in cell culture and in rat models of Parkinson's Disease (PD). Acta Biomater 2017;54:58–68.
[115] Somani S, Blatchford DR, Millington O, Stevenson ML, Dufès C. Transferrin-bearing polypropylenimine dendrimer for targeted gene delivery to the brain. J Control Release 2014;188:78–86.
[116] Song P, Song N, Li L, Wu M, Lu Z, Zhao X. Angiopep-2-modified carboxymethyl chitosan-based ph/reduction dual-stimuli-responsive nanogels for enhanced targeting glioblastoma. Biomacromolecules 2021;22:2921–34.
[117] Vashist A, Kaushik A, Vashist A, Bala J, Nikkhah-Moshaie R, Sagar V, et al. Nanogels as potential drug nanocarriers for CNS drug delivery. Drug Discov Today 2018;23:1436–43.
[118] Zhang B, Bai M, Yang M, Wang Y, Chen X, Liu B, et al. Injectable nanocomposite hydrogel for localized precision delivery of dexamethasone after traumatic brain injury: dual modulation of neuroinflammation and blood-brain barrier restoration. J Transl Med 2025;23:579.
[119] Gao J, Song Q, Gu X, Jiang G, Huang J, Tang Y, et al. Intracerebral fate of organic and inorganic nanoparticles is dependent on microglial extracellular vesicle function. Nat Nanotechnol 2024;19:376–86.
[120] Li X, Vemireddy V, Cai Q, Xiong H, Kang P, Li X, et al. Reversibly modulating the blood–brain barrier by laser stimulation of molecular-targeted nanoparticles. Nano Lett 2021;21:9805–15.
[121] Cheng Y, Dai Q, Morshed RA, Fan X, Wegscheid ML, Wainwright DA, et al. Blood-brain barrier permeable gold nanoparticles: an efficient delivery platform for enhanced malignant glioma therapy and imaging. Small 2014;10:5137–50.
[122] Kruse B, Dash BS, Kostka K, Wolff N, Prymak O, Loza K, et al. Doxorubicin-loaded ultrasmall gold nanoparticles (1.5 nm) for brain tumor therapy and assessment of their biodistribution. ACS Appl Bio Mater 2024;7:6890–907.
[123] Truong TT, Mondal S, Doan VHM, Tak S, Choi J, Oh H, et al. Precision-engineered metal and metal-oxide nanoparticles for biomedical imaging and healthcare applications. Adv Colloid Interface Sci 2024;332:103263.
[124] Fu C, Duan X, Cao M, Jiang S, Ban X, Guo N, et al. Targeted magnetic resonance imaging and modulation of hypoxia with multifunctional hyaluronic acid-MnO2 nanoparticles in glioma. Adv Healthc Mater 2019;8:1900047.
[125] Cheng KK, Chan PS, Fan S, Kwan SM, Yeung KL, Wáng Y-X-J, et al. Curcumin-conjugated magnetic nanoparticles for detecting amyloid plaques in Alzheimer's disease mice using magnetic resonance imaging (MRI). Biomaterials 2015;44:155–72.
[126] Chen Z-A, Wu C-H, Wu S-H, Huang C-Y, Mou C-Y, Wei K-C, et al. Receptor ligand-free mesoporous silica nanoparticles: a streamlined strategy for targeted drug delivery across the blood–brain barrier. ACS Nano 2024;18:12716–36.
[127] Jiao M, Li X, Liu H, Cai P, Yang X, McHugh KJ, et al. Aqueous grown quantum dots with robust near-infrared fluorescence for integrated traumatic brain injury diagnosis and surgical monitoring. ACS Nano 2024;18:19038–53.
[128] Hsu T-I, Chen Y-P, Zhang R-L, Chen Z-A, Wu C-H, Chang W-C, et al. Overcoming the blood–brain tumor barrier with docetaxel-loaded mesoporous silica nanoparticles for treatment of temozolomide-resistant glioblastoma. ACS Appl Mater Interfaces 2024;16:21722–35.
[129] Sun G, Zeng S, Liu X, Shi H, Zhang R, Wang B, et al. Synthesis and characterization of a silica-based drug delivery system for spinal cord injury therapy. Nano-Micro Letters 2019;11:23.
[130] Guo Q, Qian Z-M. Macrophage based drug delivery: key challenges and strategies. Bioact Mater 2024;38:55–72.
[131] Zhou L, Liu H, Zhang B, Wei C, Zhou S, Huang X, et al. A novel 3D-printed Bi-Layer cranial-brain patch promotes brain injury repair and bone tissue regeneration. Adv Funct Mater 2024;34:2314330.
[132] Li Z, Wang Y, Ding Y, Repp L, Kwon GS, Hu Q. Cell-based delivery systems: emerging carriers for immunotherapy. Adv Funct Mater 2021;31:2100088.
[133] Wang X, Jianqing G, Xumei O, Junbo W, Xiaoyi S, Lv Y. Mesenchymal stem cells loaded with paclitaxel-poly(lactic-co-glycolic acid) nanoparticles for glioma-targeting therapy. Int J Nanomed 2018;13:5231–48.
[134] Li W, Cheng J, He F, Zhang P, Zhang N, Wang J, et al. Cell membrane-based nanomaterials for theranostics of central nervous system diseases. J Nanobiotechnol 2023;21:276.
[135] Ma Y, Yi J, Ruan J, Ma J, Yang Q, Zhang K, et al. Engineered cell membrane-coated nanoparticles: new strategies in glioma targeted therapy and immune modulation. Adv Healthc Mater 2024;13:2400514.
[136] Parodi A, Quattrocchi N, van de Ven AL, Chiappini C, Evangelopoulos M, Martinez JO, et al. Synthetic nanoparticles functionalized with biomimetic leukocyte membranes possess cell-like functions. Nat Nanotechnol 2013;8:61–8.
[137] Liao J, Gong L, Xu Q, Wang J, Yang Y, Zhang S, et al. Revolutionizing neurocare: biomimetic nanodelivery via cell membranes. Adv Mater 2024;36:2402445.
[138] Fan Y, Cui Y, Hao W, Chen M, Liu Q, Wang Y, et al. Carrier-free highly drug-loaded biomimetic nanosuspensions encapsulated by cancer cell membrane based on homology and active targeting for the treatment of glioma. Bioact Mater 2021;6:4402–14.

[139] Wang J, Liu Y, Liu F, Gan S, Roy S, Hasan I, et al. Emerging extracellular vesicle-based carriers for glioblastoma diagnosis and therapy. Nanoscale 2023;15:10904–38.
[140] Ye Z, Zhang T, He W, Jin H, Liu C, Yang Z, et al. Methotrexate-loaded extracellular vesicles functionalized with therapeutic and targeted peptides for the treatment of glioblastoma multiforme. ACS Appl Mater Interfaces 2018;10:12341–50.
[141] Wang J, Tang W, Yang M, Yin Y, Li H, Hu F, et al. Inflammatory tumor microenvironment responsive neutrophil exosomes-based drug delivery system for targeted glioma therapy. Biomaterials 2021;273:120784.
[142] Shu M, Tang J, Chen L, Zeng Q, Li C, Xiao S, et al. Tumor microenvironment triple-responsive nanoparticles enable enhanced tumor penetration and synergetic chemo-photodynamic therapy. Biomaterials 2021;268:120574.
[143] Luo M, Lewik G, Ratcliffe JC, Choi CHJ, Mäkilä E, Tong WY, et al. Systematic evaluation of transferrin-modified porous silicon nanoparticles for targeted delivery of doxorubicin to glioblastoma. ACS Appl Mater Interfaces 2019;11:33637–49.
[144] Hu X, Guan X, Li J, Pei Q, Liu M, Xie Z, et al. Hybrid polymer micelles capable of cRGD targeting and pH-triggered surface charge conversion for tumor selective accumulation and promoted uptake. Chem Commun 2014;50:9188–91.
[145] Shi J, Tan C, Ge X, Qin Z, Xiong H. Recent advances in stimuli-responsive controlled release systems for neuromodulation. J Mater Chem B 2024;12:5769–86.
[146] Yang Z, Luo Y, Yu H, Liang K, Wang M, Wang Q, et al. Reshaping the tumor immune microenvironment based on a light-activated nanoplatform for efficient cancer therapy. Adv Mater 2022;34:2108908.
[147] Xiong S, Li Z, Liu Y, Wang Q, Luo J, Chen X, et al. Brain-targeted delivery shuttled by black phosphorus nanostructure to treat Parkinson's disease. Biomaterials 2020;260:120339.
[148] Xie J, Shen Z, Anraku Y, Kataoka K, Chen X. Nanomaterial-based blood-brain-barrier (BBB) crossing strategies. Biomaterials 2019;224:119491.
[149] Lilius TO, Blomqvist K, Hauglund NL, Liu G, Stæger FF, Bærentzen S, et al. Dexmedetomidine enhances glymphatic brain delivery of intrathecally administered drugs. J Control Release 2019;304:29–38.
[150] Noorani I, de la Rosa J. Breaking barriers for glioblastoma with a path to enhanced drug delivery. Nat Commun 2023;14:5909.
[151] Noseda L, Sakar MS. Small-scale robotic devices for medical interventions in the brain. MRS Bull 2024;49:125–35.
[152] Zhu P, Simon I, Kokalari I, Kohane DS, Rwei AY. Miniaturized therapeutic systems for ultrasound-modulated drug delivery to the central and peripheral nervous system. Adv Drug Deliv Rev 2024;208:115275.
[153] Rae AI, O'Neill BE, Godil J, Fecker AL, Ross D. Low-cost wound healing protocol reduces infection and reoperation rates after cranioplasty: a retrospective cohort study. Neurosurgery 2023:93.
[154] Pingue V, Franciotta D. Functional outcome in patients with traumatic or hemorrhagic brain injuries undergoing decompressive craniectomy versus craniotomy and 6-month rehabilitation. Sci Rep 2023;13:10624.
[155] Del Campo FA, Glück C, Droux J, Ferry Y, Frei C, Wegener S, et al. Ultrasound trapping and navigation of microrobots in the mouse brain vasculature. Nat Commun 2023;14:5889.
[156] Wu J, Jiao N, Lin D, Li N, Ma T, Tung S, et al. Dual-responsive nanorobot-based marsupial robotic system for intracranial cross-scale targeting drug delivery. Adv Mater 2024;36:2306876.
[157] Li J, Mayorga-Martinez CC, Ohl C-D, Pumera M. Ultrasonically propelled micro- and nanorobots. Adv Funct Mater 2022;32:2102265.
[158] Li L, Yu Z, Liu J, Yang M, Shi G, Feng Z, et al. Swarming responsive photonic nanorobots for motile-targeting microenvironmental mapping and mapping-guided photothermal treatment. Nano-Micro Lett 2023;15:141.
[159] Wang H, Chen X, Qi Y, Wang C, Huang L, Wang R, et al. Self-propelled nanomotors with an alloyed engine for emergency rescue of traumatic brain injury. Adv Mater 2022;34:2206779.
[160] Wang S, Liu K, Zhou Q, Xu C, Gao J, Wang Z, et al. Hydrogen-powered microswimmers for precise and active hydrogen therapy towards acute ischemic stroke. Adv Funct Mater 2021;31:2009475.
[161] Gao Y, Mao M, Li Y, Xuan M, Wu Y, He Q. A self-directed Trojanbot-enzymatic nanobot in neutrobot for active target therapy of glioblastoma. Nat Commun 2025;16:5263.
[162] Zhao D, Feng P-J, Liu J-H, Dong M, Shen X-Q, Chen Y-X, et al. Electromagnetized-nanoparticle-modulated neural plasticity and recovery of degenerative dopaminergic neurons in the mid-brain. Adv Mater 2020;32:2003800.
[163] Santos LF, Silva AS, Mano JF. Magnetic-based strategies for regenerative medicine and tissue engineering. Adv Healthc Mater 2023;12:2300605.
[164] Chung H-J, Parsons AM, Zheng L. Magnetically controlled soft robotics utilizing elastomers and gels in actuation: a review. Adv Intell Syst 2021;3:2000186.
[165] Li J, Shen H, Zhou H, Shi R, Wu C, Chu PK. Antimicrobial micro/nanorobotic materials design: from passive combat to active therapy. Mater Sci Eng R Rep 2023;152:100712.
[166] Wrede P, Degtyaruk O, Kalva SK, Deán-Ben XL, Bozuyuk U, Aghakhani A, et al. Real-time 3D optoacoustic tracking of cell-sized magnetic microrobots circulating in the mouse brain vasculature. Sci Adv 2022;8:eabm9132.
[167] Kim E, Jeon S, Yang Y-S, Jin C, Kim J-y, Oh Y-S, et al. A neurospheroid-based microrobot for targeted neural connections in a hippocampal slice. Adv Mater 2023;35:2208747.
[168] Mahoney AW, Nelson ND, Peyer KE, Nelson BJ, Abbott JJ. Behavior of rotating magnetic microrobots above the step-out frequency with application to control of multi-microrobot systems. Appl Phys Lett 2014;104:144101.
[169] Agrahari V, Agrahari V, Chou M-L, Chew CH, Noll J, Burnouf T. Intelligent micro-/nanorobots as drug and cell carrier devices for biomedical therapeutic advancement: promising development opportunities and translational challenges. Biomaterials 2020;260:120163.
[170] Soto F, Wang J, Ahmed R, Demirci U. Medical micro/nanorobots in precision medicine. Adv Sci 2020;7:2002203.
[171] Ye M, Zhou Y, Zhao H, Wang X. Magnetic microrobots with folate targeting for drug delivery. Cyborg Bionic Syst 2023;4:0019.
[172] Ye Z, Sitti M. Dynamic trapping and two-dimensional transport of swimming microorganisms using a rotating magnetic microrobot. Lab Chip 2014;14:2177–82.
[173] Jin D, Zhang L. Collective behaviors of magnetic active matter: recent progress toward reconfigurable, adaptive, and multifunctional swarming micro/nanorobots. Acc Chem Res 2022;55:98–109.
[174] Wang Y, Shen J, Handschuh-Wang S, Qiu M, Du S, Wang B. Microrobots for targeted delivery and therapy in digestive system. ACS Nano 2023;17:27–50.
[175] Go G, Song H-W, Nan M, Lee J, Kim S, Park J-O, et al. A soft biodegradable chitosan-based medical microrobot with optimized structural design and X-ray visibility for targeted vessel chemoembolization. Adv Funct Mater 2023;33:2305205.
[176] Li J, Esteban-Fernández de Ávila B, Gao W, Zhang L, Wang J. Micro/nanorobots for biomedicine: delivery, surgery, sensing, and detoxification. Sci Rob 2017;2:eaam6431.
[177] Chen Y, Chen D, Liang S, Dai Y, Bai X, Song B, et al. Recent advances in field-controlled micro–nano manipulations and micro–nano robots. Adv Intell Syst 2022;4:2100116.
[178] Sun Z, Hou Y. Micro/nanorobots as active delivery systems for biomedicine: from self-propulsion to controllable navigation. Adv Therapeutics 2022;5:2100228.
[179] Wang Q, Wang Q, Ning Z, Chan KF, Jiang J, Wang Y, et al. Tracking and navigation of a microswarm under laser speckle contrast imaging for targeted delivery. Sci Rob 2024;9:eadh1978.
[180] Dong H, Lin J, Tao Y, Jia Y, Sun L, Li WJ, et al. AI-enhanced biomedical micro/nanorobots in microfluidics. Lab Chip 2024;24:1419–40.
[181] Li M, Wu J, Li N, Zhou J, Cheng W, Wu A, et al. Cross-scale drug delivery of diatom microrobots based on a magnetic continuum robot for combined chemical and photodynamic therapy of glioblastoma. Adv Funct Mater 2024;34:2402333.
[182] Wang J, Dong Y, Ma P, Wang Y, Zhang F, Cai B, et al. Intelligent micro-/nanorobots for cancer theragnostic. Adv Mater 2022;34:2201051.
[183] Wang B, Chan KF, Yuan K, Wang Q, Xia X, Yang L, et al. Endoscopy-assisted magnetic navigation of biohybrid soft microrobots with rapid endoluminal delivery and imaging. Sci Rob 2021;6:eabd2813.

[184] Su L, Jin D, Wang Y, Wang Q, Pan C, Jiang S, et al. Modularized microrobot with lock-and-detachable modules for targeted cell delivery in bile duct. Sci Adv 2023;9:eadj0883.
[185] Yang H, Yang Z, Jin D, Su L, Chan KF, Chong KKL, et al. Magnetic micro-driller system for nasolacrimal duct recanalization. IEEE Rob Autom Lett 2022;7:7367–74.
[186] Law J, Wang X, Luo M, Xin L, Du X, Dou W, et al. Microrobotic swarms for selective embolization. Sci Adv 2022;8:eabm5752.
[187] Bozuyuk U, Ozturk H, Sitti M. Microrobotic locomotion in blood vessels: a computational study on the performance of surface microrollers in the cardiovascular system. Adv Intell Syst 2023;5:2300099.
[188] Lin D, Jiao N, Wang Z, Liu L. A magnetic continuum robot with multi-mode control using opposite-magnetized magnets. IEEE Rob Autom Lett 2021;6:2485–92.
[189] Mao L, Yang P, Tian C, Shen X, Wang F, Zhang H, et al. Magnetic steering continuum robot for transluminal procedures with programmable shape and functionalities. Nat Commun 2024;15:3759.
[190] Huang Y, Zhao Q, Hu J, Liu H. Design and modeling of a multi-DoF magnetic continuum robot with diverse deformation modes. IEEE Rob Autom Lett 2024;9:3956–63.
[191] Yang P, Mao L, Tian C, Meng X, Xie H. A cooperative and multifunctional magnetic continuum robot for noninteractive access, dexterous navigation, and versatile manipulation. Adv Funct Mater 2025;35:2412543.
[192] Kim Y, Parada GA, Liu S, Zhao X. Ferromagnetic soft continuum robots. Sci Rob 2019;4:eaax7329.
[193] Sitti M. Microscale and nanoscale robotics systems[Grand challenges of robotics]. IEEE Rob Autom Mag 2007;14:53–60.
[194] Sitti M, Wiersma DS. Pros and cons: magnetic versus optical microrobots. Adv Mater 2020;32:1906766.
[195] Yan X, Zhou Q, Vincent M, Deng Y, Yu J, Xu J, et al. Multifunctional biohybrid magnetite microrobots for imaging-guided therapy. Sci Rob 2017;2:eaaq1155.
[196] Cao Y, Sathish CI, Guan X, Wang S, Palanisami T, Vinu A, et al. Advances in magnetic materials for microplastic separation and degradation. J Hazard Mater 2024;461:132537.
[197] Yang Y, Li Z, Fan X, Jiang C, Wang J, Rastegar-Kashkooli Y, et al. Nanozymes: potential therapies for reactive oxygen species overproduction and inflammation in ischemic stroke and traumatic brain injury. ACS Nano 2024;18:16450–67.
[198] Quan Z, Wang S, Xie H, Zhang J, Duan R, Li M, et al. ROS regulation in CNS disorder therapy: unveiling the dual roles of nanomedicine. Small 2025;21:2410031.
[199] Stolp HB, Dziegielewska KM. Review: Role of developmental inflammation and blood–brain barrier dysfunction in neurodevelopmental and neurodegenerative diseases. Neuropathol Appl Neurobiol 2009;35:132–46.
[200] Shi K, Zhang J, Dong J-f, Shi F-D. Dissemination of brain inflammation in traumatic brain injury. Cell Mol Immunol 2019;16:523–30.
[201] Cheng Y, Liu X, Rutkowski S, Badaraev AD, Kozelskaya AI, Tverdokhlebov SI, et al. Investigation of the antibacterial properties of janus micromotors catalytic propelled by manganese dioxide and hydrogen peroxide to reduce bacterial density. ACS Appl Bio Mater 2024;7:6529–41.
[202] Neettiyath A, Pumera M. Micro/nanorobots for advanced light-based biosensing and imaging. Adv Funct Mater 2025;35:2415875.
[203] Zhang Z, Wang L, Chan TKF, Chen Z, Ip M, Chan PKS, et al. Micro-/nanorobots in antimicrobial applications: recent progress, challenges, and opportunities. Adv Healthc Mater 2022;11:2101991.
[204] Srivastava SK, Guix M, Schmidt OG. Wastewater mediated activation of micromotors for efficient water cleaning. Nano Lett 2016;16:817–21.
[205] Fu L-H, Qi C, Lin J, Huang P. Catalytic chemistry of glucose oxidase in cancer diagnosis and treatment. Chem Soc Rev 2018;47:6454–72.
[206] Arqué X, Romero-Rivera A, Feixas F, Patiño T, Osuna S, Sánchez S. Intrinsic enzymatic properties modulate the self-propulsion of micromotors. Nat Commun 2019;10:2826.
[207] Yang G, Zhang Z, He S, Yuan L, Yang X. Advances in micro/nanomotor linked with bioenzymes: Design and applications. Appl Mater Today 2024;39:102287.
[208] Chen C, Karshalev E, Li J, Soto F, Castillo R, Campos I, et al. Transient micromotors that disappear when no longer needed. ACS Nano 2016;10:10389–96.
[209] Lin Z, Gao C, Wang D, He Q. Bubble-propelled janus gallium/zinc micromotors for the active treatment of bacterial infections. Angew Chem Int Ed 2021;60:8750–4.
[210] Yu Y, Liang L, Sun T, Lu H, Yang P, Li J, et al. Micro/nanomotor-driven intelligent targeted delivery systems: dynamics sources and frontier applications. Adv Healthc Mater 2024;13:2400163.
[211] Chen C, Karshalev E, Guan J, Wang J. Magnesium-based micromotors: water-powered propulsion, multifunctionality, and biomedical and environmental applications. Small 2018;14:1704252.
[212] Dutta S, Noh S, Gual RS, Chen X, Pané S, Nelson BJ, et al. Recent developments in metallic degradable micromotors for biomedical and environmental remediation applications. Nano-Micro Letters 2023;16:41.
[213] Ji X, Tian Y, Xie K, Liu W, Qu Y, Fei Z. Protective effects of hydrogen-rich saline in a rat model of traumatic brain injury via reducing oxidative stress. J Surg Res 2012;178:e9–16.
[214] Xu M, Wu G, You Q, Chen X. The landscape of smart biomaterial-based hydrogen therapy. Adv Sci 2024;11:2401310.
[215] Elnaggar A, Kang S, Tian M, Han B, Keshavarz M. State of the art in actuation of micro/nanorobots for biomedical applications. Small Sci 2024;4:2300211.
[216] Ruiz-González N, Esporrín-Ubieto D, Kim I-D, Wang J, Sánchez S. Micro- and nanomotors: engineered tools for targeted and efficient biomedicine. ACS Nano 2025;19:8411–32.
[217] Li D, Liu C, Yang Y, Wang L, Shen Y. Micro-rocket robot with all-optic actuating and tracking in blood. Light Sci Appl 2020;9:84.
[218] Esteban-Fernández de Ávila B, Ramírez-Herrera DE, Campuzano S, Angsantikul P, Zhang L, Wang J. Nanomotor-enabled pH-responsive intracellular delivery of caspase-3: toward rapid cell apoptosis. ACS Nano 2017;11:5367–74.
[219] Wu Z, Li L, Yang Y, Hu P, Li Y, Yang S-Y, et al. A microrobotic system guided by photoacoustic computed tomography for targeted navigation in intestines in vivo. Sci Rob 2019;4. eaax0613.
[220] Dayton P, Klibanov A, Brandenburger G, Ferrara K. Acoustic radiation force in vivo: a mechanism to assist targeting of microbubbles. Ultrasound Med Biol 1999;25:1195–201.
[221] Liu Q, Yang Y, Fan X. Microvascular pericytes in brain-associated vascular disease. Biomed Pharmacother 2020;121:109633.
[222] Chen T, Dai Y, Hu C, Lin Z, Wang S, Yang J, et al. Cellular and molecular mechanisms of the blood–brain barrier dysfunction in neurodegenerative diseases. Fluids Barriers CNS 2024;21:60.
[223] Varghese SM, Patel S, Nandan A, Jose A, Ghosh S, Sah RK, et al. Unraveling the role of the blood-brain barrier in the pathophysiology of depression: recent advances and future perspectives. Mol Neurobiol 2024;61:10398–447.
[224] Coureuil M, Lécuyer H, Bourdoulous S, Nassif X. A journey into the brain: insight into how bacterial pathogens cross blood–brain barriers. Nat Rev Microbiol 2017;15:149–59.
[225] Tang W, Fan W, Lau J, Deng L, Shen Z, Chen X. Emerging blood–brain-barrier-crossing nanotechnology for brain cancer theranostics. Chem Soc Rev 2019;48:2967–3014.
[226] Fan K, Jia X, Zhou M, Wang K, Conde J, He J, et al. Ferritin nanocarrier traverses the blood brain barrier and kills glioma. ACS Nano 2018;12:4105–15.
[227] Rosa LCS, Argolo CO, Nascimento CMC, Pimentel AS. Identifying substructures that facilitate compounds to penetrate the blood–brain barrier via passive transport using machine learning explainer models. ACS Chem Neurosci 2024;15:2144–59.
[228] Wang X, Yin Y, Zhou H, Chi B, Guan L, Li P, et al. Drug delivery pathways to the central nervous system via the brain glymphatic system circumventing the blood-brain barrier. Exploration 2024:20240036.
[229] Monge-Fuentes V, Biolchi Mayer A, Lima MR, Geraldes LR, Zanotto LN, Moreira KG, et al. Dopamine-loaded nanoparticle systems circumvent the blood–brain barrier restoring motor function in mouse model for Parkinson's Disease. Sci Rep 2021;11:15185.
[230] Culkins C, Adomanis R, Phan N, Robinson B, Slaton E, Lothrop E, et al. Unlocking the gates: therapeutic agents for noninvasive drug delivery across the blood-brain barrier. Mol Pharm 2024;21:5430–54.
[231] Pardridge WM. Blood–brain barrier endogenous transporters as therapeutic targets: a new model for small molecule CNS drug discovery. Expert Opin Ther Targets 2015;19:1059–72.

[232] Anraku Y, Kuwahara H, Fukusato Y, Mizoguchi A, Ishii T, Nitta K, et al. Glycaemic control boosts glucosylated nanocarrier crossing the BBB into the brain. Nat Commun 2017;8:1001.
[233] Montaser AB, Järvinen J, Löffler S, Huttunen J, Auriola S, Lehtonen M, et al. L-type amino acid transporter 1 enables the efficient brain delivery of small-sized prodrug across the blood–brain barrier and into human and mouse brain parenchymal cells. ACS Chem Neurosci 2020;11:4301–15.
[234] Ahmed HS. The multifaceted role of L-type amino acid transporter 1 at the blood–brain barrier: structural implications and therapeutic potential. Mol Neurobiol 2025;62:3813–32.
[235] Piantino M, Louis F, Shigemoto-Mogami Y, Kitamura K, Sato K, Yamaguchi T, et al. Brain microvascular endothelial cells derived from human induced pluripotent stem cells as in vitro model for assessing blood-brain barrier transferrin receptor-mediated transcytosis. Mater Today Bio 2022;14:100232.
[236] Johnsen KB, Burkhart A, Melander F, Kempen PJ, Vejlebo JB, Siupka P, et al. Targeting transferrin receptors at the blood-brain barrier improves the uptake of immunoliposomes and subsequent cargo transport into the brain parenchyma. Sci Rep 2017;7:10396.
[237] Zhang W, Liu QY, Haqqani AS, Leclerc S, Liu Z, Fauteux F, et al. Differential expression of receptors mediating receptor-mediated transcytosis (RMT) in brain microvessels, brain parenchyma and peripheral tissues of the mouse and the human. Fluids Barriers CNS 2020;17:47.
[238] Gray SM, Aylor KW, Barrett EJ. Unravelling the regulation of insulin transport across the brain endothelial cell. Diabetologia 2017;60:1512–21.
[239] Xia X, Zhou Y, Gao H. Prodrug strategy for enhanced therapy of central nervous system disease. Chem Commun 2021;57:8842–55.
[240] Luo Y, Che X, Zheng G, Liu Z, Xie D, Wang L. Microfluidic preparation and evaluation of multivesicular liposomes containing gastrodin for oral delivery across the blood–brain barrier. Mol Pharm 2024;21:5607–18.
[241] Lu L, Zhao X, Fu T, Li K, He Y, Luo Z, et al. An iRGD-conjugated prodrug micelle with blood-brain-barrier penetrability for anti-glioma therapy. Biomaterials 2020;230:119666.
[242] Patel MM, Patel BM. Crossing the blood–brain barrier: recent advances in drug delivery to the brain. CNS Drugs 2017;31:109–33.
[243] Zhou Y, Peng Z, Seven ES, Leblanc RM. Crossing the blood-brain barrier with nanoparticles. J Control Release 2018;270:290–303.
[244] Zhang W, Mehta A, Tong Z, Esser L, Voelcker NH. Development of polymeric nanoparticles for blood–brain barrier transfer—strategies and challenges. Adv Sci 2021;8:2003937.
[245] Rezai AR, Ranjan M, Haut MW, Carpenter J, D'Haese P-F, Mehta RI, et al. Focused ultrasound–mediated blood-brain barrier opening in Alzheimer's disease: long-term safety, imaging, and cognitive outcomes. J Neurosurg 2023;139:275–83.
[246] Daniels TR, Bernabeu E, Rodríguez JA, Patel S, Kozman M, Chiappetta DA, et al. The transferrin receptor and the targeted delivery of therapeutic agents against cancer. Biochim Biophys Acta Gen Subj 2012;1820:291–317.
[247] Sjöström DJ, Mohlin C, Ambrosetti E, Garforth SJ, Teixeira AI, Bjelic S. Motif-driven protein binder design towards transferrin receptor helical domain. FEBS J 2022;289:2935–47.
[248] Hultqvist G, Syvänen S, Fang XT, Lannfelt L, Sehlin D, Xie B-S, et al. Bivalent brain shuttle increases antibody uptake by monovalent binding to the transferrin receptor apolipoprotein E, low-density lipoprotein receptor, and immune cells control blood-brain barrier penetration by AAV-PHP.eB in mice. Theranostics 2017;7:308–18.
[249] Moura RP, Cláudia M, Soraia P, Flávia S, Sarmento B. Blood-brain barrier receptors and transporters: an insight on their function and how to exploit them through nanotechnology. Expert Opin Drug Deliv 2019;16:271–85.
[250] Reimund M, Dearborn AD, Graziano G, Lei H, Ciancone AM, Kumar A, et al. Structure of apolipoprotein B100 bound to the low-density lipoprotein receptor. Nature 2025;638:829–35.
[251] Xie B-S, Wang X, Pan Y-H, Jiang G, Feng J-F, Lin Y. Apolipoprotein E, low-density lipoprotein receptor, and immune cells control blood-brain barrier penetration by AAV-PHP.eB in mice. Theranostics 2021;11:1177–91.
[252] Banks WA, Owen JB, Erickson MA. Insulin in the brain: there and back again. Pharmacol Ther 2012;136:82–93.
[253] Werner H, LeRoith D. Insulin and insulin-like growth factor receptors in the brain: physiological and pathological aspects. Eur Neuropsychopharmacol 2014; 24:1947–53.
[254] Pardridge WM. Kinetics of blood–brain barrier transport of monoclonal antibodies targeting the insulin receptor and the transferrin receptor. Pharmaceuticals 2022.
[255] Kzhyshkowska J, Neyen C, Gordon S. Role of macrophage scavenger receptors in atherosclerosis. Immunobiology 2012;217:492–502.
[256] Srimanee A, Regberg J, Hällbrink M, Vajragupta O, Langel Ü. Role of scavenger receptors in peptide-based delivery of plasmid DNA across a blood–brain barrier model. Int J Pharm 2016;500:128–35.
[257] Zani IA, Stephen SL, Mughal NA, Russell D, Homer-Vanniasinkam S, Wheatcroft SB, et al. Scavenger receptor structure and function in health and disease. Cells 2015:178–201.
[258] McCord E, Pawar S, Koneru T, Tatiparti K, Sau S, Iyer AK. Folate receptors' expression in gliomas may possess potential nanoparticle-based drug delivery opportunities. ACS Omega 2021;6:4111–8.
[259] Alam C, Hoque MT, Finnell RH, Goldman ID, Bendayan R. Regulation of reduced folate carrier (RFC) by vitamin D receptor at the blood-brain barrier. Mol Pharm 2017;14:3848–58.
[260] Wei X, Zhan C, Shen Q, Fu W, Xie C, Gao J, et al. A D-peptide ligand of nicotine acetylcholine receptors for brain-targeted drug delivery. Angew Chem Int Ed 2015;54:3023–7.
[261] Xiao X, Gao Y, Liu S, Wang M, Zhong M, Wang J, et al. A "nano-courier" for precise delivery of acetylcholine and melatonin by C5a-targeted aptamers effectively attenuates reperfusion injury of ischemic stroke. Adv Funct Mater 2023;33:2213633.
[262] Butiaeva LI, Slutzki T, Swick HE, Bourguignon C, Robins SC, Liu X, et al. Leptin receptor-expressing pericytes mediate access of hypothalamic feeding centers to circulating leptin. Cell Metab 2021;33. 1433 48.e5.
[263] Aloss K, Hamar P. Recent preclinical and clinical progress in liposomal doxorubicin. Pharmaceutics 2023.
[264] Wang P, Xue Y, Shang X, Liu Y. Diphtheria toxin mutant CRM197-mediated transcytosis across blood–brain barrier in vitro. Cell Mol Neurobiol 2010;30: 717–25.
[265] Tosi G, Vilella A, Veratti P, Belletti D, Pederzoli F, Ruozi B, et al. Exploiting bacterial pathways for BBB crossing with PLGA nanoparticles modified with a mutated form of diphtheria toxin (CRM197). In Vivo Exp Mol Pharm 2015;12:3672–84.
[266] Christianson HC, Belting M. Heparan sulfate proteoglycan as a cell-surface endocytosis receptor. Matrix Biol 2014;35:51–5.
[267] Zhang X, Wang B, Li J-P. Implications of heparan sulfate and heparanase in neuroinflammation. Matrix Biol 2014;35:174–81.
[268] Kuo TT, Baker K, Yoshida M, Qiao S-W, Aveson VG, Lencer WI, et al. Neonatal Fc receptor: from immunity to therapeutics. J Clin Immunol 2010;30:777–89.
[269] Nortley R, Attwell D. Control of brain energy supply by astrocytes. Curr Opin Neurobiol 2017;47:80–5.
[270] Ouyang M, Detre JA, Hyland JL, Sindabizera KL, Kuschner ES, Edgar JC, et al. Spatiotemporal cerebral blood flow dynamics underlies emergence of the limbic-sensorimotor-association cortical gradient in human infancy. Nat Commun 2024;15:8944.
[271] Adusei KM, Ngo TB, Sadtler K. T lymphocytes as critical mediators in tissue regeneration, fibrosis, and the foreign body response. Acta Biomater 2021;133: 17–33.
[272] Fu D, Wang Z, Tu Y, Peng F. Interactions between biomedical micro-/nano-motors and the immune molecules, immune cells, and the immune system: challenges and opportunities. Adv Healthc Mater 2021;10:2001788.
[273] Yuan D, Zhao Y, Banks WA, Bullock KM, Haney M, Batrakova E, et al. Macrophage exosomes as natural nanocarriers for protein delivery to inflamed brain. Biomaterials 2017;142:1–12.
[274] Yin Y, Tang W, Ma X, Tang L, Zhang Y, Yang M, et al. Biomimetic neutrophil and macrophage dual membrane-coated nanoplatform with orchestrated tumor-microenvironment responsive capability promotes therapeutic efficacy against glioma. Chem Eng J 2022;433:133848.
[275] Chen J, Zeng S, Xue Q, Hong Y, Liu L, Song L, et al. Photoacoustic image-guided biomimetic nanoparticles targeting rheumatoid arthritis. Proc Natl Acad Sci 2022;119:e2213373119.
[276] Wen W, Cheng J, Tang Y. Brain perivascular macrophages: current understanding and future prospects. Brain 2024;147:39–55.

[277] Royse MK, Fowler M, Mai AK, He Y, Durante MR, Buist N, et al. Development of a 3D printed perfusable in vitro blood–brain barrier model for use as a scalable screening tool. Biomater Sci 2024;12:4363–75.
[278] Ding S, Khan AI, Cai X, Song Y, Lyu Z, Du D, et al. Overcoming blood–brain barrier transport: advances in nanoparticle-based drug delivery strategies. Mater Today 2020;37:112–25.
[279] Wu D, Chen Q, Chen X, Han F, Chen Z, Wang Y. The blood–brain barrier: structure, regulation and drug delivery. Signal Transduct Target Ther 2023;8:217.
[280] Wu H, Wang Y, Ren Z, Cong H, Shen Y, Yu B. The nanocarrier strategy for crossing the blood-brain barrier in glioma therapy. Chin Chem Lett 2025;36:109996.
[281] Oller-Salvia B, Sánchez-Navarro M, Giralt E, Teixidó M. Blood–brain barrier shuttle peptides: an emerging paradigm for brain delivery. Chem Soc Rev 2016;45:4690–707.
[282] Zhurenkov KE, Svirskis D, Connor B, Malmström J. Actuated hydrogel platforms to study brain cell behavior. Adv Healthc Mater 2025:2404484.
[283] Tuladhar A, Morshead CM, Shoichet MS. Circumventing the blood–brain barrier: local delivery of cyclosporin a stimulates stem cells in stroke-injured rat brain. J Control Release 2015;215:1–11.
[284] Kang T, Cha GD, Park OK, Cho HR, Kim M, Lee J, et al. Penetrative and sustained drug delivery using injectable hydrogel nanocomposites for postsurgical brain tumor treatment. ACS Nano 2023;17:5435–47.
[285] Catania G, Rodella G, Vanvarenberg K, Préat V, Malfanti A. Combination of hyaluronic acid conjugates with immunogenic cell death inducer and CpG for glioblastoma local chemo-immunotherapy elicits an immune response and induces long-term survival. Biomaterials 2023;294:122006.
[286] Cousins O, Hodges A, Schubert J, Veronese M, Turkheimer F, Miyan J, et al. The blood–CSF–brain route of neurological disease: the indirect pathway into the brain. Neuropathol Appl Neurobiol 2022;48:e12789.
[287] Fowler MJ, Cotter JD, Knight BE, Sevick-Muraca EM, Sandberg DI, Sirianni RW. Intrathecal drug delivery in the era of nanomedicine. Adv Drug Deliv Rev 2020;165–166:77–95.
[288] Nie T, He Z, Zhu J, Chen K, Howard GP, Pacheco-Torres J, et al. Non-invasive delivery of levodopa-loaded nanoparticles to the brain via lymphatic vasculature to enhance treatment of Parkinson's disease. Nano Res 2021;14:2749–61.
[289] Liu J, Gao D, Hu D, Lan S, Liu Y, Zheng H, et al. Delivery of biomimetic liposomes via meningeal lymphatic vessels route for targeted therapy of Parkinson's disease. Research 2023;6:0030.
[290] Nance E, Pun SH, Saigal R, Sellers DL. Drug delivery to the central nervous system. Nat Rev Mater 2022;7:314–31.
[291] Lian H, Meng Z. Melt electrospinning of daunorubicin hydrochloride-loaded poly (ε-caprolactone) fibrous membrane for tumor therapy. Bioact Mater 2017;2:96–100.
[292] Nance E, Zhang C, Shih T-Y, Xu Q, Schuster BS, Hanes J. Brain-penetrating nanoparticles improve paclitaxel efficacy in malignant glioma following local administration. ACS Nano 2014;8:10655–64.
[293] Khang M, Bindra RS, Mark SW. Intrathecal delivery and its applications in leptomeningeal disease. Adv Drug Deliv Rev 2022;186:114338.
[294] Casaca-Carreira J, Temel Y, Hescham S-A, Jahanshahi A. Transependymal cerebrospinal fluid flow: opportunity for drug delivery? Mol Neurobiol 2018;55:2780–8.
[295] Uriarte M, De Francesco PN, Fernandez G, Cabral A, Castrogiovanni D, Lalonde T, et al. Evidence supporting a role for the blood-cerebrospinal fluid barrier transporting circulating ghrelin into the brain. Mol Neurobiol 2019;56:4120–34.
[296] Lin T, Liu E, He H, Shin MC, Moon C, Yang VC, et al. Nose-to-brain delivery of macromolecules mediated by cell-penetrating peptides. Acta Pharm Sin B 2016;6:352–8.
[297] Jeon S, Park SH, Kim E, Kim J-y, Kim SW, Choi H. A magnetically powered stem cell-based microrobot for minimally invasive stem cell delivery via the intranasal pathway in a mouse brain. Adv Healthc Mater 2021;10:2100801.
[298] Mazzitelli JA, Smyth LCD, Cross KA, Dykstra T, Sun J, Du S, et al. Cerebrospinal fluid regulates skull bone marrow niches via direct access through dural channels. Nat Neurosci 2022;25:555–60.
[299] Pulous FE, Cruz-Hernández JC, Yang C, Kaya Z, Paccalet A, Wojtkiewicz G, et al. Cerebrospinal fluid can exit into the skull bone marrow and instruct cranial hematopoiesis in mice with bacterial meningitis. Nat Neurosci 2022;25:567–76.
[300] Mazzitelli JA, Pulous FE, Smyth LCD, Kaya Z, Rustenhoven J, Moskowitz MA, et al. Skull bone marrow channels as immune gateways to the central nervous system. Nat Neurosci 2023;26:2052–62.
[301] Kim D-I, Lee H, Kwon S-H, Sung YJ, Song WK, Park S. Bilayer hydrogel sheet-type intraocular microrobot for drug delivery and magnetic nanoparticles retrieval. Adv Healthc Mater 2020;9:2000118.
[302] Wu Y, Song Z, Deng G, Jiang K, Wang H, Zhang X, et al. Gastric acid powered nanomotors release antibiotics for in vivo treatment of helicobacter pylori infection. Small 2021;17:2006877.
[303] Wang W, Luo H, Wang H. Recent advances in micro/nanomotors for antibacterial applications. J Mater Chem B 2024;12:5000–23.
[304] Sun Z, Hou Y. Intelligent micro/nanorobots for improved tumor therapy. BMEMat 2023;1:e12012.
[305] Zhu Y-X, Jia H-R, Jiang Y-W, Guo Y, Duan Q-Y, Xu K-F, et al. A red blood cell-derived bionic microrobot capable of hierarchically adapting to five critical stages in systemic drug delivery. Exploration 2023:20230105.
[306] Tang X, Chen L, Wu Z, Li Y, Zeng J, Jiang W, et al. Lipophilic NO-driven nanomotors as drug balloon coating for the treatment of atherosclerosis. Small 2023;19:2203238.
[307] Zhang J, Dong Y, Liu X, Jin H, Wang S, An N, et al. Effective myocardial infarction treatment by targeted accumulation of sulforaphane using porous magnetic silica nanoparticles. Int J Pharm 2023;645:123389.
[308] Cai L, Zhao C, Cao X, Lu M, Li N, Luo Y, et al. Chinese herb pollen derived micromotors as active oral drug delivery system for gastric ulcer treatment. Bioact Mater 2024;32:28–36.
[309] Zhao Y, Xiong H, Li Y, Gao W, Hua C, Wu J, et al. Magnetically actuated reactive oxygen species scavenging nano-robots for targeted treatment. Adv Intell Syst 2022;4:2200061.
[310] Zhang L, Zhang B, Liang R, Ran H, Zhu D, Ren J, et al. A dual-biomineralized yeast micro-/nanorobot with self-driving penetration for gastritis therapy and motility recovery. ACS Nano 2023;17:6410–22.
[311] Zhang N, Fan M, Zhao Y, Hu X, Zhu Q, Jiao X, et al. Biomimetic and NOS-responsive nanomotor deeply delivery a combination of MSC-EV and mitochondrial ROS scavenger and promote heart repair and regeneration. Adv Sci 2023;10:2301440.
[312] de Ávila B-E-F, Angsantikul P, Li J, Angel Lopez-Ramirez M, Ramírez-Herrera DE, Thamphiwatana S, et al. Micromotor-enabled active drug delivery for in vivo treatment of stomach infection. Nat Commun 2017;8:272.
[313] Xu C, Jiang Y, Wang H, Zhang Y, Ye Y, Qin H, et al. Arthritic microenvironment actuated nanomotors for active rheumatoid arthritis therapy. Adv Sci 2023;10:2204881.
[314] Cao W, Wei W, Qiu B, Liu Y, Xie S, Fang Q, et al. Ultrasound-powered hydrogen peroxide-responsive Janus micromotors for targeted thrombolysis and recurrence inhibition. Chem Eng J 2024;483:149187.
[315] Go G, Jeong S-G, Yoo A, Han J, Kang B, Kim S, et al. Human adipose–derived mesenchymal stem cell–based medical microrobot system for knee cartilage regeneration in vivo. Sci Rob 2020;5:eaay6626.
[316] Go G, Han J, Zhen J, Zheng S, Yoo A, Jeon M-J, et al. A magnetically actuated microscaffold containing mesenchymal stem cells for articular cartilage repair. Adv Healthc Mater 2017;6:1601378.
[317] Wang F, Zhang Y, Jin D, Jiang Z, Liu Y, Knoll A, et al. Magnetic soft microrobot design for cell grasping and transportation. Cyborg Bionic Syst 2024;5:0109.
[318] Wu Z, Chen L, Guo W, Wang J, Ni H, Liu J, et al. Oral mitochondrial transplantation using nanomotors to treat ischaemic heart disease. Nat Nanotechnol 2024;19:1375–85.
[319] Chen X-Z, Hoop M, Shamsudhin N, Huang T, Özkale B, Li Q, et al. Hybrid magnetoelectric nanowires for nanorobotic applications: fabrication, magnetoelectric coupling, and magnetically assisted in vitro targeted drug delivery. Adv Mater 2017;29:1605458.

[320] Weerarathna IN, Kumar P, Dzoagbe HY, Kiwanuka L. Advancements in micro/nanorobots in medicine: design, actuation, and transformative application. ACS Omega 2025;10:5214–50.
[321] Cong Z, Li Y, Xie L, Chen Q, Tang M, Thongpon P, et al. Engineered microrobots for targeted delivery of bacterial outer membrane vesicles (OMV) in thrombus therapy. Small 2024;20:2400847.
[322] Darmawan BA, Lee SB, Nguyen VD, Go G, Nguyen KT, Lee H-S, et al. Self-folded microrobot for active drug delivery and rapid ultrasound-triggered drug release. Sens Actuators B 2020;324:128752.
[323] Xu Y, Bian Q, Wang R, Gao J. Micro/nanorobots for precise drug delivery via targeted transport and triggered release: a review. Int J Pharm 2022;616:121551.
[324] Luo M, Feng Y, Wang T, Guan J. Micro-/nanorobots at work in active drug delivery. Adv Funct Mater 2018;28:1706100.
[325] Kim H, Jo K, Choi H, Hahn SK. Biocompatible polymer-based micro/nanorobots for theranostic translational applications. J Control Release 2024;374:606–26.
[326] Bozuyuk U, Yasa O, Yasa IC, Ceylan H, Kizilel S, Sitti M. Light-triggered drug release from 3D-printed magnetic chitosan microswimmers. ACS Nano 2018;12:9617–25.
[327] Nguyen KT, Go G, Jin Z, Darmawan BA, Yoo A, Kim S, et al. A magnetically guided self-rolled microrobot for targeted drug delivery, real-time X-ray imaging, and microrobot retrieval. Adv Healthc Mater 2021;10:2001681.
[328] Kim J, Mayorga-Burrezo P, Song S-J, Mayorga-Martinez CC, Medina-Sánchez M, Pané S, et al. Advanced materials for micro/nanorobotics. Chem Soc Rev 2024;53:9190–253.
[329] Esteban-Fernández de Ávila B, Lopez-Ramirez MA, Mundaca-Uribe R, Wei X, Ramírez-Herrera DE, Karshalev E, et al. Multicompartment tubular micromotors toward enhanced localized active delivery. Adv Mater 2020;32:2000091.
[330] Li M, Wu J, Lin D, Yang J, Jiao N, Wang Y, et al. A diatom-based biohybrid microrobot with a high drug-loading capacity and pH-sensitive drug release for target therapy. Acta Biomater 2022;154:443–53.
[331] He T, Yang Y, Chen X-B. Propulsion mechanisms of micro/nanorobots: a review. Nanoscale 2024;16:12696–734.
[332] Kroupa T, Hermanová S, Mayorga-Martinez CC, Novotný F, Sofer Z, Pumera M. Micromotors as “motherships”: a concept for the transport, delivery, and enzymatic release of molecular cargo via nanoparticles. Langmuir 2019;35:10618–24.
[333] Hortelão AC, Patiño T, Perez-Jiménez A, Blanco À, Sánchez S. Enzyme-powered nanobots enhance anticancer drug delivery. Adv Funct Mater 2018;28:1705086.
[334] Ma R, Hou Y, Wang S. Combatting cancer with tiny intelligent warriors: stimuli-responsive micro/nanorobots in chemotherapeutic delivery. Sci China Mater 2024;67:2469–76.
[335] Wang X, Cai J, Sun L, Zhang S, Gong D, Li X, et al. Facile fabrication of magnetic microrobots based on spirulina templates for targeted delivery and synergistic chemo-photothermal therapy. ACS Appl Mater Interfaces 2019;11:4745–56.
[336] Chai Z, Ran D, Lu L, Zhan C, Ruan H, Hu X, et al. Ligand-modified cell membrane enables the targeted delivery of drug nanocrystals to glioma. ACS Nano 2019;13:5591–601.
[337] Zhang X, Yao S, Liu C, Jiang Y. Tumor tropic delivery of doxorubicin-polymer conjugates using mesenchymal stem cells for glioma therapy. Biomaterials 2015;39:269–81.
[338] Lu G, Wang X, Li F, Wang S, Zhao J, Wang J, et al. Engineered biomimetic nanoparticles achieve targeted delivery and efficient metabolism-based synergistic therapy against glioblastoma. Nat Commun 2022;13:4214.
[339] Wang B, Shen J, Huang C, Ye Z, He J, Wu X, et al. Magnetically driven biohybrid blood hydrogel fibres for personalized intracranial tumour therapy under fluoroscopic tracking. Nat Biomed Eng 2025;1–15.
[340] Wang B, Wang Q, Chan KF, Ning Z, Wang Q, Ji F, et al. tPA-anchored nanorobots for in vivo arterial recanalization at submillimeter-scale segments. Sci Adv 2024;10:eadk8970.
[341] Ghanbari A. Bioinspired reorientation strategies for application in micro/nanorobotic control. J Micro-Bio Robot 2020;16:173–97.
[342] Bachmann F, Giltinan J, Codutti A, Klumpp S, Sitti M, Faivre D. Opportunities and utilization of branching and step-out behavior in magnetic microswimmers with a nonlinear response. Appl Phys Lett 2021;118:174102.
[343] Banerjee A, Qi J, Gogoi R, Wong J, Mitragotri S. Role of nanoparticle size, shape and surface chemistry in oral drug delivery. J Control Release 2016;238:176–85.
[344] Nowak M, Brown TD, Graham A, Helgeson ME, Mitragotri S. Size, shape, and flexibility influence nanoparticle transport across brain endothelium under flow. Bioeng Transl Med 2020;5:e10153.
[345] Wang Y, Bao Z, Shi M, Liang Z, Cao R, Zheng H. The role of surface curvature in electrocatalysts. Chem – Eur J 2022;28:e202102915.
[346] Yue Z-G, Wei W, Lv P-P, Yue H, Wang L-Y, Su Z-G, et al. Surface charge affects cellular uptake and intracellular trafficking of chitosan-based nanoparticles. Biomacromolecules 2011;12:2440–6.
[347] Kim S, Lee S, Lee J, Nelson BJ, Zhang L, Choi H. Fabrication and manipulation of ciliary microrobots with non-reciprocal magnetic actuation. Sci Rep 2016;6:30713.
[348] Dreyfus R, Boehler Q, Lyttle S, Gruber P, Lussi J, Chautems C, et al. Dexterous helical magnetic robot for improved endovascular access. Sci Rob 2024;9:eadh0298.
[349] Servant A, Qiu F, Mazza M, Kostarelos K, Nelson BJ. Controlled in vivo swimming of a swarm of bacteria-like microrobotic flagella. Adv Mater 2015;27:2981–8.
[350] Wang H, Pumera M. Fabrication of micro/nanoscale motors. Chem Rev 2015;115:8704–35.
[351] Fan X, Sun M, Sun L, Xie H. Ferrofluid droplets as liquid microrobots with multiple deformabilities. Adv Funct Mater 2020;30:2000138.
[352] Song G, Cheng L, Chao Y, Yang K, Liu Z. Emerging nanotechnology and advanced materials for cancer radiation therapy. Adv Mater 2017;29:1700996.
[353] Liu Y, Zhang N, Wen Y, Wen J. Head and neck cancer: pathogenesis and targeted therapy. MedComm 2024;5:e702.
[354] Zhao W, Wang L, Zhang M, Liu Z, Wu C, Pan X, et al. Photodynamic therapy for cancer: mechanisms, photosensitizers, nanocarriers, and clinical studies. MedComm 2024;5:e603.
[355] Wang J, Dong Y, Li Y, Li W, Cheng K, Qian Y, et al. Designer exosomes for active targeted chemo-photothermal synergistic tumor therapy. Adv Funct Mater 2018;28:1707360.
[356] Liu B, Zhou H, Tan L, Siu KTH, Guan X-Y. Exploring treatment options in cancer: tumor treatment strategies. Signal Transduct Target Ther 2024;9:175.
[357] Hu T, Shen C, Wang X, Wu F, He Z. Tumor microenvironment-sensitive polymeric nanoparticles for synergetic chemo-photo therapy. Chin Chem Lett 2024;35:109562.
[358] Gotwals P, Cameron S, Cipolletta D, Cremasco V, Crystal A, Hewes B, et al. Prospects for combining targeted and conventional cancer therapy with immunotherapy. Nat Rev Cancer 2017;17:286–301.
[359] Liu Y, Yan Q, Zeng Z, Fan C, Xiong W. Advances and prospects of mRNA vaccines in cancer immunotherapy. Biochimica et Biophysica Acta (BBA) - Rev Cancer 2024;1879:189068.
[360] Chen Y, Zhou Q, Jia Z, Cheng N, Zhang S, Chen W, et al. Enhancing cancer immunotherapy: nanotechnology-mediated immunotherapy overcoming immunosuppression. Acta Pharm Sin B 2024;14:3834–54.
[361] Dougan M, Luoma AM, Dougan SK, Wucherpfennig KW. Understanding and treating the inflammatory adverse events of cancer immunotherapy. Cell 2021;184:1575–88.
[362] Motevasseli M, Darvishi M, Khoshnevisan A, Zeinalizadeh M, Saffar H, Bayat S, et al. Distinct tumor-TAM interactions in IDH-stratified glioma microenvironments unveiled by single-cell and spatial transcriptomics. Acta Neuropathol Commun 2024;12:133.
[363] Xiong J, Wang H, Wang Q. Suppressive myeloid cells shape the tumor immune microenvironment. Advanced Biology 2021;5:1900311.
[364] Zhu Y, An X, Zhang X, Qiao Y, Zheng T, Li X. STING: a master regulator in the cancer-immunity cycle. Mol Cancer 2019;18:152.
[365] Fu G, Zhao Y, Mao C, Liu Y. Enhancing nano-immunotherapy of cancer through cGAS–STING pathway modulation. Biomater Sci 2025.

[366] Zhao X, Chen R, Liu M, Feng J, Chen J, Hu K. Remodeling the blood–brain barrier microenvironment by natural products for brain tumor therapy. Acta Pharm Sin B 2017;7:541–53.
[367] Li T, Chen L, Xue Y, Xiao X, Dai W, Tan K, et al. Chemotactic nanomotor for multimodal combined therapy of glioblastoma. Sci China Chem 2024;67:1277–88.
[368] Huang Y, Wu Z, Wang H, An H, Zhang J, Bao Z. Nanogenerators with l-arginine loading: new choices as cascade and synergistic nitric oxide/photodynamic antitumor agents. Mater Chem Front 2025;9:204–22.
[369] Chen Y, Shu X, Guo J-Y, Xiang Y, Liang S-Y, Lai J-M, et al. Nanodrugs mediate TAMs-related arginine metabolism interference to boost photodynamic immunotherapy. J Control Release 2024;367:248–64.
[370] Li S-L, Jiang P, Jiang F-L, Liu Y. Recent advances in nanomaterial-based nanoplatforms for chemodynamic cancer therapy. Adv Funct Mater 2021;31:2100243.
[371] Yasa IC, Ceylan H, Bozuyuk U, Wild A-M, Sitti M. Elucidating the interaction dynamics between microswimmer body and immune system for medical microrobots. Sci Rob 2020;5:eaaz3867.
[372] Li W, Liu B, Ou L, Li G, Lei D, Xiong Z, et al. Arbitrary construction of versatile NIR-driven microrobots. Adv Mater 2024;36:2402482.
[373] Ding Q, Huang S, Zhang Z, Yu D, Li M, He Q, et al. Integration of photodiagnosis and therapy guided by micro/nanorobots. Adv Mater 2025:n/a:2420359.
[374] Hou Y, Dan X, Babbar M, Wei Y, Hasselbalch SG, Croteau DL, et al. Ageing as a risk factor for neurodegenerative disease. Nat Rev Neurol 2019;15:565–81.
[375] Massimini M, Corbetta M, Sanchez-Vives MV, Andrillon T, Deco G, Rosanova M, et al. Sleep-like cortical dynamics during wakefulness and their network effects following brain injury. Nat Commun 2024;15:7207.
[376] Galgano M, Toshkezi G, Qiu X, Russell T, Chin L, Zhao L-R. Traumatic brain injury: current treatment strategies and future endeavors. Cell Transplant 2017;26:1118–30.
[377] Klein P, Kaminski RM, Koepp M, Löscher W. New epilepsy therapies in development. Nat Rev Drug Discov 2024;23:682–708.
[378] Hosseini SM, Borys B, Karimi-Abdolrezaee S. Neural stem cell therapies for spinal cord injury repair: an update on recent preclinical and clinical advances. Brain 2024;147:766–93.
[379] Svendsen SP, Svendsen CN. Cell therapy for neurological disorders. Nat Med 2024;30:2756–70.
[380] Polanía R, Nitsche MA, Ruff CC. Studying and modifying brain function with non-invasive brain stimulation. Nat Neurosci 2018;21:174–87.
[381] Oganesian LL, Shanechi MM. Brain–computer interfaces for neuropsychiatric disorders. Nat Rev Bioeng 2024;2:653–70.
[382] De Paolis ML, Paoletti I, Zaccone C, Capone F, D'Amelio M, Krashia P. Transcranial alternating current stimulation (tACS) at gamma frequency: an up-and-coming tool to modify the progression of Alzheimer's Disease. Trans Neurodegen 2024;13:33.
[383] Liu L, Li Y, Liu R, Shen Q, Li Y, Shi Z, et al. Switchable nanoparticle for programmed gene-chem delivery with enhanced neuronal recovery and CT imaging for neurodegenerative disease treatment. Mater Horiz 2019;6:1923–9.
[384] Mahar M, Cavalli V. Intrinsic mechanisms of neuronal axon regeneration. Nat Rev Neurosci 2018;19:323–37.
[385] Grinsell D, Keating CP. Peripheral nerve reconstruction after injury: a review of clinical and experimental therapies. Biomed Res Int 2014;2014:698256.
[386] Burrell JC, Ali ZS, Zager EL, Rosen JM, Tatarchuk MM, Cullen DK. Engineering the future of restorative clinical peripheral nerve surgery. Adv Healthc Mater 2025:2404293.
[387] Liao W, Shi Y, Li Z, Yin X. Advances in 3D printing combined with tissue engineering for nerve regeneration and repair. J Nanobiotechnol 2025;23:5.
[388] Manoukian OS, Arul MR, Rudraiah S, Kalajzic I, Kumbar SG. Aligned microchannel polymer-nanotube composites for peripheral nerve regeneration: small molecule drug delivery. J Control Release 2019;296:54–67.
[389] Lyden PD, Lamb J, Kothari S, Toossi S, Boitano P, Rajput PS. Differential effects of hypothermia on neurovascular unit determine protective or toxic results: toward optimized therapeutic hypothermia. J Cereb Blood Flow Metab 2018;39:1693–709.
[390] Yu Y, Liu S, Yang L, Song P, Liu Z, Liu X, et al. Roles of reactive oxygen species in inflammation and cancer. MedComm 2024;5:e519.
[391] Tuo Q-z, Zhang S-t, Lei P. Mechanisms of neuronal cell death in ischemic stroke and their therapeutic implications. Med Res Rev 2022;42:259–305.
[392] Fan W, Chen H, Li M, Fan X, Jiang F, Xu C, et al. NRF2 activation ameliorates blood–brain barrier injury after cerebral ischemic stroke by regulating ferroptosis and inflammation. Sci Rep 2024;14:5300.
[393] Zhang LM, Liang XL, Xiong GF, Xing XL, Zhang QJ, Zhang BR, et al. Analysis and identification of oxidative stress-ferroptosis related biomarkers in ischemic stroke. Sci Rep 2024;14:3803.
[394] Sabelli M, Montosi G, Garuti C, Caleffi A, Oliveto S, Biffo S, et al. Human macrophage ferroportin biology and the basis for the ferroportin disease. Hepatology 2017;65.
[395] Tao Y, Chan HF, Shi B, Li M, Leong KW. Light: a magical tool for controlled drug delivery. Adv Funct Mater 2020;30:2005029.
[396] Yang Y, Long K, Chu Y, Lu H, Wang W, Zhan C. Photoresponsive drug delivery systems: challenges and progress. Adv Funct Mater 2024;34:2402975.
[397] Sia CS, Tey BT, Low LE. Light-responsive nanoassemblies: advancing biomedical innovation. Adv Funct Mater 2024;34:2314278.
[398] Gao Y, Guo Y, Yang Y, Tang Y, Wang B, Yan Q, et al. Magnetically manipulated optoelectronic hybrid microrobots for optically targeted non-genetic neuromodulation. Adv Mater 2024;36:2305632.
[399] Luo L. Architectures of neuronal circuits. Science 2021;373:eabg7285.
[400] Pillai EK, Franze K. Mechanics in the nervous system: from development to disease. Neuron 2024;112:342–61.
[401] Marcus M, Baranes K, Park M, Choi IS, Kang K, Shefi O. Interactions of neurons with physical environments. Adv Healthc Mater 2017;6:1700267.
[402] Hennig K, Wang I, Moreau P, Valon L, DeBeco S, Coppey M, et al. Stick-slip dynamics of cell adhesion triggers spontaneous symmetry breaking and directional migration of mesenchymal cells on one-dimensional lines. Sci Adv 2020;6. eaau5670.
[403] Aliakbarshirazi S, Ghobeira R, Asadian M, Narimisa M, Nikiforov A, De Baere I, et al. Advanced hollow cathode discharge plasma treatment of unique bilayered fibrous nerve guidance conduits for enhanced/oriented neurite outgrowth. Biomacromolecules 2024;25:1448–67.
[404] Kim E, Jeon S, An H-K, Kianpour M, Yu S-W, Kim J-y, et al. A magnetically actuated microrobot for targeted neural cell delivery and selective connection of neural networks. Sci Adv 2020;6:eabb5696.
[405] Venkat P, Chopp M, Chen J. Blood–brain barrier disruption, vascular impairment, and ischemia/reperfusion damage in diabetic stroke. J Am Heart Assoc 2017;6. e005819.
[406] Mackman N, Bergmeier W, Stouffer GA, Weitz JI. Therapeutic strategies for thrombosis: new targets and approaches. Nat Rev Drug Discov 2020;19:333–52.
[407] Zhang S, Zhou Y, Li R, Chen Z, Fan X. Advanced drug delivery system against ischemic stroke. J Control Release 2022;344:173–201.
[408] Woodland MLD, Thompson A, Lipford A, Goyal N, Schexnaildre JC, Mottamal M, et al. New triazole-based potent inhibitors of human factor XIIa as anticoagulants. ACS Omega 2024;9:10694–708.
[409] Liu X, Wang L, Xiang Y, Liao F, Li N, Li J, et al. Magnetic soft microfiberbots for robotic embolization. Sci Rob 2024;9:eadh2479.
[410] Wei J, Jiang J, Zhu Y, Wei X, Sun Z, Sun J, et al. Clot-based time attenuation curve as a novel imaging predictor of mechanical thrombectomy functional outcome in acute ischemia stroke. Eur Radiol 2024;34:2198–208.
[411] Wang L, Wang J, Hao J, Dong Z, Wu J, Shen G, et al. Guiding drug through interrupted bloodstream for potentiated thrombolysis by C-shaped magnetic actuation system in vivo. Adv Mater 2021;33:2105351.
[412] Sommer CJ. Ischemic stroke: experimental models and reality. Acta Neuropathol 2017;133:245–61.
[413] Barakzie A, Jansen AJG, Cavalcante F, Nagy M, Dippel DWJ, van der Lugt A, et al. Association of primary and secondary hemostasis biomarkers with acute ischemic stroke outcome in patients undergoing thrombectomy, with or without thrombolytics: post hoc analysis of the Multicenter Randomized Clinical Trial of Endovascular Treatment for Acute Ischemic Stroke in the Netherlands-NO IV. J Thromb Haemost 2025;23:235–47.
[414] Hackam DG, Spence JD. Antiplatelet therapy in ischemic stroke and transient ischemic attack: an overview of major trials and meta-analyses. Stroke 2019;50:773–8.
[415] Barnes GD. New targets for antithrombotic medications: seeking to decouple thrombosis from hemostasis. J Thromb Haemost 2025;23:1146–59.
[416] Fisher M, Saver JL. Future directions of acute ischaemic stroke therapy. The Lancet Neurology 2015;14:758–67.
[417] Li F, Liu J, Zhang F, Wu X, Dai T, Kuang J, et al. Anticoagulation therapy after reperfusion treatment for acute ischemic stroke with non-valvular atrial fibrillation: a multicenter retrospective study. Sci Rep 2025;15:9619.

[418] Refaat A, del Rosal B, Palasubramaniam J, Pietersz G, Wang X, Peter K, et al. Smart delivery of plasminogen activators for efficient thrombolysis; recent trends and future perspectives. Adv Therapeutics 2021;4:2100047.
[419] Mega JL, Simon T. Pharmacology of antithrombotic drugs: an assessment of oral antiplatelet and anticoagulant treatments. Lancet 2015;386:281–91.
[420] Tsikis ST, Hirsch TI, Fligor SC, Pan A, Joiner MM, Devietro A, et al. Direct thrombin inhibitors as alternatives to heparin to preserve lung growth and function in a murine model of compensatory lung growth. Sci Rep 2022;12:21117.
[421] Yang Z, Tu Q, Maitz MF, Zhou S, Wang J, Huang N. Direct thrombin inhibitor-bivalirudin functionalized plasma polymerized allylamine coating for improved biocompatibility of vascular devices. Biomaterials 2012;33:7959–71.
[422] Zhao Y, Xie R, Yodsanit N, Ye M, Wang Y, Wang B, et al. Hydrogen peroxide-responsive platelet membrane-coated nanoparticles for thrombus therapy. Biomater Sci 2021;9:2696–708.
[423] Wang Q, Jin D, Wang B, Xia N, Ko H, Ip BYM, et al. Reconfigurable magnetic microswarm for accelerating tPA-mediated thrombolysis under ultrasound imaging. IEEE/ASME Trans Mechatron 2022;27:2267–77.
[424] Cheng R, Huang W, Huang L, Yang B, Mao L, Jin K, et al. Acceleration of tissue plasminogen activator-mediated thrombolysis by magnetically powered nanomotors. ACS Nano 2014;8:7746–54.
[425] Xie M, Zhang W, Fan C, Wu C, Feng Q, Wu J, et al. Bioinspired soft microrobots with precise magneto-collective control for microvascular thrombolysis. Adv Mater 2020;32:2000366.
[426] Wan M, Wang Q, Wang R, Wu R, Li T, Fang D, et al. Platelet-derived porous nanomotor for thrombus therapy. Sci Adv 2020;6. eaaz9014.
[427] Yang M, Zhang Y, Mou F, Cao C, Yu L, Li Z, et al. Swarming magnetic nanorobots bio-interfaced by heparinoid-polymer brushes for in vivo safe synergistic thrombolysis. Sci Adv 2023;9:eadk7251.
[428] Qin C, Yang S, Chu Y-H, Zhang H, Pang X-W, Chen L, et al. Signaling pathways involved in ischemic stroke: molecular mechanisms and therapeutic interventions. Signal Transduct Target Ther 2022;7:215.
[429] Blennow K, Brody DL, Kochanek PM, Levin H, McKee A, Ribbers GM, et al. Traumatic brain injuries. Nat Rev Dis Primers 2016;2:16084.
[430] Donat CK, Yanez Lopez M, Sastre M, Baxan N, Goldfinger M, Seeamber R, et al. From biomechanics to pathology: predicting axonal injury from patterns of strain after traumatic brain injury. Brain 2021;144:70–91.
[431] Shao X, Liu Z, Mao S, Han L. Unraveling the mechanobiology underlying traumatic brain injury with advanced technologies and biomaterials. Adv Healthc Mater 2022;11:2200760.
[432] Hemphill Matthew A, Dauth S, Yu Chung J, Dabiri Borna E, Parker KK. Traumatic brain injury and the neuronal microenvironment: a potential role for neuropathological mechanotransduction. Neuron 2015;85:1177–92.
[433] Dutta D, Khan N, Wu J, Jay SM. Extracellular vesicles as an emerging frontier in spinal cord injury pathobiology and therapy. Trends Neurosci 2021;44:492–506.
[434] Wang J, Jiang C, Zhang K, Lan X, Chen X, Zang W, et al. Melatonin receptor activation provides cerebral protection after traumatic brain injury by mitigating oxidative stress and inflammation via the Nrf2 signaling pathway. Free Radic Biol Med 2019;131:345–55.
[435] Shi Z-f, Fang Q, Chen Y, Xu L-x, Wu M, Jia M, et al. Methylene blue ameliorates brain edema in rats with experimental ischemic stroke via inhibiting aquaporin 4 expression. Acta Pharmacol Sin 2021;42:382–92.
[436] Ahn H, Kang SG, Yoon S-i, Ko H-J, Kim P-H, Hong E-J, et al. Methylene blue inhibits NLRP3, NLRC4, AIM2, and non-canonical inflammasome activation. Sci Rep 2017;7:12409.
[437] Liu Y, Tan Y, Cheng G, Ni Y, Xie A, Zhu X, et al. Customized intranasal hydrogel delivering methylene blue ameliorates cognitive dysfunction against Alzheimer's disease. Adv Mater 2024;36:2307081.
[438] Li X, Hua S, Zhong D, Zhou M, Ding Z. Metal-organic framework-edaravone nanoparticles for radiotherapy-induced brain injury treatment. Biomaterials 2025;314:122868.
[439] Bao Q, Hu P, Xu Y, Cheng T, Wei C, Pan L, et al. Simultaneous blood–brain barrier crossing and protection for stroke treatment based on edaravone-loaded ceria nanoparticles. ACS Nano 2018;12:6794–805.
[440] Barati A, Moghimi S, Taghavi Zanjani K, Rohani M, Sohrabi Hesar M, Arfaie A, et al. Acute administration of edaravone improves cognitive impairment in a mouse model of mPFC ischemia: crosstalk between necroptosis, neuroinflammation, and antioxidant defense. Mol Neurobiol 2025;62:4420–34.
[441] Scott G, Zetterberg H, Jolly A, Cole JH, De Simoni S, Jenkins PO, et al. Minocycline reduces chronic microglial activation after brain trauma but increases neurodegeneration. Brain 2018;141:459–71.
[442] Pernici CD, Rowe RK, Doughty PT, Madadi M, Lifshitz J, Murray TA. Longitudinal optical imaging technique to visualize progressive axonal damage after brain injury in mice reveals responses to different minocycline treatments. Sci Rep 2020;10:7815.
[443] Cheng G, Liu Z, Yan Z, Wu J, Li Z, Gao S, et al. Minocycline nanoplatform penetrates the BBB and enables the targeted treatment of Parkinson's disease with cognitive impairment. J Control Release 2025;377:591–605.
[444] Park J, Choi E, Shin S, Lim S, Kim D, Baek S, et al. Nootropic nanocomplex with enhanced blood-brain barrier permeability for treatment of traumatic brain injury-associated neurodegeneration. J Control Release 2018;284:152–9.
[445] Bayat Tork MA, Saberifar M, Joneidi Yekta H, Hajinejad M, Hosseini Ravandi H, Gorji A, et al. Nano-scaffold containing functional motif of stromal cell-derived factor 1 enhances neural stem cell behavior and synaptogenesis in traumatic brain injury. Sci Rep 2025;15:5811.
[446] Ciryam P, Kundra R, Morimoto RI, Dobson CM, Vendruscolo M. Supersaturation is a major driving force for protein aggregation in neurodegenerative diseases. Trends Pharmacol Sci 2015;36:72–7.
[447] Soto C, Pritzkow S. Protein misfolding, aggregation, and conformational strains in neurodegenerative diseases. Nat Neurosci 2018;21:1332–40.
[448] Böken D, Xia Z, Lam JYL, Fertan E, Wu Y, English EA, et al. Ultrasensitive protein aggregate quantification assays for neurodegenerative diseases on the simoa platform. Anal Chem 2025;97:290–9.
[449] Niedzielska E, Smaga I, Gawlik M, Moniczewski A, Stankowicz P, Pera J, et al. Oxidative stress in neurodegenerative diseases. Mol Neurobiol 2016;53:4094–125.
[450] Bhat AH, Dar KB, Anees S, Zargar MA, Masood A, Sofi MA, et al. Oxidative stress, mitochondrial dysfunction and neurodegenerative diseases; a mechanistic insight. Biomed Pharmacother 2015;74:101–10.
[451] Fan Y-G, Wu T-Y, Zhao L-X, Jia R-J, Ren H, Hou W-J, et al. From zinc homeostasis to disease progression: unveiling the neurodegenerative puzzle. Pharmacol Res 2024;199:107039.
[452] Lin M-m, Liu N, Qin Z-h, Wang Y. Mitochondrial-derived damage-associated molecular patterns amplify neuroinflammation in neurodegenerative diseases. Acta Pharmacol Sin 2022;43:2439–47.
[453] Jayaraj RL, Rodriguez EA, Wang Y, Block ML. Outdoor ambient air pollution and neurodegenerative diseases: the neuroinflammation hypothesis. Curr Environ Health Rep 2017;4:166–79.
[454] Summers RA, Fagiani F, Rowitch DH, Absinta M, Reich DS. Novel human iPSC models of neuroinflammation in neurodegenerative disease and regenerative medicine. Trends Immunol 2024;45:799–813.
[455] Chen Y, Wu W, Zhao S, Lv X, Hu J, Han C, et al. Increased accumulation of α-synuclein in inflamed appendices of Parkinson's disease patients. Mov Disord 2021;36:1911–8.
[456] Wu K-M, Xu Q-H, Liu Y-Q, Feng Y-W, Han S-D, Zhang Y-R, et al. Neuronal FAM171A2 mediates α-synuclein fibril uptake and drives Parkinson's disease. Science 2025;387:892–900.
[457] He M, Zhang X, Ran X, Zhang Y, Nie X, Xiao B, et al. Black phosphorus nanosheets protect neurons by degrading aggregative α-syn and clearing ROS in Parkinson's disease. Adv Mater 2024;36:2404576.
[458] Hou J, Wang H, Ge Z, Zuo T, Chen Q, Liu X, et al. Treating acute kidney injury with antioxidative black phosphorus nanosheets. Nano Lett 2020;20:1447–54.
[459] Liu W, Dong A, Wang B, Zhang H. Current advances in black phosphorus-based drug delivery systems for cancer therapy. Adv Sci 2021;8:2003033.

[460] Zhang C, Shao W, Yuan H, Xiao R, Zhang Y, Wei C, et al. Engineered extracellular vesicle-based nanoformulations that coordinate neuroinflammation and immune homeostasis, enhancing Parkinson's disease therapy. ACS Nano 2024;18:23014–31.
[461] Zhao Z, Chen L, Yang C, Guo W, Huang Y, Wang W, et al. Nanomotor-based H2S donor with mitochondrial targeting function for treatment of Parkinson's disease. Bioact Mater 2024;31:578–89.
[462] Wang W, Zhao Z, Zhang Z, Wu Z, Zhang Y, Wang K, et al. Delivery of small interfering RNA by hydrogen sulfide-releasing nanomotor for the treatment of Parkinson's disease. J Control Release 2025;377:648–60.
[463] Lei T, Yang Z, Jiang C, Wang X, Yang W, Yang X, et al. Mannose-integrated nanoparticle hitchhike glucose transporter 1 recycling to overcome various barriers of oral delivery for Alzheimer's disease therapy. ACS Nano 2024;18:3234–50.
[464] Gilbert MAG, Fatima N, Jenkins J, O'Sullivan TJ, Schertel A, Halfon Y, et al. CryoET of β-amyloid and tau within postmortem Alzheimer's disease brain. Nature 2024;631:913–9.
[465] Kang H, Ga YJ, Kim SH, Cho YH, Kim JW, Kim C, et al. Small interfering RNA (siRNA)-based therapeutic applications against viruses: principles, potential, and challenges. J Biomed Sci 2023;30:88.
[466] Xu R, Huang L, Liu J, Zhang Y, Xu Y, Li R, et al. Remodeling of mitochondrial metabolism by a mitochondria-targeted RNAi nanoplatform for effective cancer therapy. Small 2024;20:2305923.
[467] Jiang S, Cai G, Yang Z, Shi H, Zeng H, Ye Q, et al. Biomimetic nanovesicles as a dual gene delivery system for the synergistic gene therapy of Alzheimer's disease. ACS Nano 2024;18:11753–68.
[468] Ning S, Sanchis-Gual R, Franco C, Wendel-Garcia PD, Ye H, Veciana A, et al. Magnetic PiezoBOTs: a microrobotic approach for targeted amyloid protein dissociation. Nanoscale 2023;15:14800–8.
[469] Luo Q, Lin Y-X, Yang P-P, Wang Y, Qi G-B, Qiao Z-Y, et al. A self-destructive nanosweeper that captures and clears amyloid β-peptides. Nat Commun 2018;9:1802.
[470] Ghosh C, Ghosh S, Chatterjee A, Bera P, Mampallil D, Ghosh P, et al. Dual enzyme-powered chemotactic cross β amyloid based functional nanomotors. Nat Commun 2023;14:5903.
[471] Yuan X, Shi J, Kang Y, Dong J, Pei Z, Ji X. Piezoelectricity, pyroelectricity, and ferroelectricity in biomaterials and biomedical applications. Adv Mater 2024;36:2308726.
[472] Yang X, Yang Z, Wang X, Guo Y, Xie Y, Yao W, et al. Piezoelectric nanomaterials for antibacterial strategies. Appl Mater Today 2024;40:102419.
[473] Chen S, Tong X, Huo Y, Liu S, Yin Y, Tan M-L, et al. Piezoelectric biomaterials inspired by nature for applications in biomedicine and nanotechnology. Adv Mater 2024;36:2406192.
[474] LaFerla FM, Green KN, Oddo S. Intracellular amyloid-β in Alzheimer's disease. Nat Rev Neurosci 2007;8:499–509.
[475] Marksteiner J, Humpel C. Beta-amyloid expression, release and extracellular deposition in aged rat brain slices. Mol Psychiatry 2008;13:939–52.
[476] Liu W, Wang W, Dong X, Sun Y. Near-infrared light-powered Janus nanomotor significantly facilitates inhibition of amyloid-β fibrillogenesis. ACS Appl Mater Interfaces 2020;12:12618–28.
[477] Lin X, Dong X, Sun Y. Dual-carbon dots composite: a multifunctional photo-propelled nanomotor against Alzheimer's β-amyloid. Small 2024;20:2407154.
[478] Mayorga-Burrezo P, Mayorga-Martinez CC, Pumera M. Light-driven micromotors to dissociate protein aggregates that cause neurodegenerative diseases. Adv Funct Mater 2022;32:2106699.
[479] Wang D, Wang S, Zhou Z, Bai D, Zhang Q, Ai X, et al. White blood cell membrane-coated nanoparticles: recent development and medical applications. Adv Healthc Mater 2022;11:2101349.
[480] Lin X, Liu W, Dong X, Sun Y. Epigallocatechin gallate-derived carbonized polymer dots: a multifunctional scavenger targeting Alzheimer's β-amyloid plaques. Acta Biomater 2023;157:524–37.
[481] Zhou J, Jangili P, Son S, Ji MS, Won M, Kim JS. Fluorescent diagnostic probes in neurodegenerative diseases. Adv Mater 2020;32:2001945.
[482] Fayazi N, Sheykhhasan M, Soleimani Asl S, Najafi R. Stem cell-derived exosomes: a new strategy of neurodegenerative disease treatment. Mol Neurobiol 2021;58:3494–514.
[483] Dong M, Wang X, Chen X-Z, Mushtaq F, Deng S, Zhu C, et al. 3D-printed soft magnetoelectric microswimmers for delivery and differentiation of neuron-like cells. Adv Funct Mater 2020;30:1910323.
[484] Hwang J, Jeon S, Kim B, Kim J-y, Jin C, Yeon A, et al. An electromagnetically controllable microrobotic interventional system for targeted, real-time cardiovascular intervention. Adv Healthc Mater 2022;11:2102529.
[485] Medina-Sánchez M, Schmidt OG. Medical microbots need better imaging and control. Nature 2017;545:406–8.
[486] Maksim S, Melanie W, Kate TC, Michael RL, Eytan R, Erez N, et al. Neuroanatomy of cranial dural vessels: implications for subdural hematoma embolization. J NeuroInterventional Surg 2021;13:471–7.
[487] Cugurra A, Mamuladze T, Rustenhoven J, Dykstra T, Beroshvili G, Greenberg ZJ, et al. Skull and vertebral bone marrow are myeloid cell reservoirs for the meninges and CNS parenchyma. Science 2021;373. eabf7844.
[488] Castellani G, Croese T, Peralta Ramos JM, Schwartz M. Transforming the understanding of brain immunity. Science 2023;380. eabo7649.
[489] Liu W, Yang M, Wang N, Liu X, Wang C, Shi K, et al. Intracalvariosseous injection: an approach for central nervous system drug delivery through skull bone marrow with a preclinical research in stroke. EBioMedicine 2025;112:105568.
[490] Herisson F, Frodermann V, Courties G, Rohde D, Sun Y, Vandoorne K, et al. Direct vascular channels connect skull bone marrow and the brain surface enabling myeloid cell migration. Nat Neurosci 2018;21:1209–17.
[491] Yao H, Price TT, Cantelli G, Ngo B, Warner MJ, Olivere L, et al. Leukaemia hijacks a neural mechanism to invade the central nervous system. Nature 2018;560:55–60.
[492] Blaber E, Marçal H, Burns BP. Bioastronautics: The Influence of Microgravity on Astronaut Health. Astrobiology 2010;10:463–73.
[493] Cucinotta FA, Alp M, Sulzman FM, Wang M. Space radiation risks to the central nervous system. Life Sciences in Space Research 2014;2:54–69.
[494] Widrow LM. Origin of galactic and extragalactic magnetic fields. Reviews of Modern Physics 2002;74:775–823.
[495] Luo H, Wang H, Cai S, Qin H, Lin Y, Jia Y, et al. Evolution of the Lunar Magnetic Field. Space: Science & Technology 2024;4:0155.